DOE/ID/12613-1

Rec'd ... JU

DOE/ID/12613--1

DE90 014391

Cascade Geothermal Drilling/Corehole N-3

Submitted to The Department of Energy
Mr. R. Jeffrey Hoyles
Dated July 19, 1988

Final report for Contract DE-FC07-85ID12613

By

Dr. Chandler A. Swanberg
Project Manager

Geothermal Resources International, Inc.
1825 S. Grant Street
Suite 900
San Mateo, Ca. 94402

DISCLAIMER

8135 Hydrothermal Systems

CORE HOLE DRILLING AND THE "RAIN CURTAIN" PHENOMENON AT NEWBERRY VOLCANO, OREGON

C. A. Swanberg, (Geothermal Resources International Inc.,1825 S. Grant Street, Suite 900, San Mateo, Ca 94402) W. C. Walkey, J. Combs

Two core holes have been completed on the flanks of Newberry Volcano, Orgeon. Core hole GEO N-1 has a heat flow of 180 mWm-2 reflecting subsurface temperature sufficient for commerical exploitation of geothermally generated electricity. GEO N-3, which has a heat flow of 86 mWm-2, is less encouraging. Considerable emphasis has been placed on the"rain curtain" effect with the hope that a detailed discussion of this phenomenon at two distinct localities will lead to a better understanding of the physical processes in operation. Core hole GEO N-1 was cored to a depth of 1,387 m at a site located 9.3 km south of the center of the volcano. Core hole GEO N-3 was cored to a depth of 1,220 m at a site located 12.6 km north of the center of the volcano. Both core holes penetrated interbedded pyroclastic lava flows and lithic tuffs ranging in composition from basalt to rhyolite with basaltic andesite being the most common rock type. Potassium-argon age dates range up to 2 Ma. Difficult drilling conditions were encountered in both core holes at depths near the regional water table. Additionally, both core holes penetrate three distinct thermal regimes (isothermal (the rain curtain), transition, and conductive) each having its own unique features based on geophysical logs, fluid geochemistry, age dates, and rock alteration. Smectite alteration, which seems to control the results of surface geoelectrical studies, begins in the isothermal regime close to and perhaps associated with the regional water table.

on the gamma ray log (N-1, N-3) and the electrical conductivity log (N-1), (2) temperatures below surface ambient measured downhole with a maximum recording thermometer (MRT) during periodic pauses in drilling operations (N-1, N-3), and (3) drilling fluids whose chemistry does not reflect an influx of geothermal fluids (N-3). In contrast, the thermally conductive regime is characterized by (1) a high and variable response on the gamma ray log (N-1, N-3) and on the electrical conductivity log (N-1), (2) temperatures (MRT) measured downhole during pauses in drilling which are above ambient and which track in situ conditions (N-1, N-3), and (3) drilling fluids whose chemistry clearly reveals a geothermal component (N-3). The transition zone is characterized by major washouts in the caliper log (N-1, N-3), a major anomaly in the mercury content of the rocks (N-1), an extremely strong response on the gamma-ray log (N-1, N-3) and electrical conductivity log (N-1), and a major SP anomaly (N-1). Smectite alteration, which seems to control the results of surface geoelectrical studies, begins in the isothermal regime close to and perhaps associated with the regional water table.

INTRODUCTION

The Cascade Range, which consists of a series of Quaternary and late Tertiary andesitic volcanoes that extend from northern California to southern British Columbia, is a geologic province with immense potential for the generation of electricity from geothermal resources. The geothermal potential for the Cascades

Province may well be thousands if not tens of thousands of megawatts [Bloomquist, et al., 1985]. Yet to date, there are no geothermal power plants operating in the Cascades Province, and none are planned. Furthermore, except for the obvious heat sources represented by the active volcanoes, very little is known about the potential geothermal resources in the Cascades.

The geothermal literature is particularly sparse on such key parameters as the chemistry of geothermal fluids, the deep thermal structure of the geothermal systems, and the nature of reservoir host rocks in the Cascades. The Northwest Power Planning Council [1986], has not even included geothermal energy in their long-range power forecasts, stating that "Because the information regarding the character and extent of the regional geothermal resource areas used to prepare the estimates of cost and availability is very preliminary, this resource (geothermal) cannot be considered as available for the resource portfolio of this power plan."

The paucity of geothermal data in the Cascades Province and the consequent reluctance of the utility companies to plan for future geothermal development can all be traced to the single phenomenon known as the "rain curtain." This term refers to the zone of hydrologic disturbance where cool meteoric water percolates downward and spreads laterally, therefore masking the surface expression of geothermal activity. The rain curtain can severely complicate, if not render useless, the standard geophysical and geochemical techniques for locating and evaluating geothermal reservoirs. For example, hot springs are typically diluted or masked completely, temperature gradient holes may be isothermal to depths in excess of a kilometer, and surface geoelectrical studies must be designed to penetrate a kilometer or more of "noise" before geothermally useful data can be obtained. A case in point is Newberry Volcano, Oregon (Figure 1), where the rain curtain ranges in thickness from less than 300 m within the caldera [Black, et al., 1984] to about 1,000 m on the southern flank [Swanberg and Combs, 1986]. The cool meteoric zone overlies a geothermal system that is at least 265°C at a depth of 900 m [Sammel, 1981], yet supresses the surface manifestations of this system to the extent that only two small warm springs exist over the entire volcano. Various geoelectric and geoelectro-magnetic studies including magnetotellurics [D. Stanley, U.S. Geological Survey, Denver, Colo.; personal communication, 1986], Schlumberger soundings [Bisdorf, 1985], and transient geoelectromagnetic soundings [Fitterman and Neev, 1985] have shown the presence of electrically conductive zones both inside and outside the caldera, but the lack of drilling data has precluded a rigorous interpretation of these conductors [Fitterman and Neev, 1985, p. 409].

In recognition of this situation, the U.S. Department of Energy (DOE), Division of Geothermal and Hydropower Technologies (DGHT), initiated a Cascade Deep Thermal Gradient Drilling Program. The stated purpose of the program is to "support industry efforts in the Cascade Volcanic region" and the stated objectives are to "cost share with industry for the drilling of gradient holes which would penetrate the'rain curtain' and obtain deep thermal, lithologic, and structural data." In exchange for the cost sharing, the industry participant would "release [the data] to the public for the benefit of the geothermal industry and the scientific community," [Cascade Newsletter, 1986].

To date, GEO Operator Corporation (GEOOC) has cored and completed five core holes at Newberry Volcano two of which were drilled under the DOE Cascades Drilling Program. The first cost-shared core hole, GEO N-1, was completed in the fall of 1985 to a depth of 1,387 m on GEO leaseholds on the south flank of the volcano. Data and core from the upper 1,219 m are in the public domain [Cascade Newsletter, 1987]. The second cost-shared core hole, GEO N-3, was completed in the summer of 1986 to a depth of 1,220 m. Data and core from all of this core hole are in the public domain [Cascade Newsletter, 1987]. In the following sections, the basic data from these two core holes are presented with some preliminary observations which pertain to the understanding of the phenomenon of the rain curtain and its physical characteristics. We hope, the data and observations will lead to an enhanced understanding of the rain curtain; to subsequent refinements in geothermal exploration techniques for use in the Cascade Province; and finally, to an increased understanding of Cascade geothermal systems and their potential for economic exploitation.

GEOLOGY OF NEWBERRY VOLCANO

Newberry Volcano, covering roughly 1,300 km^2 in central Oregon, is one of the largest volcanoes in the conterminous United States and is one of a series of Quaternary bimodal volcanoes located to the east of the main Cascade Range trend (Figure 1). The volcano lies near the juncture of the Cascade Range with the Brothers Fault Zone, a northwest trending fracture system along which silicic volcanism and rhyolitic domes become progressively younger to the northwest [MacLeod, et al., 1975]. Considerable research has been conducted at Newberry during the past several years [Sammel, 1981; MacLeod, et al., 1981; MacLeod and Sammel, 1982; MacLeod, et al., 1982; Ciancanelli, 1983; Priest, et al., 1983, 1987], which update the earlier work of Williams [1935] and Higgins [1973]. Holes drilled within the caldera by the U.S. Geological Survey (USGS) and Sandia National Laboratories attained 265°C at 932 m [Sammel, 1981] and greater than 160°C at 424 m [Black, et al., 1984], respectively. The geothermal potential of Newberry Volcano has been estimated at 740 MWe for 30 years by the USGS [Muffler, 1979] and 1,551 MWe for 30 years by Bonneville Power Administration [Bloomquist, et al., 1985].

Page 7 is unavailable

volcano in order to determine whether there is radial symmetry of the heat source. Core hole GEO N-1 was drilled near the neck of a very young basalt flow, the Surveyors flow whose age is probably comparable to the 5,835 ± 195 years B.P. date obtained for the near surface cinders at the drill site [Swanberg and Combs, 1986]. The core hole is also located near the center of a major soil mercury anomaly [Hadden, et al., 1982].

The average heat flow from GEO N-1 is 180 mWm^{-2} based on a least squares fit to temperature-depth data over the thermally conductive regime between 1,164 and 1,219 m and twelve (12) measurements of thermal conductivity representing the same interval (Table 1). Heat flow values of this magnitude imply temperatures in excess of 200°C at depths less than 3 km. Such temperatures are sufficiently high and accessible as to imply the possible commercial exploitation of geothermal resources for the generation of electricity utilizing either the single or double flash power conversion technologies, provided of course, that suitable production zones can be encountered in deep geothermal wells.

Geophysical Logging Program

The physical condition of core hole GEO N-1 caused deviation from a traditional geophysical logging program. Specifically, the interval 378 to 549 m was known to be associated with caving and sloughing. In order to minimize the risk of loosing a logging tool and possibly the entire core hole, it was decided to forego the geophysical logs over this interval. Therefore, after drilling to total depth, the rods were pulled to a depth of about 550 m, leaving the upper 550 m of the core hole, including the incompetent section, behind pipe. The remainder of the hole was open. The hole was then conditioned and a suite of logs were run from 550 m to total depth. After this first logging run, the rods were pulled out of the hole and the geophysical logs were run from the base of the surface casing at 143 m to the top of the incompetent section 378 m. The logging program called for temperature, induction, gamma-ray, caliper, sonic, BHC acoustic fraclog, and density logs; however, the density log was terminated because the tool would not freely penetrate the section.

Depth To Water Table

The depth/elevation of the water table is an important parameter in regional hydrologic studies of geothermal systems and is also useful in interpreting the results of experiments conducted at the surface or within the core hole. Unfortunately, the water table at GEO N-1 seems to be an elusive phenomenon. None of the geophysical logs indicate an obvious perturbation that might represent the water table. It is possible that the water table lies in the interval 378 to 550 m which never was logged. The driller routinely estimates and records the standing water level in the core hole and almost all such estimates fall within the unlogged interval, the most common estimate being about 490 m. This unlogged interval also represents the approximate depth at which smectite and other alteration products first occur within the subsurface section [Bargar and Keith, 1986]. These observations, coupled with the instability of the core hole (caving-sloughing), suggest a geologically plausible cause and effect relationship: i.e., geothermal fluids rising from depth spreading laterally near the water table and promoting hydrothermal alteration, which generally weakens the rocks. The closeness of the water table to physically incompetent rocks is noteworthy because it may allow difficult drilling conditions to be predicted, thus reducing the risks (drilling problems such as stuck rods and twist off) and costs.

The Temperature Log

The equilibrium temperature log is shown in Figure 3 and was taken ten (10) months after drilling. The data from all temperature logs over the interval 450 to 1,219 m are illustrated in Figure 4. At least three (3) distinct thermal regimes can easily be recognized on the logs (see Figure 3 or 4). The temperature log is isothermal at mean air temperature (6°C) down at least to the water table at about 490 m and probably beyond. The interval 1,158 m to TD is a thermally conductive regime. Between the isothermal and conductive regimes lies a third interval over which the temperatures increase very rapidly with depth (see Figures 3 and 4).

The nature and extent of the uppermost isothermal section (the rain curtain) has been the subject of debate among several workers who have examined the temperature logs. There is no doubt that the rain curtain extends at least to the water table (about 490 m), but there is a question as to whether the isothermal temperatures measured for several hundred meters below the water table indicate a rain curtain, or merely water percolating downward in the annulus between the completion tubing and the walls of the core hole.

One scenario has the rain curtain extending to an approximate depth of 1,005 m., at which point the downward percolating groundwater exits the volcano along the highly permeable horizons depicted on the geophysical well logs (Figure 5). In this first model, the rain curtain is located in a suite of volcanics whose geological character (including porosity and permeability) is distinct from the suite of rocks lying below. This model is favored by the fact that the volcanic section does in fact change character at depths near the bottom of the isothermal section (Figure 5), and also by the fact that temperatures measured during pauses in drilling operations were never above ambient until depths of 500 meters below the water table.

A second scenario [Blackwell and Steele, 1987] has the rain curtain extending to a depth of 350 to 400 m, while the remaining isothermal interval is a consequence of intra-hole fluid flow. In this second model, the rain curtain would coincide with the region above the water table. This model is favored by its simplicity and by the observation that an extrapolation upwards of the deep temperatures intersect mean air temperature at a depth which is not incompatible with the water table.

A third (preferred) hybrid possibility would accommodate limited groundwater flow within the annulus over the interval 1,005 to 1,158 m. The first or third model is favored on the assumption that the temperatures measured during drilling are diagnostic, if not highly accurate, thus precluding the second model, which associates the rain curtain with the water table. Also, the first and third models are more compatible with the fluid geochemistry data from GEO N-3 which are discussed below.

The Mercury Log

Core hole GEO N-1 was sited on one of the major soil mercury anomalies of Hadden, et al. [1982], as was the USGS core hole NB-2, which was located near the center of the volcano, and which encountered temperatures of 265°C at 932 meters [Sammel, 1981]. Because soil mercury surveys are routinely used as a surface manifestation of sub-surface geothermal conditions, it was decided to attempt a detailed mercury survey of the rocks penetrated by core hole GEO N-1 in the hopes of learning more about the migration of mercury from a geothermal reservoir to the surface. The sampling procedure was to randomly select several core fragments from each 3-m interval, pulverize and sieve the aggregate to the same mesh as typically used in soil mercury surveys, and analyze the resulting powdered core sample for mercury content. The results of the survey are shown in Figures 5 and 6. The upper part of the core hole failed to yield detectable levels of mercury so the sampling technique was modified to emphasize altered zones and fractures. This technique also failed to yield detectable mercury. However, once the hydrologically disturbed zone between 945 and 1,000 m was entered, a major mercury anomaly was encountered. This anomaly has been verified by resampling and laboratory analysis by an independent laboratory. The mercury anomaly is shown in Figure 5 in relation to other core hole data sets and the correlation among the mercury anomaly, the rapid temperature buildup, and the "washouts" in the caliper log are quite obvious. Clearly, geothermal fluids relatively enriched in mercury are migrating through this interval. But, the relationship between this mercury anomaly within the core hole and soil mercury anomaly at the surface remains unclear. None of the other fracture or rubble zones in the core hole are enriched in mercury, and the low background levels of mercury throughout the core hole would seem to preclude the volcanic pile itself as the source of the soil mercury anomaly. These data are consistent with the standard concept that soil mercury anomalies result from clay entrapment of mercury ascending along fractures from depth. However, it is not possible to prove that the mercury anomaly at depth is the origin of the soil mercury anomaly observed at the surface.

Geophysical Logs: Electrical Conductivity

A generalized electrical conductivity log derived from the induction log for core hole GEO N-1 is shown in Figure 5. It was prepared by averaging the log over 30-meter intervals and plotting the resulting average at the midpoint of the 30-meter section. Thus, any anomalous point in this log may be reflecting changes up to 15 meters on either side of the depth at which the point is plotted. The logic behind this type of presentation is the expectation that gross changes in the electrical properties of the volcanic pile might be detected from the ground surface using traditional geoelectric or geoelectromagnetic surveys. Examination of the generalized electrical conductivity log (Figure 5) shows the volcanic pile to be of generally constant conductivity down to a depth of 945 m. This interval of uniform conductivity coincides very well with the rain curtain as defined by the five temperature data sets (Figure 4). The conductivity log shows no obvious perturbations at the water table (490 m), at the onset of smectite alteration (Figure 5, Column 2), or at the depths at which smectite alteration becomes ubiquitous (Figure 5, Column 2). Below 945 m, the volcanic pile becomes significantly more conductive and more variable in its electrical conductivity. The increased electrical conductivity may result as a direct consequence of higher temperature or from the effects of increasing rock alteration (Figure 5). In either case, the increased conductivity represents a marked change in the physical properties of the volcanic pile which is related to geothermal activity and which at least in theory, should be detectable from the surface. Fitterman and Neev [1985] have published the results of a one-dimensional geoelectrical model based on a transient geoelectromagnetic sounding (TS) located at the GEO N-1 site. This model is reproduced in Figure 5, Column 1 as "TS Resist Section Ω -M." Unfortunately, the model appears to reflect smectite alteration and not the geothermal system. A similar conclusion has been published by Wright and Nelson [1986], also based on analyses of data from core hole GEO N-1.

Geophysical Logs: Gamma Ray

A generalized gamma ray log for core hole GEO N-1 is presented in Figure 5. It was prepared in a manner analogous to the electrical conductivity log, i.e., averaged over 30-meter sections and plotted at the midpoint. The generalized gamma ray log is fairly uniform from the surface to a depth of 945 m, below which the rocks become significantly more potassic (see stratigraphic column, Figure 6).

It is interesting to note that the gamma ray and electrical conductivity logs are inversely correlated throughout the nonisothermal section of the core hole (i.e., below 945 m), but not in the isothermal section (i.e., 0-945 m). A thermal origin for this inverse correlation is suggested and probably reflects the manner in which laterally migrating geothermal fluids promote rock alteration. Apparently, the more mafic glass-rich basalts are more prone to undergo alteration to highly conductive clay minerals such as smectite than are the more potassic rocks which show the strong gamma ray signature (from K^{40}). The lack of the inverse correlation throughout the isothermal section would, therefore, reflect a lack of migrating geothermal fluids (see Figures 3, 4), a general lack of felsic volcanics (see Figure 6), or a combination of both.

Geophysical Logs: Caliper

The core hole diameter over the interval 550 to 1,045 m as depicted by the caliper log is presented in Figure 5. The three lower washouts and their association with the rapid temperature increase and other anomalous features of the core hole have already been discussed. The four washouts further up the core hole do not appear to reflect migration of geothermal fluid (i.e., they are in the rain curtain).

Geophysical Logs: SP

The SP log (Figure 5) undergoes a drop of 70 mV over the interval from about 1,000 to 1,020 m. This feature probably reflects fluid movement, and is the only such feature on the SP log.

Rock Alteration

Bargar and Keith [1986] have studied the alteration mineralogy of core hole GEO N-1. A generalized depiction of smectite alteration, taken directly from Bargar and Keith [1986], is shown in Figure 5. The relationships among alteration mineralogy, the electrical conductivity log, and surface geoelectromagnetic studies are discussed elsewhere in this report.

Potassium Argon (K-Ar) Age Dates

K-Ar age dates representing surface samples collected from around Newberry volcano are presented in Figure 2 and typically are less than 2 Ma although ages as old as 5 to 7 Ma are reported for the outer flanks of the volcano. Age dates representing samples taken from core hole GEO N-1 increase systematically with increasing depth from values of 27,000 and 29,000 years B.P. at 481 and 491 meters, respectively, to 1.63 Ma at 1,081 meters (Figure 7, Table 2). In addition, in an earlier report, Swanberg and Combs [1987], reported the results of a single C^{14} age date based upon charcoal discovered while digging the mud sumps. This date of 5835 ± 195 years B.P. establishes the age of the basaltic cinders at the surface near the core hole.

Whenever age dates are determined in a geothermal environment, the possibility always exists of nonrepresentative ages due to argon diffusion and subsequent resetting of the K-Ar clock. Perhaps the best testament to the reliability of the age dates presented in Table 2 and Figure 7 is the fact that they are geologically reasonable. The dates are generally compatible with those determined from surface samples throughout the volcano. The dates increase systematically with depth throughout the core hole and there is no radical departure from this trend upon encountering the zone of ubiquitous smectite alteration near 700 meters (Figure 5) or encountering the zone of rapid temperature buildup near 1,000 meters.

Chemistry of Formation Fluids

During drilling operations, fluid samples were episodically selected for chemical analysis. Although such samples would be severely contaminated with drilling mud, it was felt that various geothermal constituents might be detectable above the background and if so, would serve to indicate any environmental problems that might be encountered during eventual production. The results of silica analyses as a function of depth are presented in Figure 8. Representative samples of the drilling fluid are also shown. Analyses of other chemical constituents are even less revealing than silica and are not reported here.

The Rain Curtain as a Lithologic Discontinuity

The coincidence that the generalized gamma ray and electrical conductivity logs both change character at a depth (945 m, Figure 5) which is compatible with the rain curtain as defined by the five temperature data sets (Figure 4) suggests the possibility that the rain curtain may represent a lithologic discontinuity. An intriguing (but speculative) extension of this logic is to associate such a discontinuity with the transition between pre- and post-Newberry strata. The pre-Newberry strata are generally more felsic than the Newberry pile [Ciancanelli personal communication, 1987], so that the pre/post Newberry transition might well produce a generalized gamma ray signature similar to that shown in Figure 5. MacLeod and Sherrod [this issue] confine the Newberry section to those normally polarized strata younger than 0.73 Ma. The K-Ar age dates shown in Figure 7 are compatible with a pre/post Newberry transition at 945 m. In fact, using selective license with the error bars on the K-Ar age dates (Table 2), indicates that all age dates shallower than 945 m are 0.737 Ma or less, while all age dates deeper than 945 m are older than 0.73 Ma. At present, however, the data do not totally support the postulation of a depth or even the existance of a pre/post Newberry discontinuity. Any K-Ar age date for extremely young, potassium poor rocks located in a geothermal regime are subject to question and although the age dates presented in Table 2 and Figure 7 are considered reliable, this issue should be tabled until the paleomagnetic studies have been completed and the K-Ar age dates have been verified.

CORE HOLE N-3

Core hole GEO N-3 was drilled at a surface elevation of 1,753 m on the north flank of the volcano at a distance of 12.6 km from the center of the volcano (see Figure 2). Of all of the Newberry core holes, GEO N-3 is the most distant from the center of the volcano. Heat flow from GEO N-3 is 86 mWm^{-2} based on a least squares fit to the temperature-depth data over the thermally conductive region between 1,170 and 1,220 meters and nine (9) measurements of thermal conductivity representing the same interval (Table 1). This value is typical of heat flow values found throughout the non-geothermal areas of the Cascade Range [Blackwell and Steele, 1987] and, therefore, does not indicate the presence of an exploitable geothermal resource. This core hole, located 12.6 km from the center of the volcano, apparently constrains the radial extent of the major geothermal system associated with the core of Newberry Volcano. If geothermal resources are to be located at such large distances from the center of the volcano, they must be associated with heat sources which are separate from the main volcanic heat source.

Geophysical Logging Program

As in core hole GEO N-1, the integrity of core hole GEO N-3 forced modifications to the geophysical logging program. Specifically, at a depth of about 520 m the rods became stuck in the core hole and were cemented in place, causing a reduction in hole size. To compound the problem, the induction tools and gamma-ray tools, required to penetrate the smaller diameter hole all failed. The gamma-ray log was recovered from the surface to total depth, since this log could be run through the completion tubing, but the induction log was lost. The temperature log and the neutron density log were also run from surface to total depth but the caliper log and BHC acoustic fraclog could only be run from 520 m to total depth. The casing schematic for core hole, GEO N-3 is shown in Figure 9.

Depth To Water Table

The depth to the regional water table is just as elusive as in GEO N-1. The standing water level in the core hole as estimated by the drillers ranges from about 455 to 565 m with a modal value of 525 m. Thus, the water table may well lie close to, and perhaps exactly at, the depth at which the drilling problems were encountered which forced the cementing of the rods in place. Therefore, the failure of the geophysical logs to clearly reveal the water table may well result from the complicating effects of the metal rods and the cement.

The Temperature Log

The final temperature log for core hole GEO N-3 is shown in Figure 10 and compared with other data sets in Figure 9. A composite of all temperature logs measured in this core hole is presented in Figure 11. At first glance, the final temperature log appears to differ significantly from the corresponding log for core hole GEO N-1 (Figure 3). Closer examination, however, reveals that the two logs contain the same basic elements. Specifically, like GEO N-1, core hole GEO N-3 is isothermal to the water table and probably beyond, it has a thermally conductive zone near the bottom, and the isothermal and conductive zones are separated by a transition region exhibiting considerable hydrologic disturbance.

The interval between the upper isothermal and lower conductive sections of core hole GEO N-3 is a complicated region because it represents two separate and overlapping patterns of groundwater circulation, one of which was induced by drilling operations. Several obvious features of the temperature log are the rapid buildup of temperature at about 580 to 610 m, the smaller temperature buildup at about 1,160 m, and the interval between them which is very nearly isothermal at 52°C. These observations are the result of artesian water ascending the annulus of the core hole. Geothermal fluids under artesian pressure appear to enter the core hole at a depth of about 1,160 m. This same depth is charactered by a significant washout as observed on the caliper log (Figure 9) and also by a thermal pulse as detected by the maximum recording thermometers (MRTs) which were run into the core hole during pauses in the drilling operations (Figure 11). The geothermal fluids appear to exit the core hole annulus at a depth of about 575 to 585 m. This zone is a major washout area as shown by the caliper log (Figure 9). It is significant that the ascending geothermal fluids seem to ignore the numerous washouts throughout the core hole interval 610 to 1,100 m (Figure 9) and choose instead to exit the core hole annulus at a washout located at or near the regional water table estimated at about 455 to 564 m. If a man-induced vertical conduit such as a core hole will cause artesian fluids to rise and spread laterally near the water table, it might be expected that a natural conduit such as a vertical fracture might also cause the same phenomenon. If so, geothermal fluids migrating laterally near the water table are likely to promote hydrothermal alteration, reduce the mechanical strength of the rocks, and help explain why there seem to be difficult drilling conditions coincident with the water table.

The remaining unexplained feature of the GEO N-3 temperature log is the nature of the thermal regime which existed before the artesian breakthrough. The germane data are the temperatures taken during drilling by maximum recording thermometers (MRTs, Figures 9 and 11). As was the case for GEO N-1, these temperatures showed no tendency to increase near the water table and in fact, readings did not exceed ambient temperatures until a depth of about 935 m. On this basis, it is suggested that the rain curtain extends to an approximate depth of 915 to 975 m at which point the section becomes significantly more potassic as indicated by the gamma ray and lithologic logs (Figures 9 and 12). Having the rain curtain extend to a signficant depth below the water table is supported by the close association between washouts as depicted by the caliper log and small temperature anomalies measured by the MRTs during drilling operations. Careful inspection of Figure 9 shows that below 915 m, the MRT readings taken at or near the washouts are slightly but consistently elevated relative to the remaining MRT values: as if thermal fluids were moving through these horizons. Above 915 m no such correlation exists. If the washouts above 915 m represent horizons which permit lateral flow of groundwater, it is not thermal fluid that is migrating through these horzions but rather cold, descending groundwater, i.e., the rain curtain. As a final comment for those researchers who prefer to associate the rain curtain with the region above the water table, it can be noted that an upward extrapolation of temperature from the thermally conductive region, intersects the mean annual air temperature at a depth which is not incompatible with the water table.

Ages Dates

The seven K-Ar age dates from core hole GEO N-3, range from 0.1 to 1.5 Ma and are presented in Figure 13 and Table 2. These dates are similar to those measured in core hole GEO N-1 (Figure 7) and throughout the volcano (Figure 2). There is also a tendency for the age dates to increase with depth although the date of 1.5 Ma at 324 m is contrary to this trend.

Chemistry of Formation Fluids

During the drilling operations for core hole GEO N-3, fluid samples were systematically collected from the core hole for routine chemical analyses. As was the case for GEO N-1, these samples were not collected to provide reliable geochemical data of formation fluids, but rather to try to detect the presence of geothermal fluids and any associated chemical species that may require special treatment during eventual production. The results of silica concentration, a typical indicator of geothermal fluid, is shown as a function of depth in Figure 14. As shown in Figure 14, the bottom four (4) samples, which were collected from depths below 1,050 m, are greatly enriched in silica relative to samples taken at other depths and this enrichment reflects the strong presence of geothermal fluids near the bottom of the core hole. Vertical zonation of the silica content of fluids sampled from GEO N-3 is an interesting feature of the core hole that may relate directly to the depth of the rain curtain. To examine the phenomenon further, a composite of all anomalous chemical constituents was prepared and their distribution with depth was plotted in histogram form (Figure 15). Also shown in Figure 15 is a histogram of sample depth and a comparison of the two histograms should reveal the depths at which the anomalous chemical constituents are located. As can be seen in Figure 15, the anomalous constituents are found primarily below the arbitrary depth of 915 m and reflect the presence of geothermal fluids below this depth. Above 915 m, nearly all samples collected are depleated in almost every chemical constituent analyzed and these samples are thought to represent the cold descending groundwater of the rain curtain. A comparison of the data in Figure 15 with that in Figures 9 and 11 shows the anticipated result that the depths at which the chemically anomalous (geothermal) fluids were sampled are precisely the same depths at which the highest temperatures were recorded during drilling operations. This almost trivial observation would probably not be worth reporting were it not for the important role played by the rain curtain in the exploration for and evaluation of geothermal resources.

SUMMARY

In the preceding sections, the data and some observations for two core holes on the flanks of Newberry Volcano, Oregon have been presented. Particular emphasis has been placed on the rain curtain with the purpose that a detailed discussion of this phenomenon at two discrete localities will lead to a better understanding of the physical processes in operation. It is further expected that the data will spark scientific debate and additional research on the rain curtain phenomenon, with emphasis directed towards surface geophysical techniques that can "see through" the rain curtain and provide valuable exploration information on the underlying geothermal reservoirs. Unfortunately, most geoelectric and geoelectromagnetic surveys to date have been strongly affected by smectite alteration which prevails at depths that are shallower than the geothermal reservoir (Figure 5; see also Fitterman and Neev, 1985; Wright and Neilson, 1986) Wright and Neilson [1986] have noted that "delineation of the high temperature (geothermal) system by electrical surveys may be difficult or impossible because of effects from altered rocks." While the problem is formidable, sufficient documentation has been provided that the rain curtain and the underlying geothermal systems are sufficiently different in their physical characteristics to justify continued search for a surface geophysical technique or a combination of techniques which will detect and provide information on geothermal systems, in spite of the complicating effects of the rain curtain and the smectite alteration. The goal is certainly worthwhile, since mile-deep core holes are rather expensive for reconnaissance exploration.

ACKNOWLEDGEMENTS

We thank the management of Geothermal Resources International, Inc. (GEO), and its wholly owned subsidiary, GEO Operator Corporation (GEOOC), for financial support of, and permission to publish, this work. We also thank Bruce Sibbett (University of Utah Research Institute) for his outstanding job as technical liaison between GEOOC and the U.S. DOE, M. Johnson, W. J. Dansart, M. C. Hagood and M. Woodruff (GEOOC), for providing the core descriptions, and acknowledge the professional services of Tonto Drilling Services, Vancouver, Canada (drilling), Dresser-Atlas, Houston, Tex. (geophysical logging), and Geotech Data, Poway, Calif. (temperature logging and thermal conductivity measurements). The figures were prepared by M. Maloney and the manuscript typed by Y. Stallings and S. Ballin of GEO. S. Prestwich and R. King acted as DOE technical and administrative monitors, respectively. The project was funded by U.S. DOE cooperative agreements DE-FC07-85ID12612 and DE-FC07-85ID12613 (49%) and GEO corporate funds (51%).

REFERENCES

Bacon, C. R., Eruptive history of Mount Mazama and Crater Lake Caldera, Cascade Range, U.S.A., J. Volcanol. Geotherm. Res., 18, 57, 1983.

Bargar, K. E., and T. E.C. Keith, Hydrothermal mineralization in GEO N-1 drill hole, Newberry volcano, Oregon, U.S. Geol. Surv., Open File Rpt., 86-440, 12 pp., 1986.

Bisdorf, R. J., Schlumberger sounding results over the Newberry Volcano area, Oregon, Geotherm. Resour. Council Trans., 9, 389, 1985.

Black, G. L., G. R. Priest, and N. M. Woller, Temperature data and drilling history of the Sandia National Laboratories well at Newberry Caldera, Oreg. Geol., 46, 7, 1984.

Blackwell, D. D., and J. L. Steele, Geothermal data from deep holes in the Oregon Cascade Range, Geotherm. Resour. Council Trans, in press, 1987.

Bloomquist, R. G., G. L. Black, D. S. Parker, A. Sifford, S. J. Simpson, and L. V. Street, Evaluation and ranking of geothermal resources for electrical generation or electrical offset in Idaho, Montana, Oregon, and Washington, Rep. DOE/BP-13609-1, 504 pp., U.S. Department of Energy, Washington, D.C., 1985.

Cascade Newsletter, No. 2, Earth Sci. Lab./Univ. Utah Res. Inst., Salt Lake City, February 7, 1986.

Cascade Newsletter, No. 3, Earth Sci. Lab./Univ. Utah Res. Inst., Salt Lake City, February 6, 1987.

Ciancanelli, E. V., Geology of Newberry Volcano, Oregon, Geotherm. Resour. Council Trans., 7, 129, 1983.

Fiebelkorn, R. G., G. W. Walker, N. S. MacLeod, E. H. MacKee, and J. G. Smith, Index to K-Ar age determinations for the State of Oregon, U.S. Geol. Survey, Open File Rpt., 82-546, 39 pp., 1982.

Fitterman, D. V., and D. K. Neev, Transient sounding investigation of Newberry Volcano, Oregon, Geotherm. Resour. Council Trans., 9, 407, 1985.

Friedman, I., Hydration dating of volcanism at Newberry Crater, Oregon, J. Res. U.S. Geol. Surv., 5, 337, 1977.

Hadden, M. M., G. R. Priest, and N. M. Woller, Preliminary soil-mercury survey of Newberry Volcano, Deschutes County, Oregon, Ore. Dept. Geol. and Min. Ind., Bonneville Power Administration Cooperative Agreement No. DE-AC79-82BP36734, 1982.

Higgins, M. W., Petrology of Newberry Volcano, central Oregon, Geol. Soc. Am. Bull., 84, 455, 1973.

MacLeod, N. S., and E. A. Sammel, Newberry Volcano, Oregon: A Cascade Range geothermal prospect, Oreg. Geol., 44, 123, 1982.

MacLeod, N. S., and D. R. Sherrod, Geologic Evidence for a Magma Chamber Beneath Newberry Volcano, Oregon, J. Geophys. Res., This issue.

MacLeod, N. S., D. R. Sherrod, L. A. Chitwood, and E. H. McKee, Newberry Volcano, Oregon, U.S. Geol. Surv. Circ., 838, 85, 1981.

MacLeod, N. S., D. R. Sherrod, and L. A. Chitwood, Geologic map of Newberry Volcano, Deschutes, Klamath, and Lake Counties, Oregon, U.S. Geol. Surv. Open File Rep., 82-847, 1982.

MacLeod, N. S., G. W. Walker, and E. H. McKee, Geothermal significance of eastward increase in age of upper Cenozoic rhyolite domes in southeastern Oregon, in Second United Nations Symposium on the Development and Uses of Geothermal Resources, 1, 465, 1975.

Muffler, L. J. P. (Ed.), Assessment of geothermal resources of the United States--1978, U.S. Geol. Surv. Circ. 790, 163 pp., 1979.

Northwest Power Planning Council, Northwest Conservation and Electric Power Plan, vol. 2, 271 pp., Portland, Oreg., 1986.

Pierson, F. J., Jr., E. M. Davis, and M. A. Tanners, University of Texas radiocarbon dates 4, Radiocarbon, 8, 453, 1966.

Priest, G. R., B. F. Vogt, and G. L. Black, Survey of potential geothermal exploration sites at Newberry Volcano, Deschutes County, Oregon, Open File Rep., 0-83-3, 174 pp., Oreg. Dept. of Geol. and Min. Ind., Portland, 1983.

Priest, G. R., N. M. Woller, and D. D. Blackwell, Geothermal exploration in Oregon, 1986, Oregon Geol., 49, 67, 1987.

Sammel, E. A., Results of test drilling at Newberry Volcano, Oregon, Geotherm. Resour. Council Bull., 10(11), 7, 1981.

Swanberg, C. A., and J. Combs, Geothermal drilling in the Cascade Range: Preliminary results from a 1387-m core hole, Newberry Volcano, Oregon, EOS, 67, 578, 1986.

Williams, H., Newberry volcano of central Oregon, Geol. Soc. Am. Bull., 46, 253, 1935.

Wright, P. M., and D. L. Neilson, Electrical resistivity anomalies at Newberry Volcano, Oregon; comparison with alteration mineralogy in GEO core hole N-1, Geotherm. Resour. Council Trans., 10, 247, 1986.

TABLE 1

HEAT FLOW - NEWBERRY VOLCANO, OREGON

Depth Range (meters)	Gradient ($^{o}C/km$)	Thermal Conductivity ($Wm^{-1}K^{-1}$)	Number of Samples	Heat Flow (mWm^{-2})
		GEO N-1		
1,164 - 1,177	122.7	1.76 ± 0.40	5	216
1,180 - 1,192	86.7	2.01	1	174
1,195 - 1,219	74.9	2.00 ± 0.08	6	150
			AVERAGE =	180
		GEO N-3		
1,172 - 1,220	54.3	1.59 ± 0.14	9	86

TABLE 2

K-Ar AGE DATES - NEWBERRY VOLCANO, OREGON

feet	Depth (meters)	Age (Ma)	Description
		GEO N-1	
1213	370	0.306 ± 0.075	Basaltic andesite
1578	481	0.027 ± 0.009	Basaltic andesite
1610	491	0.029 ± 0.081	Basaltic andesite
2299	701	0.090 ± 0.026	Basaltic intrusive
2375	724	0.847 ± 0.110	Basaltic andesite
2926	892	0.768 ± 0.147	Basalt
2995	913	0.746 ± 0.110	Basalt _
3238	987	0.943 ± 0.053	Andesite
3261	994	0.997 ± 0.050	Andesite
3546	1,081	1.630 ± 0.13	Basaltic andesite
		GEO N-3	
1062	324	1.50 + 0.63	Phyric basalt
	594	0.911 + 0.188	Phyric basaltic andesite
	769	0.109 + 0.081	Lithic tuff
	853	0.819 + 0.113	Basalt
	1,010	1.04 + 0.03	Rhyodacitic flow
	1,100	1.54 + 0.05	Rhyodacitic flow
	1,207	1.18 + 0.30	Basalt

FIGURE CAPTIONS

FIGURE 1 Index map showing the location of Newberry Volcano in relation to the Oregon Cascades (stippled area).

FIGURE 2 Potassium Argon age dates (Ma) for surface samples at Newberry Volcano, Oregon. Data from Fiebelkorn, et al. [1982] are plotted as age dates with the plot point representing the decimal point. Two GEO determinations are presented with errors indicated. The location of the Newberry Flank Federal Geothermal Unit (area between the two boundaries), The Newberry Known Geothermal Resource Area (KGRA - inside the inner boundary), and the location of the two small lakes inside the crater are also shown.

FIGURE 3 Equilibrium temperature log for GEO N-1. Original data were collected (9/25/86) by D. D. Blackwell and R. E. Spafford and were measured at 2-m intervals with a precision of 0.01°C. Data plotted at 10-m intervals.

FIGURE 4 Summary of all temperature data below 500 m for GEO N-1. Plotted points labeled "1" represent maximum recording thermometers (MRTs) which were allowed to sit on bottom for roughly 10 minutes without circulation. Logs 2 through 4 were obtained by Geotech Data and represent discrete measurements at 3-m interval with a precision of 0.01°C. Log 5 is the same as that presented in Figure 3.

FIGURE 5 Comparison of GEO N-1 logs. From left to right: (1) the one dimensional geoelectric section determined from the surface measurements of Fitterman and Neev [1985] using transient geoelectromagnetic soundings (TS), (2) smectite alteration from Bargar and Keith [1986], (3) generalized electrical conductivity (see text for discussion), (4) generalized gamma ray log (see text for discussion), (5) the location of the SP anomaly, (6) mercury log (see Figure 6 for detail), (7) location of washouts below 500 m as determined by the caliper log, (8) the bottom part of the temperature log shown in Figure 3, and (9) the core hole completion. Note the unlogged section (conductivity log) which reflects the depth interval of difficult drilling conditions and also the relationship between the zone of rapid temperature buildup and anomalies in the other geophysical logs.

FIGURE 6 Generalized litholgic log and detailed rock mercury analyses for GEO N-1. The detection thresholds for the Cascadia and Bondar-Clegg analyses are 1 and 5 ppb, respectively.

FIGURE 7 Potassium-argon age dates from GEO N-1. Note the agreement with the surface data shown in Figure 2.

FIGURE 8 Silica content of fluids recovered from GEO N-1. Surface samples depicted as open symbols while downhole samples are shaded symbols. Note that all downhole samples are contaminated with drilling fluid.

FIGURE 9 Comparison of the temperature data from GEO N-3 with the generalized gamma ray log and the washouts as depicted by the caliper log. Note: (1) the relation between the large washout in the caliper log and the intermediate drill string (drill rods cemented in place) reflecting the difficult drilling conditions, (2) the anomalous temperatures measured during drilling (triangles) and the washouts at depths below 915 m, and (3) the washouts which allow the artesian fluids to enter and exit the annulus of the core hole. The detailed temperature log is reproduced in Figure 10. Core hole completion presented on the far right.

FIGURE 10 Detailed equilibrium temperature log of GEO N-3. Measurements were taken every 6 m with a precision of 0.01°C by Geotech Data on 8/18/86. Data plotted at 10-m intervals.

FIGURE 11 Summary of all temperature data obtained below 500 m in GEO N-3. Note the highest MRT temperature reading coincides with the artesian aquifer (compare Figure 9).

FIGURE 12 Thermal conductivity from GEO N-3. Note the generalized lithologic log shows a rhyodacitic flow unit centered at 1,100 m (compare Figure 9) and that the remainder of the core hole is essentially a series of basaltic andesite flows. Data from Geotech Data.

FIGURE 13 Potassium-argon age dates from GEO N-3. Note the agreement among these dates and those from GEO N-1 (Figure 7) and the surface samples (Figure 2).

FIGURE 14 Silica content of fluids taken from GEO N-3. Note the increase in silica below 1,100 m and that all downhole samples are contaminated by drilling fluids.

FIGURE 15 Distribution of anomalous constituents of fluids taken at intervals of about 75 m from GEO N-3. Chemical species used in constructing this figure are Si, Hg, K, Al, Sr, B, and F. The highest 10% of each of the species are considered anomalous and their distribution plotted as a function of depth in histogram form. The shaded area reflects the depth distribution of sample depths. The difference between the two should qualitatively reflect drilling fluids mixing with formation fluids. Note that effects of geothermal fluids are basically lacking above 915 m (compare with Figure 9).

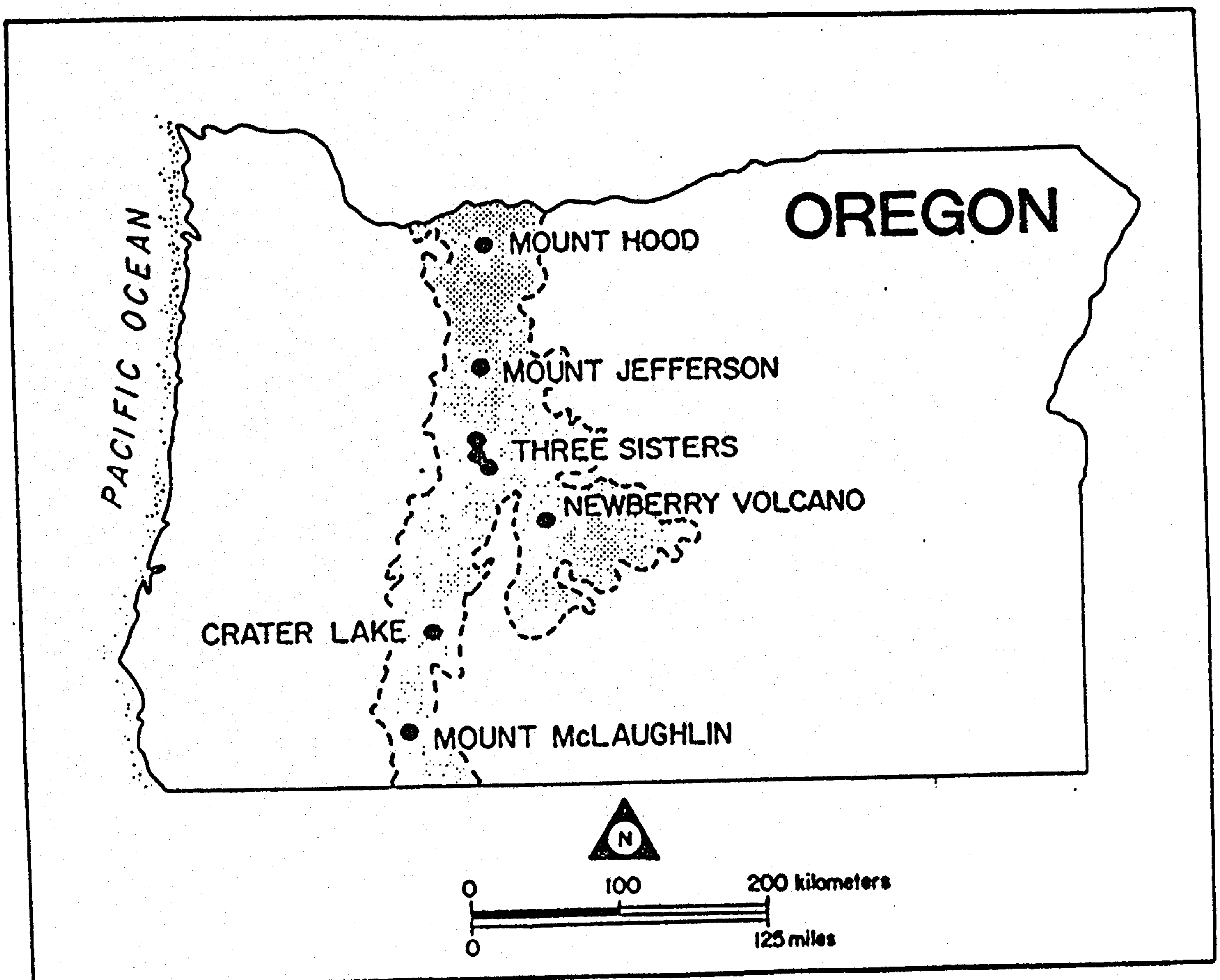

OREGON
PACIFIC OCEAN
MOUNT HOOD
MOUNT JEFFERSON
THREE SISTERS
NEWBERRY VOLCANO
CRATER LAKE
MOUNT McLAUGHLIN
N
0
100
200 kilometers
0
125 miles

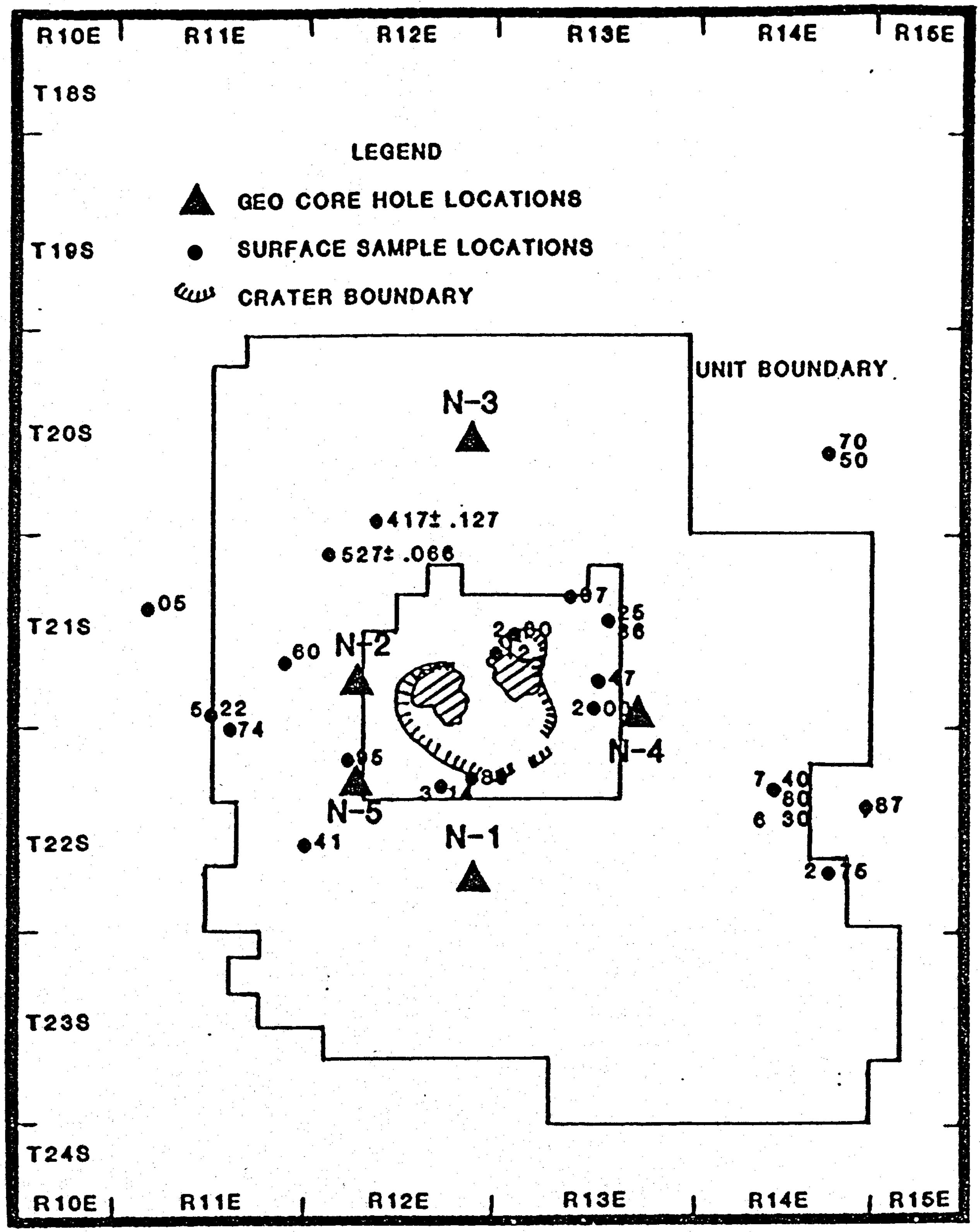
R10E
R11E
R12E
R13E
R14E
R15E
T18S
T19S
T20S
T21S
T22S
T23S
T24S
LEGEND
GEO CORE HOLE LOCATIONS
SURFACE SAMPLE LOCATIONS
CRATER BOUNDARY
UNIT BOUNDARY
N-1
N-2
N-3
N-4
N-5
.417± .127
.527± .066
70
50
05
60
22
74
41
87
47
40
80
30

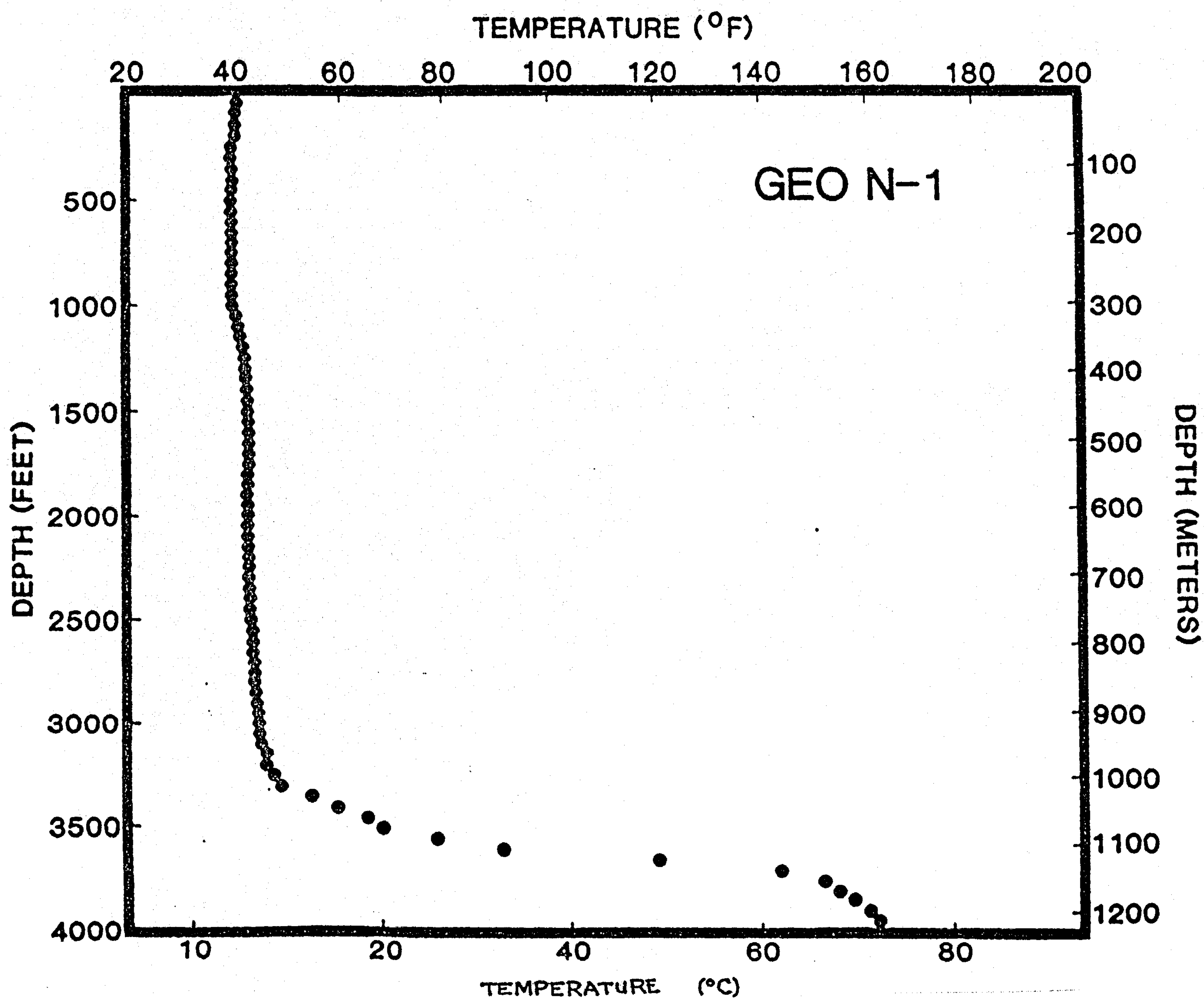
TEMPERATURE (°F)
20
40
60
80
100
120
140
160
180
200
GEO N-1
DEPTH (FEET)
500
1000
1500
2000
2500
3000
3500
4000
DEPTH (METERS)
100
200
300
400
500
600
700
800
900
1000
1100
1200
10
20
40
60
80
TEMPERATURE (°C)

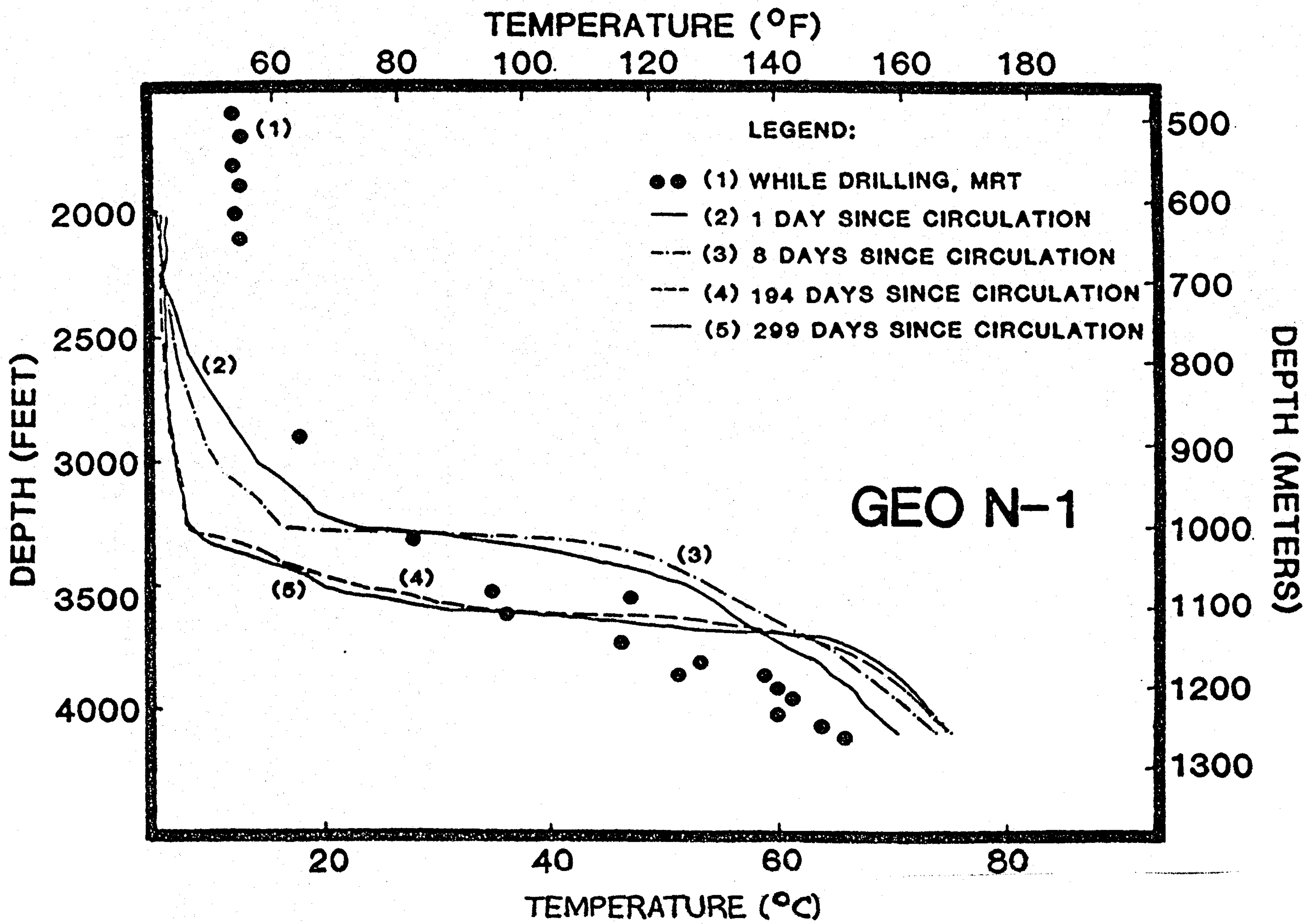

TEMPERATURE (°F)
60
80
100
120
140
160
180
LEGEND:
(1) WHILE DRILLING, MRT
(2) 1 DAY SINCE CIRCULATION
(3) 8 DAYS SINCE CIRCULATION
(4) 194 DAYS SINCE CIRCULATION
(5) 299 DAYS SINCE CIRCULATION
(1)
(2)
(3)
(4)
(5)
GEO N-1
DEPTH (FEET)
2000
2500
3000
3500
4000
DEPTH (METERS)
500
600
700
800
900
1000
1100
1200
1300
20
40
60
80
TEMPERATURE (°C)

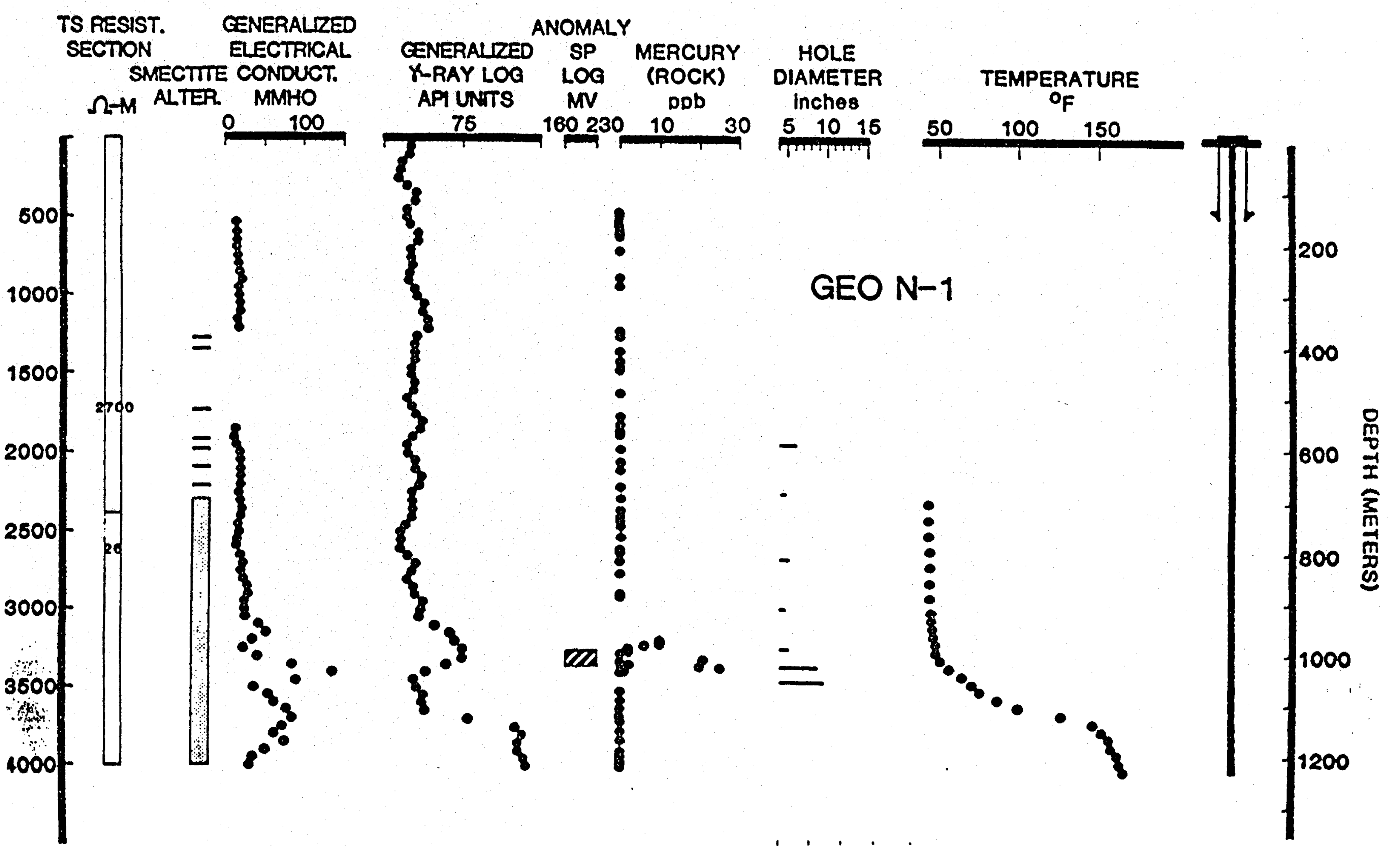
TS RESIST. SECTION
Ω-M
SMECTITE ALTER.
GENERALIZED ELECTRICAL CONDUCT. MMHO
0 100
GENERALIZED γ-RAY LOG API UNITS
75
ANOMALY SP LOG MV
160 230
MERCURY (ROCK) ppb
10 30
HOLE DIAMETER inches
5 10 15
TEMPERATURE °F
50 100 150
2700
26
500
1000
1500
2000
2500
3000
3500
4000
GEO N-1
200
400
600
800
1000
1200
DEPTH (METERS)

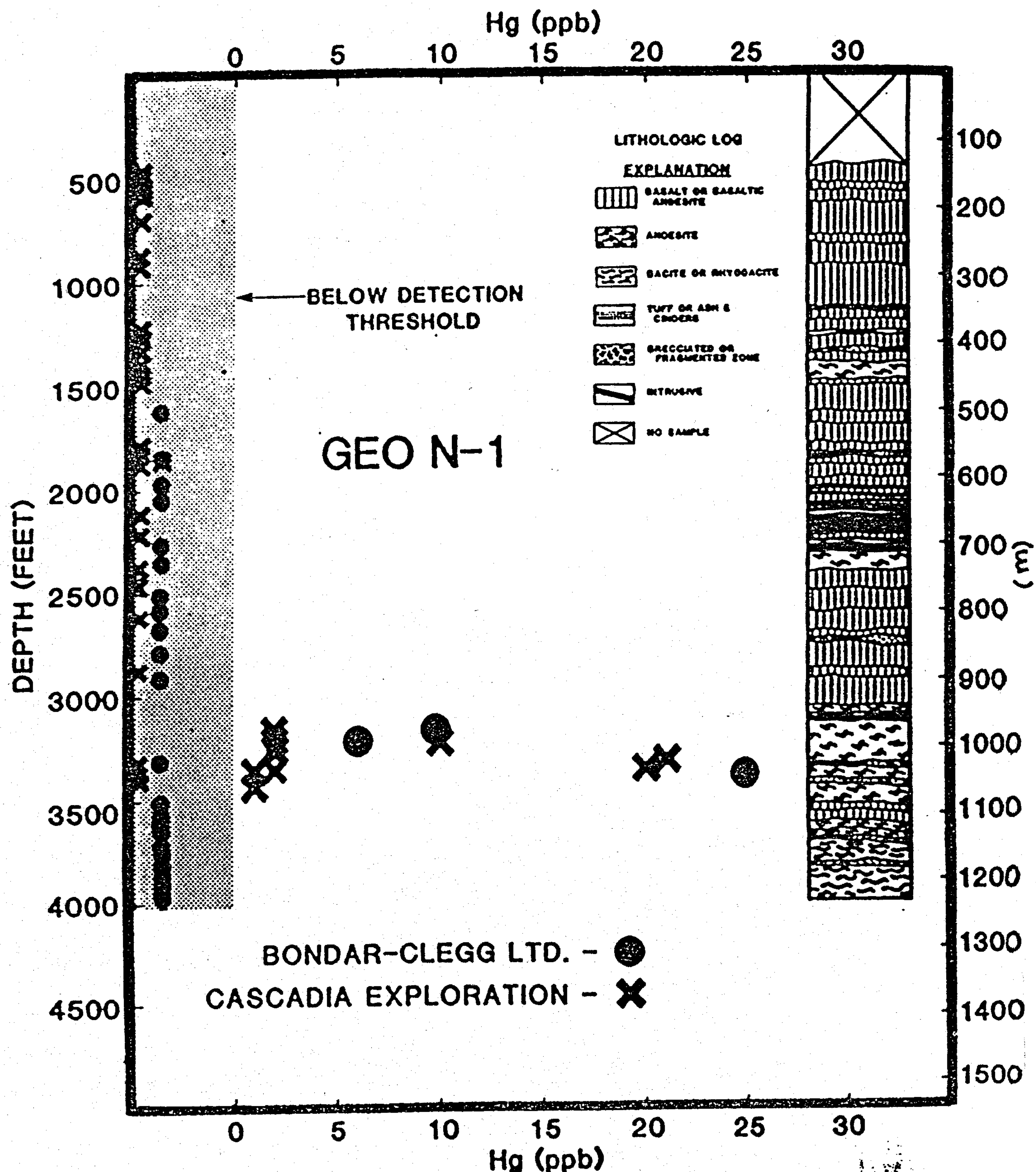
Hg (ppb)
0
5
10
15
20
25
30
LITHOLOGIC LOG
EXPLANATION
500
1000
1500
2000
2500
3000
3500
4000
4500
DEPTH (FEET)
100
200
300
400
500
600
700
800
900
1000
1100
1200
1300
1400
1500
(m)
BELOW DETECTION THRESHOLD
GEO N-1
BONDAR-CLEGG LTD. -
CASCADIA EXPLORATION -

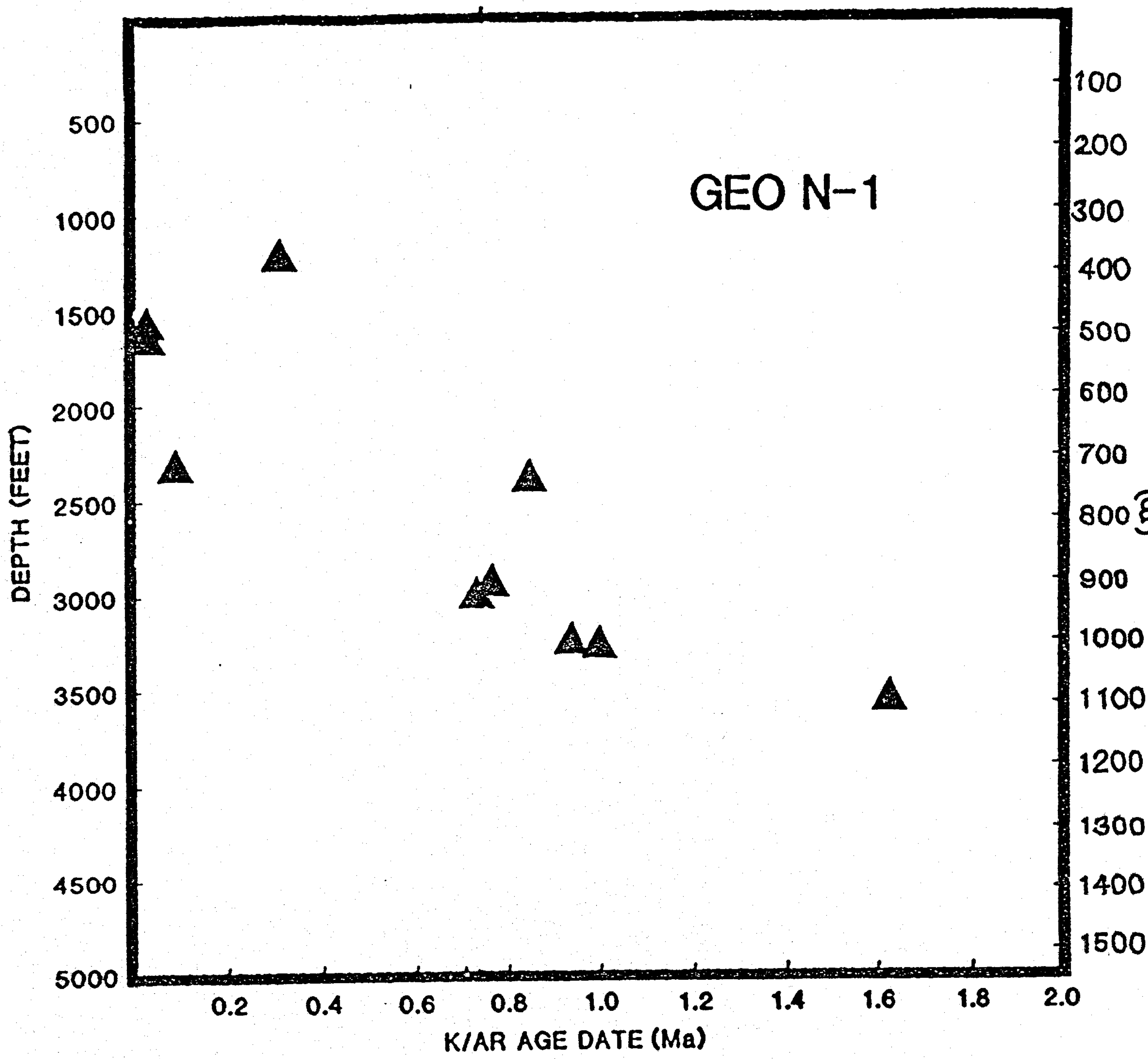

GEO N-1
DEPTH (FEET)
500
1000
1500
2000
2500
3000
3500
4000
4500
5000
100
200
300
400
500
600
700
800
900
1000
1100
1200
1300
1400
1500
(m)
0.2
0.4
0.6
0.8
1.0
1.2
1.4
1.6
1.8
2.0
K/AR AGE DATE (Ma)

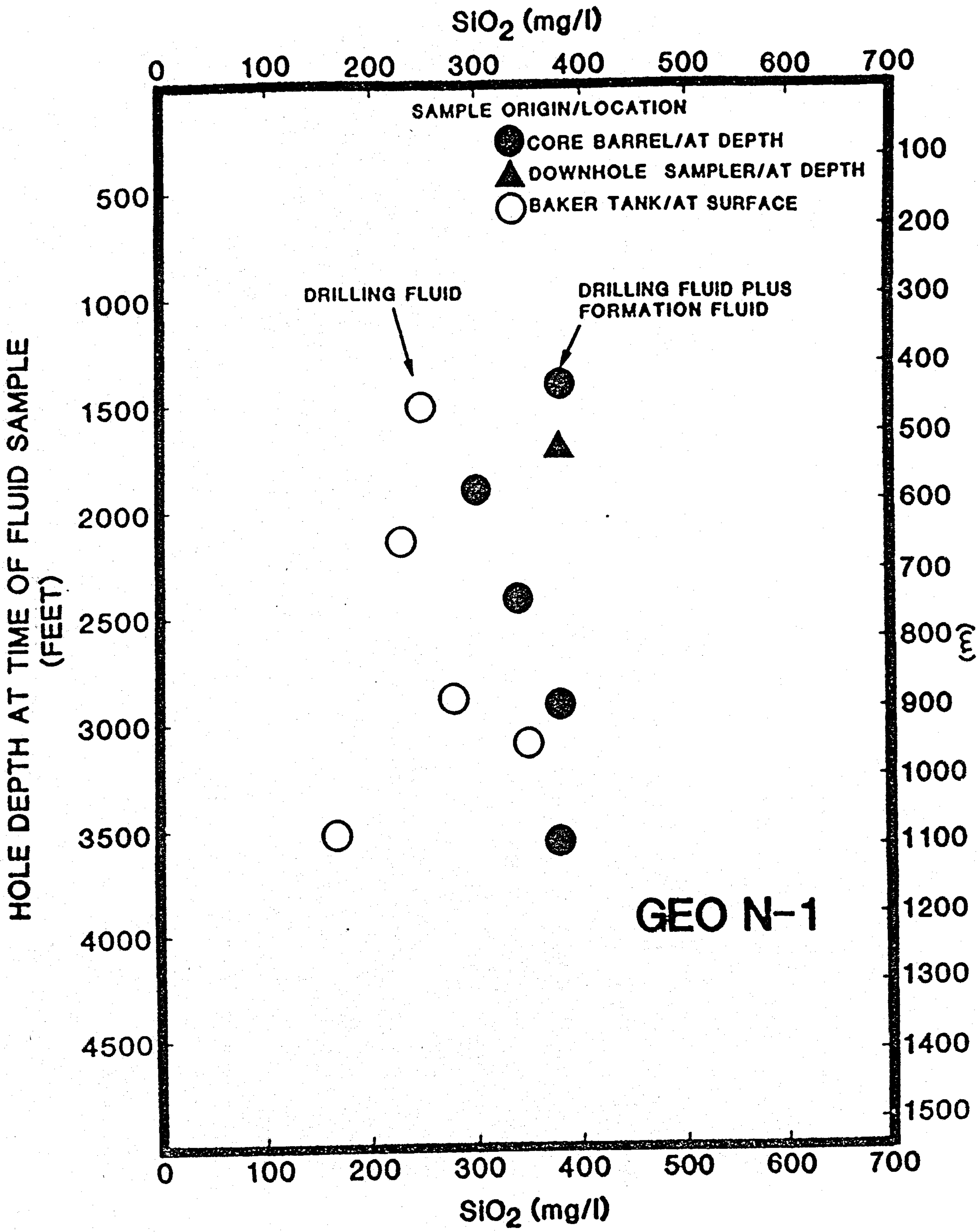

SiO2 (mg/l)
0
100
200
300
400
500
600
700
SAMPLE ORIGIN/LOCATION
CORE BARREL/AT DEPTH
DOWNHOLE SAMPLER/AT DEPTH
BAKER TANK/AT SURFACE
DRILLING FLUID
DRILLING FLUID PLUS FORMATION FLUID
HOLE DEPTH AT TIME OF FLUID SAMPLE (FEET)
500
1000
1500
2000
2500
3000
3500
4000
4500
(m)
100
200
300
400
500
600
700
800
900
1000
1100
1200
1300
1400
1500
GEO N-1

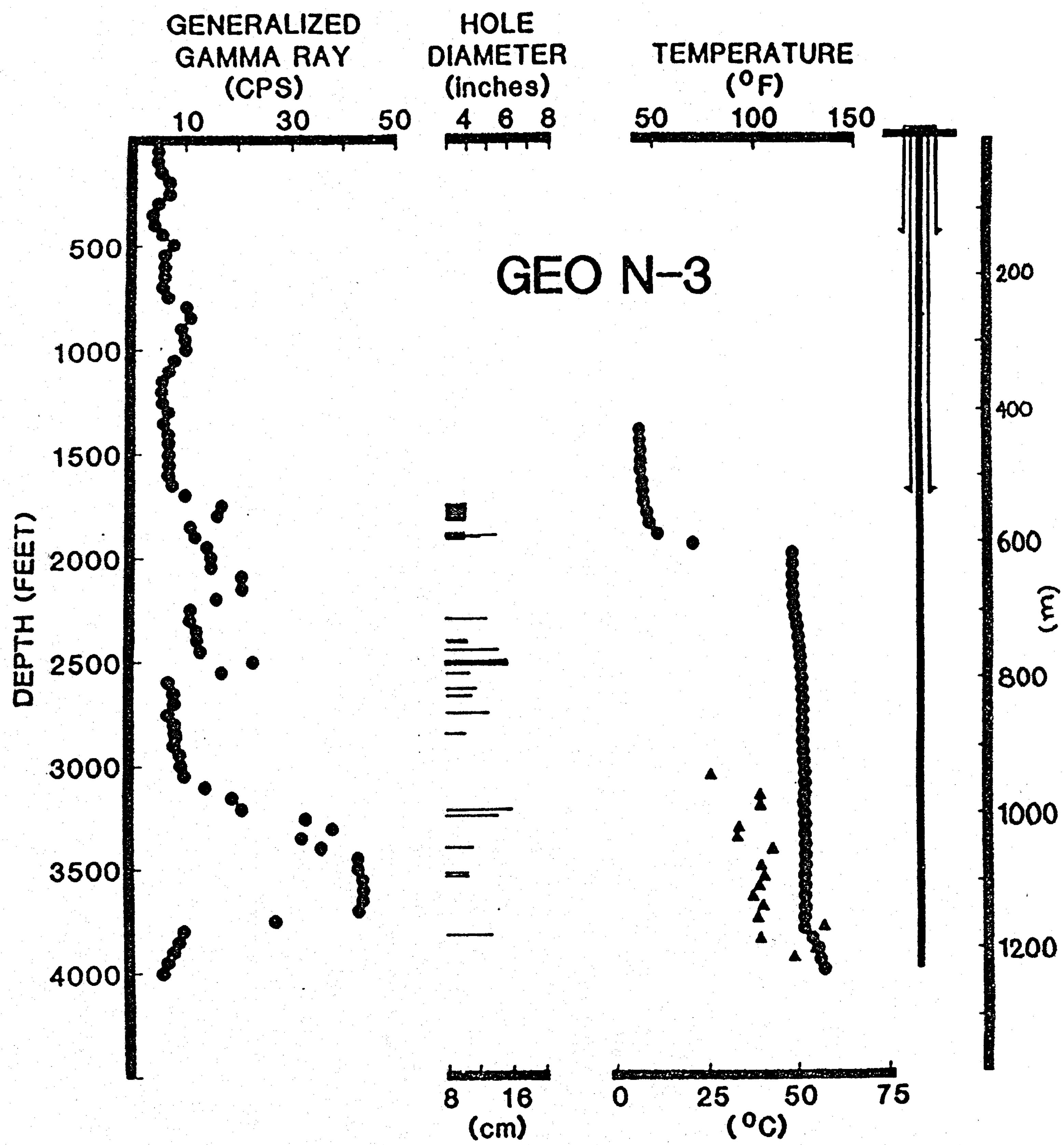
GENERALIZED
GAMMA RAY
(CPS)
10 30 50
HOLE
DIAMETER
(inches)
4 6 8
TEMPERATURE
(°F)
50 100 150
GEO N-3
DEPTH (FEET)
500
1000
1500
2000
2500
3000
3500
4000
8 16
(cm)
0 25 50 75
(°C)
(m)
200
400
600
800
1000
1200

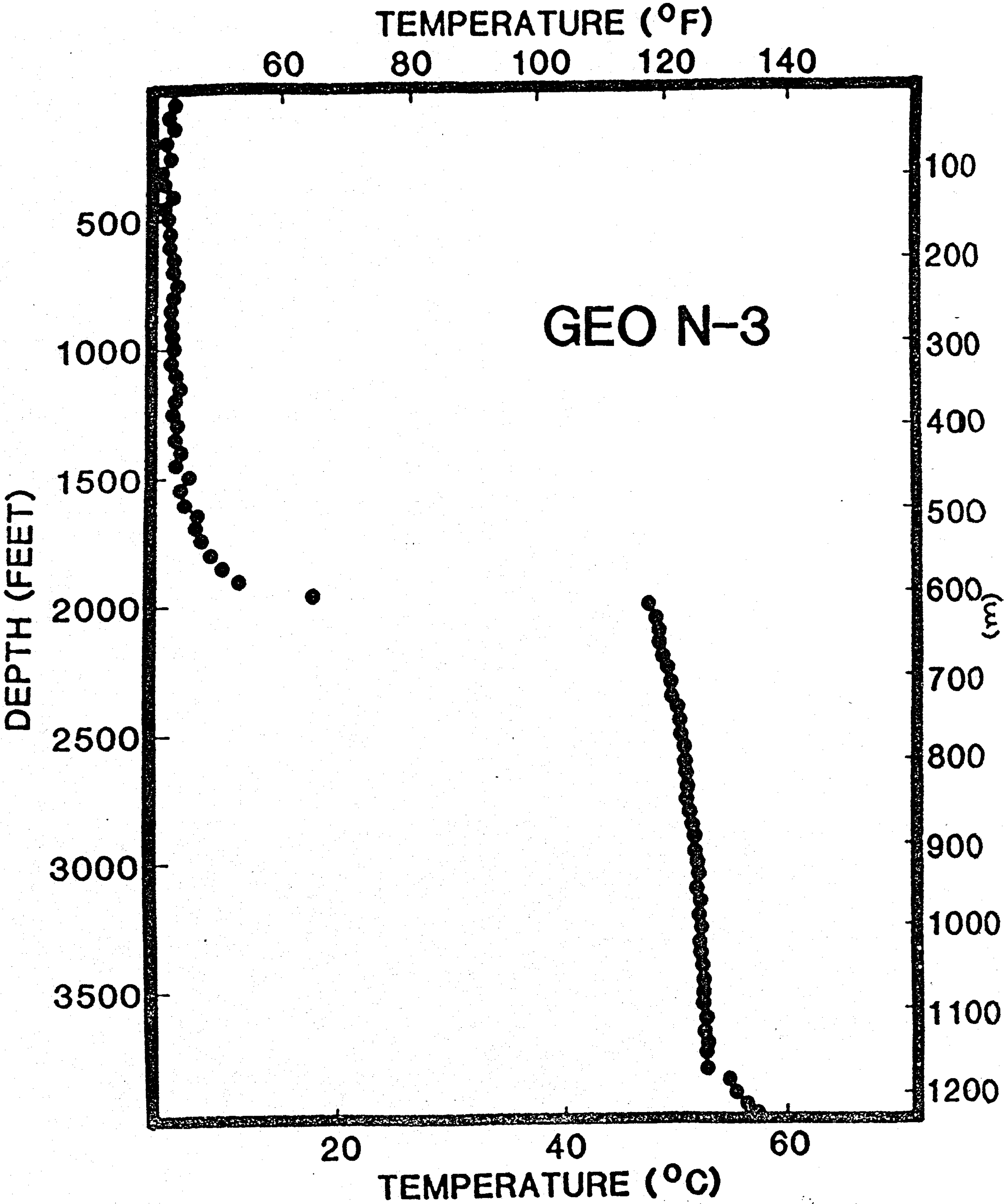
TEMPERATURE (°F)
60
80
100
120
140
GEO N-3
DEPTH (FEET)
500
1000
1500
2000
2500
3000
3500
(m)
100
200
300
400
500
600
700
800
900
1000
1100
1200
20
40
60
TEMPERATURE (°C)

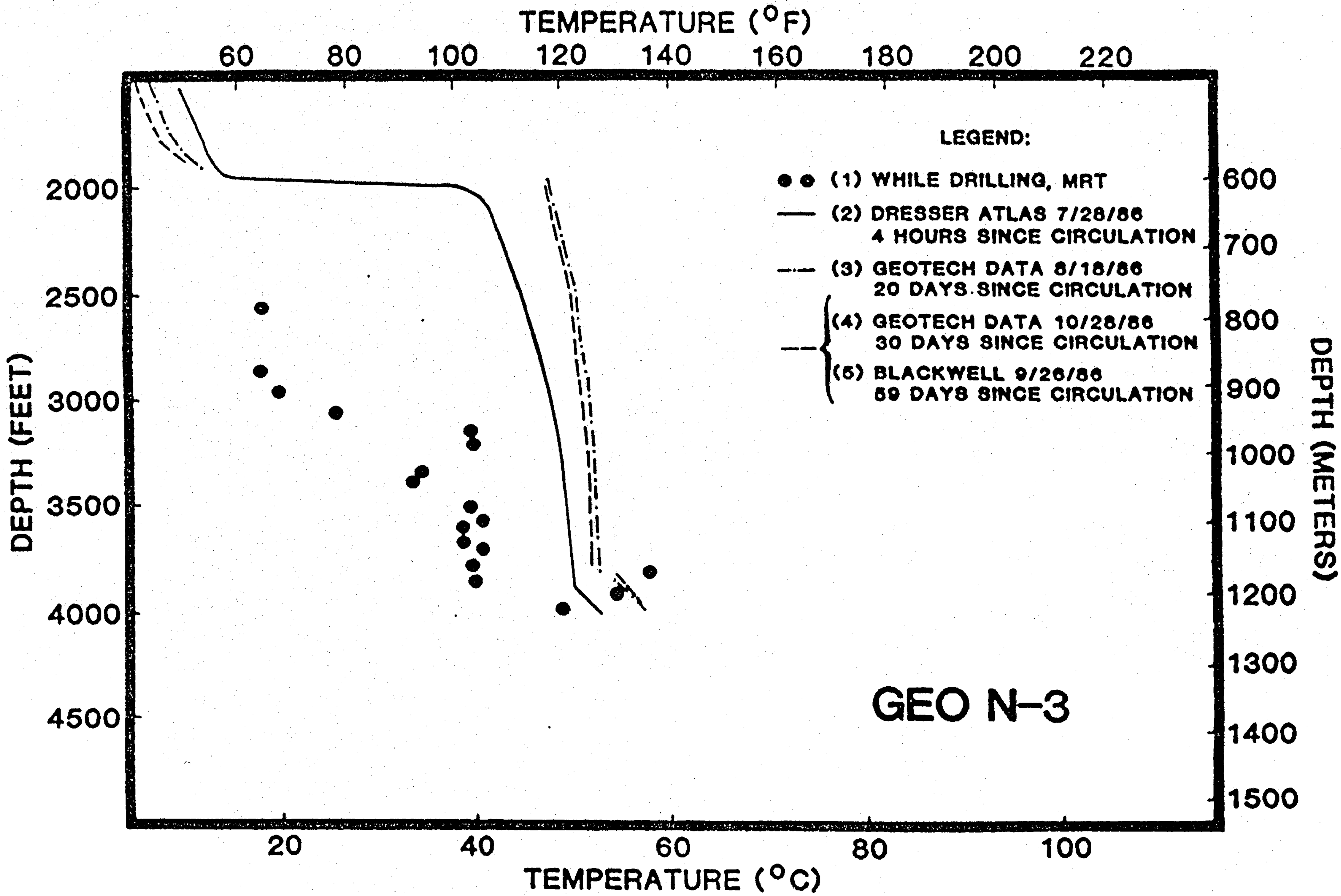
TEMPERATURE (°F)
60
80
100
120
140
160
180
200
220
LEGEND:
(1) WHILE DRILLING, MRT
(2) DRESSER ATLAS 7/28/86
4 HOURS SINCE CIRCULATION
(3) GEOTECH DATA 8/18/86
20 DAYS SINCE CIRCULATION
(4) GEOTECH DATA 10/28/86
30 DAYS SINCE CIRCULATION
(5) BLACKWELL 9/26/86
59 DAYS SINCE CIRCULATION
DEPTH (FEET)
2000
2500
3000
3500
4000
4500
DEPTH (METERS)
600
700
800
900
1000
1100
1200
1300
1400
1500
GEO N-3
20
40
60
80
100
TEMPERATURE (°C)

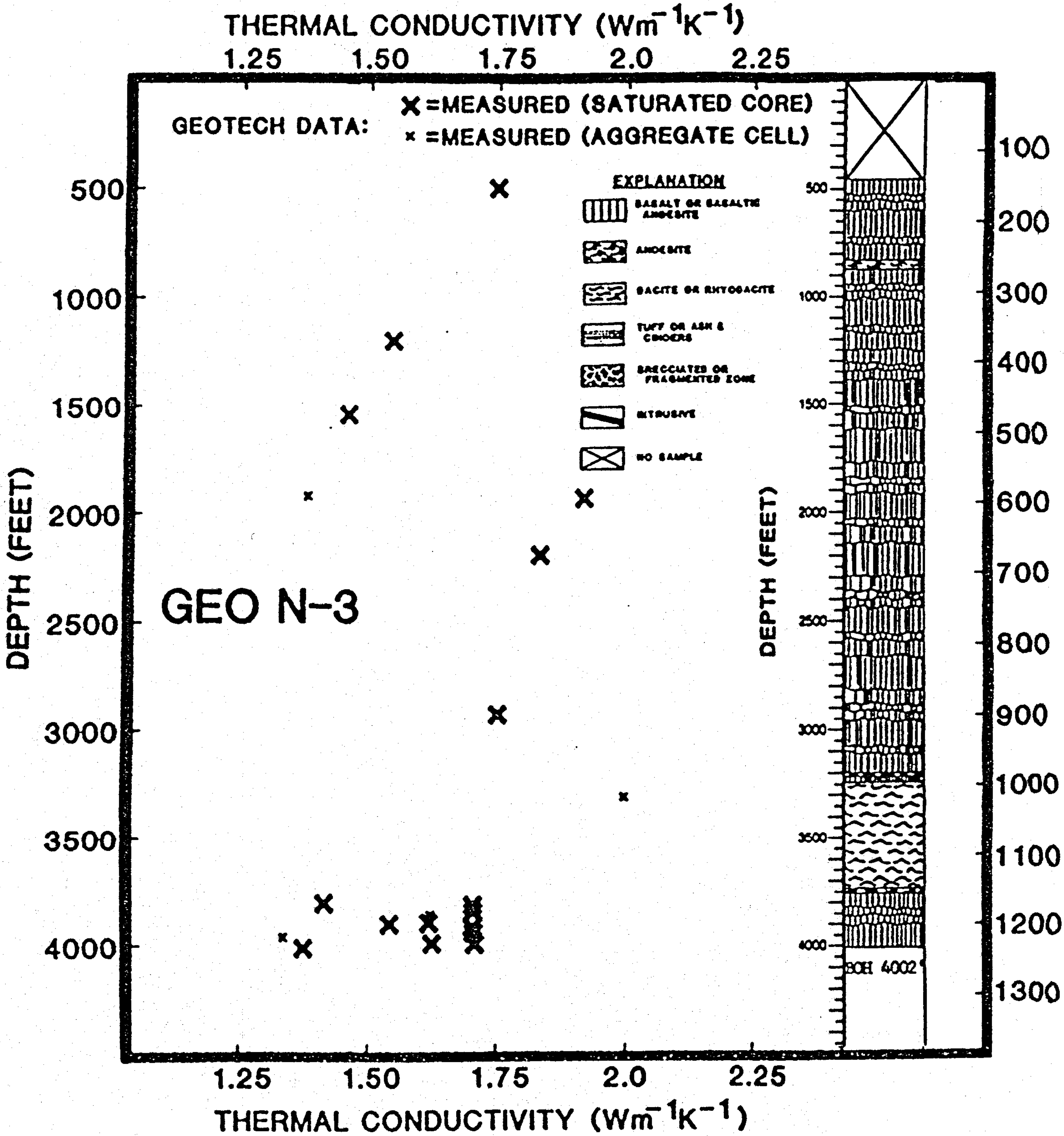

THERMAL CONDUCTIVITY (Wm⁻¹K⁻¹)
1.25 1.50 1.75 2.0 2.25
GEOTECH DATA:
X =MEASURED (SATURATED CORE)
× =MEASURED (AGGREGATE CELL)
EXPLANATION
BASALT OR BASALTIC ANDESITE
ANDESITE
DACITE OR RHYODACITE
TUFF OR ASH & CINDERS
BRECCIATED OR FRAGMENTED ZONE
INTRUSIVE
NO SAMPLE
GEO N-3
DEPTH (FEET)
500 1000 1500 2000 2500 3000 3500 4000
DEPTH (FEET)
100 200 300 400 500 600 700 800 900 1000 1100 1200 1300
BOH 4002
1.25 1.50 1.75 2.0 2.25
THERMAL CONDUCTIVITY (Wm⁻¹K⁻¹)

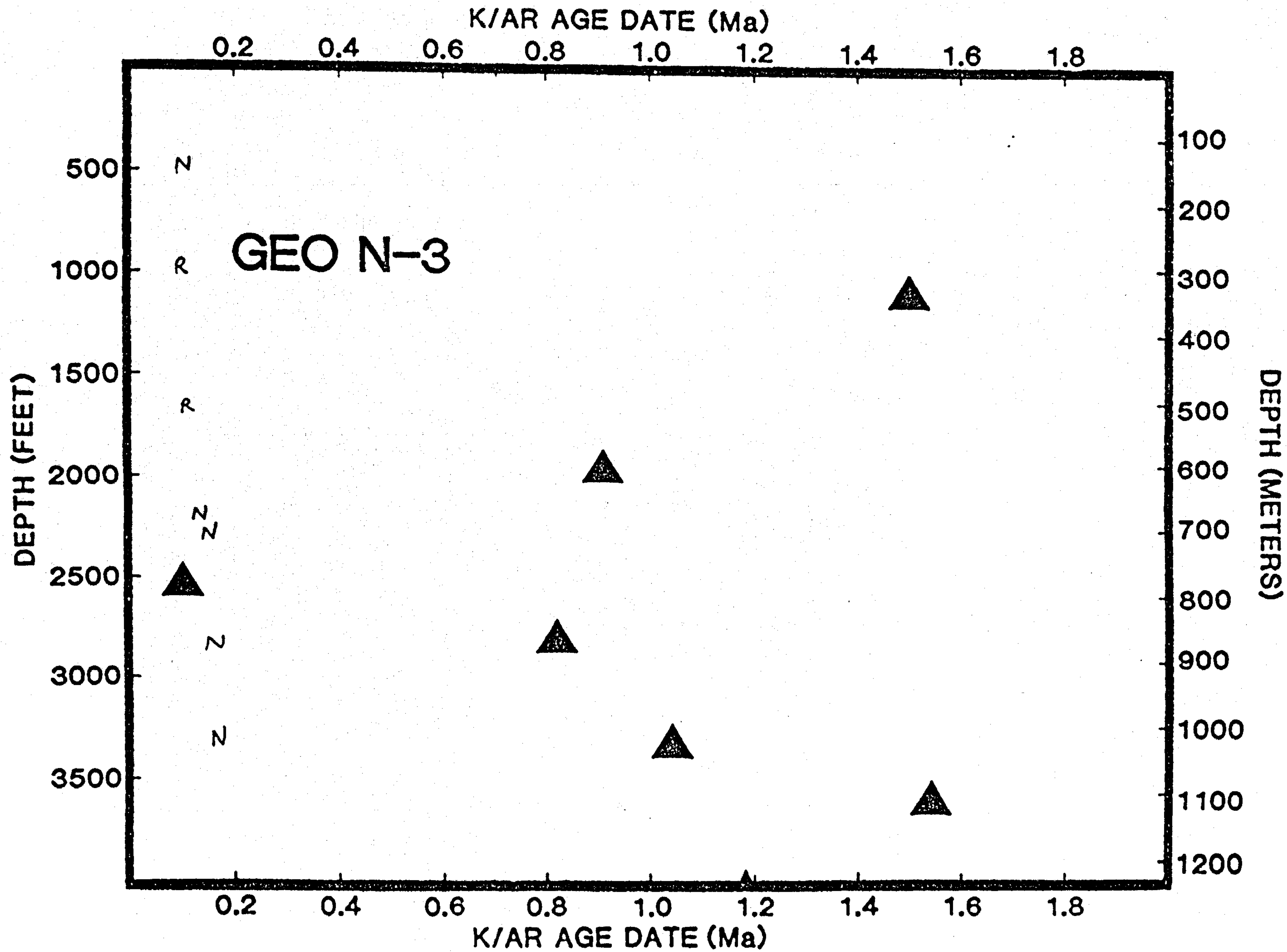

K/AR AGE DATE (Ma)
0.2
0.4
0.6
0.8
1.0
1.2
1.4
1.6
1.8
GEO N-3
DEPTH (FEET)
500
1000
1500
2000
2500
3000
3500
DEPTH (METERS)
100
200
300
400
500
600
700
800
900
1000
1100
1200
N
R
R
N
N
N
N
K/AR AGE DATE (Ma)

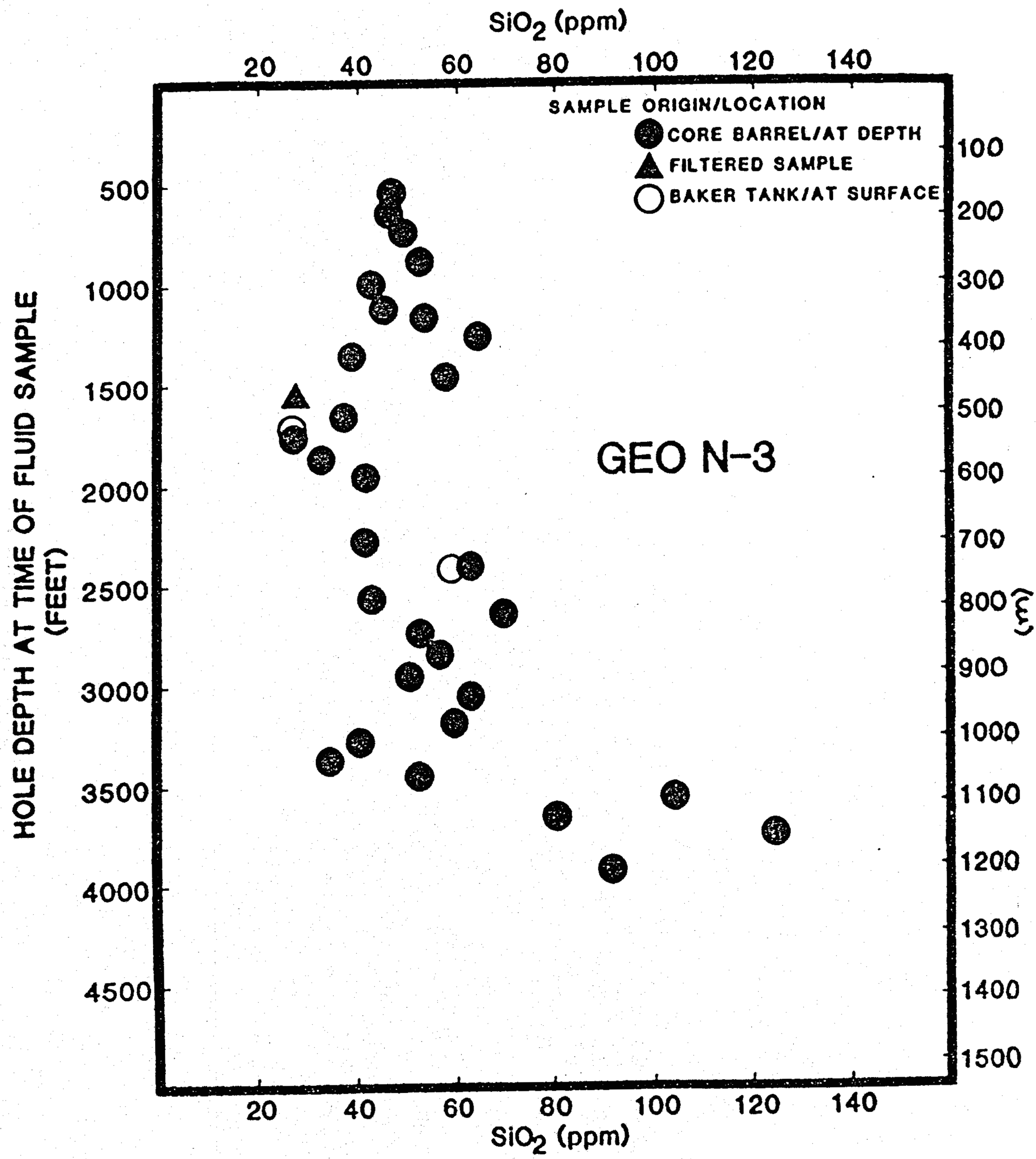
SiO2 (ppm)
20 40 60 80 100 120 140
SAMPLE ORIGIN/LOCATION
CORE BARREL/AT DEPTH
FILTERED SAMPLE
BAKER TANK/AT SURFACE
HOLE DEPTH AT TIME OF FLUID SAMPLE (FEET)
500 1000 1500 2000 2500 3000 3500 4000 4500
100 200 300 400 500 600 700 800 900 1000 1100 1200 1300 1400 1500
(m)
GEO N-3
20 40 60 80 100 120 140
SiO2 (ppm)

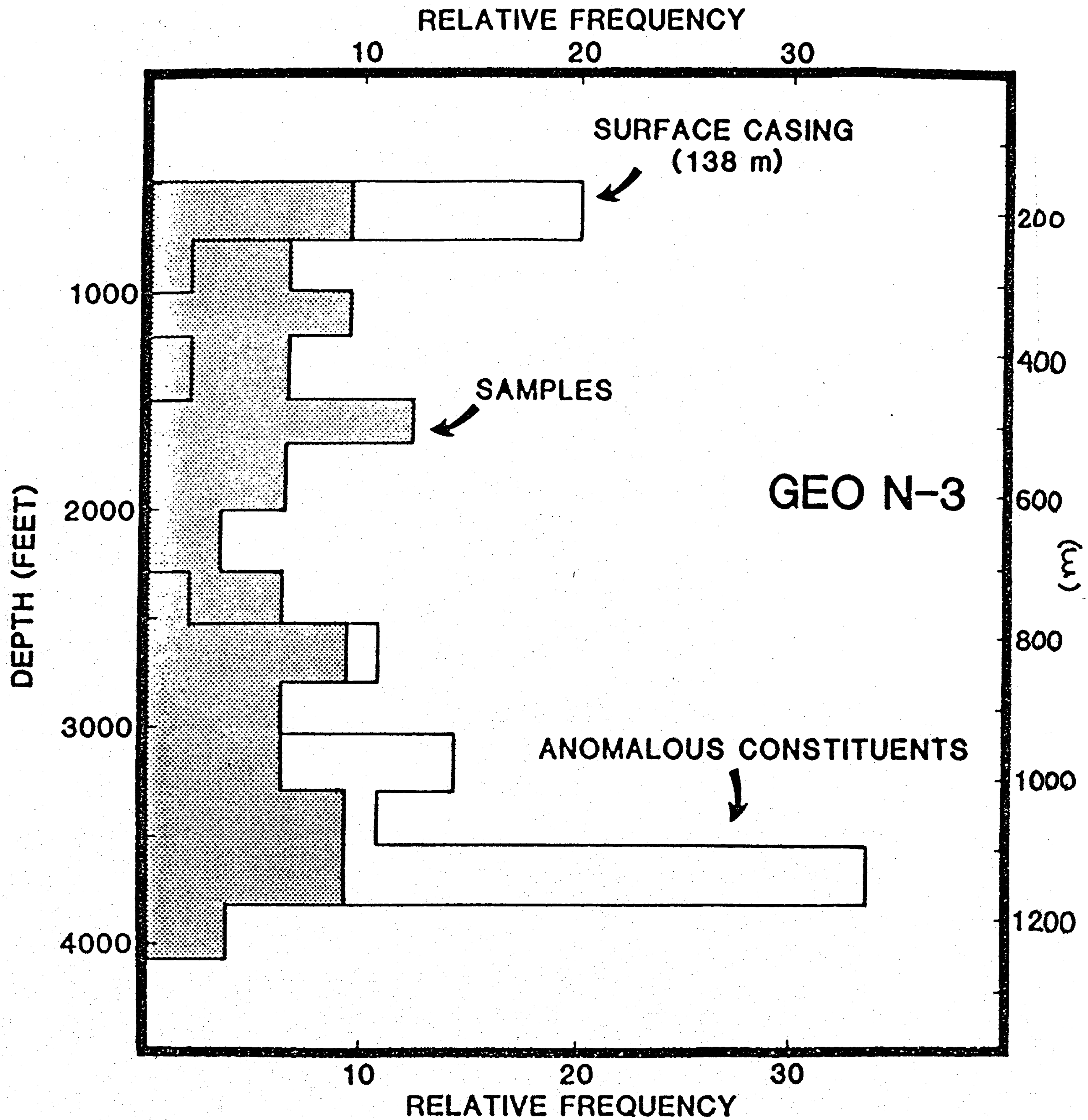
RELATIVE FREQUENCY
10
20
30
SURFACE CASING
(138 m)
SAMPLES
GEO N-3
ANOMALOUS CONSTITUENTS
DEPTH (FEET)
1000
2000
3000
4000
(m)
200
400
600
800
1000
1200
10
20
30
RELATIVE FREQUENCY

GEO N-3 CORE HOLE

D.O.E. phase 11 submittal

Cooperative Agreement No. DE-FC07-851D12613

Newberry Flank Unit

TABLE OF CONTENTS

FIGURE C2

GEOCHEMISTRY OF FLUIDS IN CORE HOLE GEO N-3. Fluid samples of the borehole were routinely collected from the core barrel during core retrieval. Clearly, these fluids are primarily drilling muds. However, value above background suggest the presence of aquifers which contribute formation fluids. Although Figure C2 illustrates only silica values, analyses were conducted for a variety of constituents (Table C2). Fluid samples were also collected from Baker tanks. Note that increasing silica content of fluids correlate with a conductive temperature gradient at 3700-3800 feet (see temperature profile Figure B6).

CORE HOLE GEO N-3

SILICA CONTENT

NEWBERRY VOLCANO, OREGON

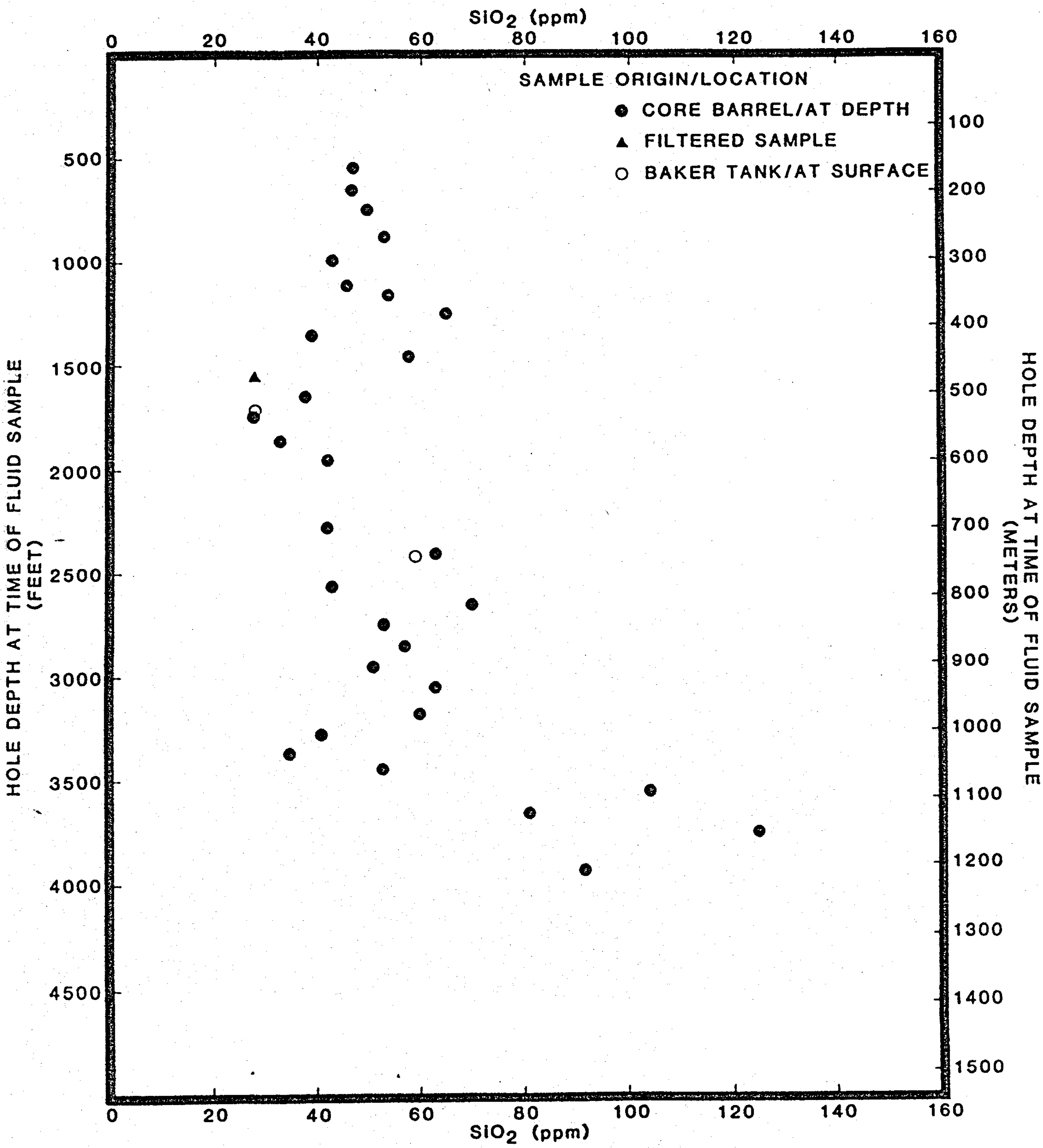

Figure C2

TABLE C2

Fluid Geochemistry for Core Hole GEO N-3

Sample #	Descriptor	PPM BA	V	Ag	Li	LA	CE	MN	ZN	B
1	549'	-	-	0.06	-	0.1	0.5	-	-	-
2	668'	-	-	0.07	-	0.2	0.5	-	-	-
3	746'	2.1	-	0.10	0.09	0.2	0.7	-	-	-
4	866'	-	1.0	0.08	-	0.2	0.5	-	-	-
5	982'	-	-	0.07	-	0.1	0.4	-	-	-
6	1113'	-	-	0.06	-	0.1	0.5	-	-	-
7	1172'	-	-	0.07	-	0.2	0.5	-	-	-
8	1242'	-	-	0.07	-	0.2	0.4	-	-	-
9	1345'	-	1	0.08	-	0.2	0.5	-	-	-
10	1462'	-	-	-	0.05	-	0.2	-	-	-
11	*1549.5'	-	-	0.06	-	0.1	0.4	-	-	-
12	1637.5'	-	-	0.06	-	0.1	0.4	-	-	-
13	**1710'	-	-	0.05	-	-	0.4	-	-	-
14	1740.5'	-	-	0.05	-	-	0.4	-	-	-
15	1859.5'	-	-	0.06	-	0.1	0.4	-	-	-
16	1969'	-	-	0.05	-	-	0.4	-	-	-
17	2271'	-	-	-	-	-	0.4	-	-	-
18	2402'	-	-	-	-	-	0.4	-	-	-
19	**2409'	-	-	-	-	-	0.3	-	-	-
20	2557'	-	-	-	-	-	0.3	-	-	-
21	2641.5'	-	-	-	-	-	-	0.4	-	-
22	2742'	-	-	-	-	-	0.3	-	0.2	-
23	2842'	-	-	-	-	-	0.3	-	-	-
24	2948'	-	-	-	-	-	0.3	-	-	-
25	3041'	-	-	-	-	-	0.3	-	-	-
26	3173'	-	-	-	0.19	-	-	-	-	4.9
27	3276'	-	-	-	-	-	0.3	-	-	0.3
28	3364'	-	-	-	-	-	0.4	-	-	-
29	3440'	-	1	0.08	0.05	0.2	0.6	-	-	-
30	3542'	0.9	-	-	0.07	-	-	0.8	1.1	-
31	3652'	-	-	-	-	-	-	-	-	-
32	3743'	-	-	-	-	-	-	-	0.3	-
33	3923'	-	-	-	-	-	-	-	-	0.1
34	***	-	-	-	-	-	0.3	-	-	-

- below detection limits
* filtered
** Bakertank
***no depth reported

TABLE C2

Fluid Geochemistry for Core Hole GEO N-3

Sample #	Descriptor	ppm CL	ppb Hg	ppmw CO_2	PPM NA	K	CA	Mg	Fe	AL	SiO_2	SR
1	549'	15	-	412	143	1	0.9	-	0.1	1.3	47	0.04
2	668'	6	-	344	119	1	0.7	-	0.08	-	47	0.04
3	746'	5	-	315	221	3	4	1.0	0.93	2.5	50	0.24
4	866'	6	-	386	135	1	0.6	-	0.03	-	53	0.04
5	982'	3	-	364	122	1	1	-	0.08	1.3	43	0.05
6	1113'	3	-	371	141	1	1	-	0.12	1.4	46	0.04
7	1172'	8	-	383	144	1	0.9	-	0.02	-	54	0.04
8	1242'	3	-	367	164	1	0.6	-	0.03	0.6	65	0.04
9	1345'	4	-	257	95	1	1	0.6	0.05	0.7	39	0.03
10	1462'	3	-	223	168	1	2	0.7	0.64	1.1	58	0.04
11	*1549.5'	4	1.4	208	67	-	0.9	-	-	-	28	0.03
12	1637.5'	4	1.4	285	72	-	1.0	-	0.03	0.6	38	0.03
13	**1710'	4	1.7	306	66	-	0.5	-	-	-	28	0.01
14	1740.5'	6	1.7	246	69	-	0.5	-	-	-	28	0.01
15	1859.5'	5	1.9	199	68	-	0.6	-	-	-	33	0.01
16	1969'	4	64	293	70	-	0.9	-	0.06	-	42	0.02
17	2271'	4	1.8	255	98	-	0.6	-	-	-	42	0.02
18	2402'	5	1.7	292	119	-	1.0	-	0.21	1.0	63	0.04
19	**2409'	11	2.0	224	128	1	1	-	0.18	0.9	59	0.04
20	2557'	7	-	395	91	-	0.9	-	0.03	-	43	0.03
21	2641.5'	4	-	315	258	-	7	2	0.24	-	70	0.10
22	2742'	4	3.7	277	118	-	1	-	0.49	0.9	53	-
23	2842'	4	3.5	264	116	-	0.8	-	0.90	0.7	57	0.02
24	2948'	6	1.6	265	115	1	1	0.6	0.21	1.2	51	0.03
25	3041'	6	1.6	596	137	1	1	-	0.14	1.0	63	0.03
26	3173'	108	-	304	438	20	7	16	0.10	-	60	0.14
27	3276'	18	1.9	272	127	1	1	-	0.05	0.61	41	0.04
28	3364'	5	1.9	267	101	-	0.5	-	-	-	35	0.02
29	3440'	6	1.7	741	112	2	1	0.6	0.08	0.9	53	0.04
30	3542'	18	-	241	720	3	29	7	5.79	-	104	0.41
31	3652'	3	4.0	273	207	-	3	1	0.76	1.5	81	0.09
32	3743'	6	3.5	230	224	-	3	1	1.83	4.1	125	0.07
33	3923'	-	-	232	167	-	2	1.0	0.85	2.4	92	0.06
34	***	-	-	-	145	-	2	1	1.1	2.9	104	0.05

- below detection limits
* filtered
** Bakertank
*** no depth reported

UNIVERSITY OF UTAH RESEARCH INSTITUTE

UURI

EARTH SCIENCE LABORATORY
391 CHIPETA WAY, SUITE C
SALT LAKE CITY, UTAH 84108—1295
TELEPHONE 801-524-3422

October 15, 1986

Thermochem, Inc.
6119 Old Redwood Hwy., Suite A-2
Santa Rosa, CA 95401
707 575-1310
Attention: Paul Hirtz

REPORT

Sample	ppm Cl	ppb Hg	Sample	ppm Cl	ppb Hg
3340-1A	15	< .5	3340-18A	11	2.0
3340-2A	6	< .5	3340-19A	7	< 0.5
3340-3A	5	< .5	3340-20A	4	< 0.5
3340-4A	6	< .5	3340-21A	4	3.7
3340-5A	3	< .5	3340-22A	4	3.5
3340-6A	3	< .5	3340-23A	6	1.6
3340-7A	8	< .5	3340-24A	6	1.6
3340-8A	3	< .5	3340-25A	108	< 0.5
3340-9A	4	< .5	3340-26A	18	1.9
3340-10A	3	< .5	3340-27A	5	1.9
3340-11A	4	1.4	3340-28A	6	1.7
3340-12A	4	1.7	3340-29A	18	< 0.5
3340-13A	6	1.7	3340-30A	3	4.0
3340-14A	5	1.9	3340-31A	6	3.5
3340-15A	4	64	3340-32A	7	2.6
3340-16A	4	1.8	3340-33A	4	2.3
3340-17A	5	1.7			

Sample # 3340-11A was run on the ICP both filtered and unfiltered. The other two labled filtered (#3A and 29A) would not settle. Filtration was necessary in order to analyze them. The remaining samples were decanted.

RECEIVED
DATE 10/22/86 TIME
BY
S. R.
GEO NEWBERRY

Ruth L. Kroneman
Chemist

File: UURI

Thermochem, Inc.
Analytical Laboratory & Consulting Service
6119 Old Redwood Hwy., Ste. A-2
Santa Rosa, CA 95401
(707) 575-1310

Report of Analysis

Lab Number	Descriptor	PPM_w CO_2
3340-1	N-3 549'	412
3340-2	N-3 668'	344
3340-3	N-3 746'	315
3340-4	N-3 866'	386
3340-5	N-3 982'	364
3340-6	N-3 1113'	371
3340-7	N-3 1172'	383
3340-8	N-3 1242'	367
3340-9	N-3 1345'	257
3340-10	N-3 1462'	223
3340-11	N-3 1549.5'	208
3340-12	N-3 1637.5'	285
3340-13	MUDTANK @ 1710'	306
3340-14	N-3 1740.5'	246
3340-15	N-3 1859.5'	199
3340-16	N-3 1969'	293
3340-17	N-3 2271'	255
3340-18	N-3 2402'	292
3340-19	MUDTANK 2409'	224
3340-20	N-3 2557'	395
3340-21	N-3 2641.5'	315
3340-22	N-3 2742'	277
3340-23	N-3 2842'	264
3340-24	N-3 2948'	265
3340-25	N-3 3041'	596
3340-26	N-3 3173'	304
3340-27	N-3 3276'	272
3340-28	N-3 3364'	267
3340-29	N-3 3440'	741
3340-30	N-3 3542'	241
3340-31	N-3 3652'	273
3340-32	N-3 3743'	230
3340-33	N-3 3923'	232

THERMOCHEM/GEO

1 1A

ELEMENT		CONCENTRATION (PPM)
NA		143
K		1
CA		0.9
MG	<	0.488
FE		0.10
AL		1.3
SIO2		47
TI	<	0.122
P	<	0.610
SR		0.04
BA	<	0.610
V	<	1.22
CR	<	0.049
MN	<	0.244
CO	<	0.024
NI	<	0.122
CU	<	0.061
MO	<	1.22
PB	<	0.244
ZN	<	0.122
CD	<	0.061
AG		0.06
AU	<	0.098
AS	<	0.610
SB	<	0.732
BI	<	2.44
U	<	6.10
TE	<	1.22
SN		0.1
W	<	0.122
LI	<	0.049
BE	<	0.005
B	<	0.122
ZR	<	0.122
LA		0.1
CE		0.5
TH	<	2.44

THERMOCHEM/GEO

2 2

ELEMENT		CONCENTRATION (PPM)
NA		119
K		1
CA		0.7
MG	<	0.488
FE		0.08
AL	<	0.610
SIO2		47
TI	<	0.122
P	<	0.610
SR		0.04
BA	<	0.610
V	<	1.22
CR	<	0.049
MN	<	0.244
CO	<	0.024
NI	<	0.122
CU	<	0.061
MO	<	1.22
PB	<	0.244
ZN	<	0.122
CD	<	0.061
AG		0.07
AU	<	0.098
AS	<	0.610
SB	<	0.732
BI	<	2.44
U	<	6.10
TE	<	1.22
SN	<	0.122
W	<	0.122
LI	<	0.049
BE	<	0.005
B	<	0.122
ZR	<	0.122
LA		0.2
CE		0.5
TH		2.44

THERMOCHEM/GEO

3 3A FILT

ELEMENT		CONCENTRATION (PPM)
NA		221
K		3
CA		4
MG		1.0
FE		0.93
AL		2.5
SIO2		50
TI	<	0.200
P	<	1.00
SR		0.24
BA		2.1
V	<	2.00
CR	<	0.080
MN	<	0.400
CO	<	0.040
NI	<	0.200
CU	<	0.100
MO	<	2.00
PB	<	0.400
ZN	<	0.200
CD	<	0.100
AG		0.10
AU	<	0.160
AS	<	1.00
SB	<	1.20
BI	<	4.00
U	<	10.0
TE	<	2.00
SN	<	0.200
W	<	0.200
LI		0.09
BE	<	0.008
B	<	0.200
ZR	<	0.200
LA		0.2
CE		0.7
TH	<	4.00

THERMOCHEM/GEO

4 4A

ELEMENT		CONCENTRATION (PPM)
NA		135
K		1
CA		0.6
MG	<	0.488
FE		0.03
AL	<	0.610
SIO2		53
TI	<	0.122
P	<	0.610
SR		0.04
BA	<	0.610
V		1
CR	<	0.049
MN	<	0.244
CO	<	0.024
NI	<	0.122
CU	<	0.061
MO	<	1.22
PB	<	0.244
ZN	<	0.122
CD	<	0.061
AG		0.08
AU	<	0.098
AS	<	0.610
SB	<	0.732
BI	<	2.44
U	<	6.10
TE	<	1.22
SN	<	0.122
W	<	0.122
LI	<	0.049
BE	<	0.005
B	<	0.122
ZR	<	0.122
LA		0.2
CE		0.5
TH	<	2.44

THERMOCHEM/GEO

5 5A

ELEMENT		CONCENTRATION (PPM)
NA		122
K		1
CA		1
MG	<	0.488
FE		0.08
AL		1.3
SIO2		43
TI	<	0.122
P	<	0.610
SR		0.05
BA	<	0.610
V	<	1.22
CR	<	0.049
MN	<	0.244
CO	<	0.024
NI	<	0.122
CU	<	0.061
MO	<	1.22
PB	<	0.244
ZN	<	0.122
CD	<	0.061
AG		0.07
AU	<	0.098
AS	<	0.610
SB	<	0.732
BI	<	2.44
U	<	6.10
TE	<	1.22
SN	<	0.122
W	<	0.122
LI	<	0.049
BE	<	0.005
B	<	0.122
ZR	<	0.122
LA		0.1
CE		0.4
TH	<	2.44

THERMOCHEM/GEO

6 6A

ELEMENT		CONCENTRATION (PPM)
NA		141
K		1
CA		1
MG	<	0.488
FE		0.12
AL		1.4
SIO2		46
TI	<	0.122
P	<	0.610
SR		0.04
BA	<	0.610
V	<	1.22
CR	<	0.049
MN	<	0.244
CO	<	0.024
NI	<	0.122
CU	<	0.061
MO	<	1.22
PB	<	0.244
ZN	<	0.122
CD	<	0.061
AG		0.06
AU	<	0.098
AS	<	0.610
SB	<	0.732
BI	<	2.44
U	<	6.10
TE	<	1.22
SN	<	0.122
W	<	0.122
LI	<	0.049
BE	<	0.005
B	<	0.122
ZR	<	0.122
LA		0.1
CE		0.5
TH	<	2.44

THERMOCHEM/GEO

7 7A

ELEMENT		CONCENTRATION (PPM)
NA		144
K		1
CA		0.9
MG	<	0.488
FE		0.02
AL	<	0.610
SIO2		54
TI	<	0.122
P	<	0.610
SR		0.04
BA	<	0.610
V	<	1.22
CR	<	0.049
MN	<	0.244
CO	<	0.024
NI	<	0.122
CU	<	0.061
MO	<	1.22
PB	<	0.244
ZN	<	0.122
CD	<	0.061
AG		0.07
AU	<	0.098
AS	<	0.610
SB	<	0.732
BI	<	2.44
U	<	6.10
TE	<	1.22
SN	<	0.122
W	<	0.122
LI	<	0.049
BE	<	0.005
B	<	0.122
ZR	<	0.122
LA		0.2
CE		0.5
TH	<	2.44

THERMOCHEM/GEO

8 8A

ELEMENT		CONCENTRATION (PPM)
NA		164
K		1
CA		0.6
MG	<	0.488
FE		0.03
AL		0.6
SIO2		65
TI	<	0.122
P	<	0.610
SR		0.04
BA	<	0.610
V	<	1.22
CR	<	0.049
MN	<	0.244
CO	<	0.024
NI	<	0.122
CU	<	0.061
MO	<	1.22
PB	<	0.244
ZN	<	0.122
CD	<	0.061
AG		0.07
AU	<	0.098
AS	<	0.610
SB	<	0.732
BI	<	2.44
U	<	6.10
TE	<	1.22
SN	<	0.122
W	<	0.122
LI	<	0.049
BE	<	0.005
B	<	0.122
ZR	<	0.122
LA		0.2
CE		0.4
TH	<	2.44

THERMOCHEM/GEO

9 9A

ELEMENT		CONCENTRATION (PPM)
NA		95
K		1
CA		1
MG		0.6
FE		0.05
AL		0.7
SIO2		39
TI	<	0.122
P	<	0.610
SR		0.03
BA	<	0.610
V		1
CR	<	0.049
MN	<	0.244
CO	<	0.024
NI	<	0.122
CU	<	0.061
MO	<	1.22
PB	<	0.244
ZN	<	0.122
CD	<	0.061
AG		0.08
AU	<	0.098
AS	<	0.610
SB	<	0.732
BI	<	2.44
U	<	6.10
TE	<	1.22
SN	<	0.122
W	<	0.122
LI	<	0.049
BE	<	0.005
B	<	0.122
ZR	<	0.122
LA		0.2
CE		0.5
TH	<	2.44

THERMOCHEM/GEO

10 10A

ELEMENT		CONCENTRATION (PPM)
NA		168
K		1
CA		2
MG		0.7
FE		0.64
AL		1.1
SIO2		58
TI	<	0.122
P	<	0.610
SR		0.04
BA	<	0.610
V	<	1.22
CR	<	0.049
MN	<	0.244
CO	<	0.024
NI	<	0.122
CU	<	0.061
MO	<	1.22
PB	<	0.244
ZN	<	0.122
CD	<	0.061
AG	<	0.049
AU	<	0.098
AS	<	0.610
SB	<	0.732
BI	<	2.44
U	<	6.10
TE	<	1.22
SN	<	0.122
W	<	0.122
LI		0.05
BE	<	0.005
B	<	0.122
ZR	<	0.122
LA	<	0.122
CE		0.2
TH	<	2.44

THERMOCHEM/GEO

11 11A FILT

ELEMENT		CONCENTRATION (PPM)
NA		67
K	<	1.22
CA		0.9
MG	<	0.488
FE	<	0.024
AL	<	0.610
SIO2		28
TI	<	0.122
P	<	0.610
SR		0.03
BA	<	0.610
V	<	1.22
CR	<	0.049
MN	<	0.244
CO	<	0.024
NI	<	0.122
CU	<	0.061
MO	<	1.22
PB	<	0.244
ZN	<	0.122
CD	<	0.061
AG		0.06
AU	<	0.098
AS	<	0.610
SB	<	0.732
BI	<	2.44
U	<	6.10
TE	<	1.22
SN	<	0.122
W	<	0.122
LI	<	0.049
BE	<	0.005
B	<	0.122
ZR	<	0.122
LA		0.1
CE		0.4
TH	<	2.44

THERMOCHEM/GEO

12 11A UNFILT

ELEMENT		CONCENTRATION (PPM)
NA		72
K	<	1.22
CA		1.0
MG	<	0.488
FE		0.03
AL		0.6
SIO2		38
TI	<	0.122
P	<	0.610
SR		0.03
BA	<	0.610
V	<	1.22
CR	<	0.049
MN	<	0.244
CO	<	0.024
NI	<	0.122
CU	<	0.061
MO	<	1.22
PB	<	0.244
ZN	<	0.122
CD	<	0.061
AG		0.06
AU	<	0.098
AS	<	0.610
SB	<	0.732
BI	<	2.44
U	<	6.10
TE	<	1.22
SN	<	0.122
W	<	0.122
LI	<	0.049
BE	<	0.005
B	<	0.122
ZR	<	0.122
LA		0.1
CE		0.4
TH	<	2.44

THERMOCHEM/GEO

13 12A

ELEMENT		CONCENTRATION (PPM)
NA		66
K	<	1.22
CA		0.5
MG	<	0.488
FE	<	0.024
AL	<	0.610
SIO2		28
TI	<	0.122
P	<	0.610
SR		0.01
BA	<	0.610
V	<	1.22
CR	<	0.049
MN	<	0.244
CO	<	0.024
NI	<	0.122
CU	<	0.061
MO	<	1.22
PB	<	0.244
ZN	<	0.122
CD	<	0.061
AG		0.05
AU	<	0.098
AS	<	0.610
SB	<	0.732
BI	<	2.44
U	<	6.10
TE	<	1.22
SN	<	0.122
W	<	0.122
LI	<	0.049
BE	<	0.005
B	<	0.122
ZR	<	0.122
LA	<	0.122
CE		0.4
TH	<	2.44

THERMOCHEM/GEO

14 13A

ELEMENT		CONCENTRATION (PPM)
NA		69
K	<	1.22
CA		0.5
MG	<	0.488
FE	<	0.024
AL	<	0.610
SIO2		28
TI	<	0.122
P	<	0.610
SR		0.01
BA	<	0.610
V	<	1.22
CR	<	0.049
MN	<	0.244
CO	<	0.024
NI	<	0.122
[illegible]	<	0.061
MO	<	1.22
PB	<	0.244
ZN	<	0.122
CD	<	0.061
AG		0.05
AU	<	0.098
AS	<	0.610
SB	<	0.732
BI	<	2.44
U	<	6.10
TE	<	1.22
SN	<	0.122
W	<	0.122
LI	<	0.049
BE	<	0.005
B	<	0.122
ZR	<	0.122
LA	<	0.122
CE		0.4
TH	<	2.44

THERMOCHEM/GEO

15 14A

ELEMENT		CONCENTRATION (PPM)
NA		68
K	<	1.22
CA		0.6
MG	<	0.488
FE	<	0.024
AL	<	0.610
SIO2		33
TI	<	0.122
P	<	0.610
SR		0.01
BA	<	0.610
V	<	1.22
CR	<	0.049
MN	<	0.244
CO	<	0.024
NI	<	0.122
CU	<	0.061
MO	<	1.22
PB	<	0.244
ZN	<	0.122
CD	<	0.061
AG		0.06
AU	<	0.098
AS	<	0.610
SB	<	0.732
BI	<	2.44
U	<	6.10
TE	<	1.22
SN	<	0.122
W	<	0.122
LI	<	0.049
BE	<	0.005
B	<	0.122
ZR	<	0.122
LA		0.1
CE		0.4
TH	<	2.44

THERMOCHEM/GEO

16 15A

ELEMENT		CONCENTRATION (PPM)
NA		70
K	<	1.22
CA		0.9
MG	<	0.488
FE		0.06
AL	<	0.610
SIO2		42
TI	<	0.122
P	<	0.610
SR		0.02
BA	<	0.610
V	<	1.22
CR	<	0.049
MN	<	0.244
CO	<	0.024
NI	<	0.122
CU	<	0.061
MO	<	1.22
PB	<	0.244
ZN	<	0.122
CD	<	0.061
AG		0.05
AU	<	0.098
AS	<	0.610
SB	<	0.732
BI	<	2.44
U	<	6.10
TE	<	1.22
SN	<	0.122
W	<	0.122
LI	<	0.049
BE	<	0.005
B	<	0.122
ZR	<	0.122
LA	<	0.122
CE		0.4
TH	<	2.44

THERMOCHEM/GEO

17 16A

ELEMENT		CONCENTRATION (PPM)
NA		98
K	<	1.22
CA		0.6
MG	<	0.488
FE	<	0.024
AL	<	0.610
SIO2		42
TI	<	0.122
P	<	0.610
SR		0.02
BA	<	0.610
V	<	1.22
CR	<	0.049
MN	<	0.244
CO	<	0.024
NI	<	0.122
CU	<	0.061
MO	<	1.22
PB	<	0.244
ZN	<	0.122
CD	<	0.061
AG	<	0.049
AU	<	0.098
AS	<	0.610
SB	<	0.732
BI	<	2.44
U	<	6.10
TE	<	1.22
SN	<	0.122
W	<	0.122
LI	<	0.049
BE	<	0.005
B	<	0.122
ZR	<	0.122
LA	<	0.122
CE		0.4
TH	<	2.44

THERMOCHEM/GEO

18 17A

ELEMENT		CONCENTRATION (PPM)
NA		119
K	<	1.22
CA		1
MG	<	0.488
FE		0.21
AL		1.0
SIO2		63
TI	<	0.122
P	<	0.610
SR		0.04
BA	<	0.610
V	<	1.22
CR	<	0.049
MN	<	0.244
CO	<	0.024
NI	<	0.122
CU	<	0.061
MO	<	1.22
PB	<	0.244
ZN	<	0.122
CD	<	0.061
AG	<	0.049
AU	<	0.098
AS	<	0.610
SB	<	0.732
BI	<	2.44
U	<	6.10
TE	<	1.22
SN	<	0.122
W	<	0.122
LI	<	0.049
BE	<	0.005
B	<	0.122
ZR	<	0.122
LA	<	0.122
CE		0.4
TH	<	2.44

THERMOCHEM/GEO

18 18A
19 ?

ELEMENT		CONCENTRATION (PPM)
NA		128
K		1
CA		1
MG	<	0.488
FE		0.18
AL		0.9
SIO2		59
TI	<	0.122
P	<	0.610
SR		0.04
BA	<	0.610
V	<	1.22
CR	<	0.049
MN	<	0.244
CO	<	0.024
NI	<	0.122
CU	<	0.061
MO	<	1.22
PB	<	0.244
ZN	<	0.122
CD	<	0.061
AG	<	0.049
AU	<	0.098
AS	<	0.610
SB	<	0.732
BI	<	2.44
U	<	6.10
TE	<	1.22
SN	<	0.122
W	<	0.122
LI	<	0.049
BE	<	0.005
B	<	0.122
ZR	<	0.122
LA	<	0.122
CE		0.3
TH	<	2.44

THERMOCHEM/GEO

20 19A

ELEMENT		CONCENTRATION (PPM)
NA		91
K	<	1.22
CA		0.9
MG	<	0.488
FE		0.03
AL	<	0.610
SIO2		43
TI	<	0.122
P	<	0.610
SR		0.03
BA	<	0.610
V	<	1.22
CR	<	0.049
MN	<	0.244
CO	<	0.024
NI	<	0.122
CU	<	0.061
MO	<	1.22
PB	<	0.244
ZN	<	0.122
CD	<	0.061
AG	<	0.049
AU	<	0.098
AS	<	0.610
SB	<	0.732
BI	<	2.44
U	<	6.10
TE	<	1.22
SN	<	0.122
W	<	0.122
LI	<	0.049
BE	<	0.005
B	<	0.122
ZR	<	0.122
LA	<	0.122
CE		0.3
TH	<	2.44

THERMOCHEM/GEO

21 20A

ELEMENT		CONCENTRATION (PPM)
NA		258
K	<	1.22
CA		7
MG		2
FE		0.24
AL	<	0.610
SIO2		70
TI	<	0.122
P	<	0.610
SR		0.10
BA	<	0.610
V	<	1.22
CR	<	0.049
MN		0.4
CO	<	0.024
NI	<	0.122
CU	<	0.061
MO	<	1.22
PB	<	0.244
ZN	<	0.122
CD	<	0.061
AG	<	0.049
AU	<	0.098
AS	<	0.610
SB	<	0.732
BI	<	2.44
U	<	6.10
TE	<	1.22
SN	<	0.122
W	<	0.122
LI	<	0.049
BE	<	0.005
B	<	0.122
ZR	<	0.122
LA	<	0.122
CE	<	0.244
TH	<	2.44

THERMOCHEM/GEO

22 21A

ELEMENT		CONCENTRATION (PPM)
NA		118
K	<	1.22
CA		1
MG	<	0.488
FE		0.49
AL		0.9
SIO2		53
TI	<	0.122
P	<	0.610
SR		0.02
BA	<	0.610
V	<	1.22
CR	<	0.049
MN	<	0.244
CO	<	0.024
NI	<	0.122
[illegible]	<	0.061
MO	<	1.22
PB	<	0.244
ZN		0.2
CD	<	0.061
AG	<	0.049
AU	<	0.098
AS	<	0.610
SB	<	0.732
BI	<	2.44
U	<	6.10
TE	<	1.22
SN	<	0.122
W	<	0.122
LI	<	0.049
BE	<	0.005
B	<	0.122
ZR	<	0.122
LA	<	0.122
CE		0.3
TH	<	2.44

THERMOCHEM/GEO

23 22A

ELEMENT		CONCENTRATION (PPM)
NA		116
K	<	1.22
CA		0.8
MG	<	0.488
FE		0.09
AL		0.7
SIO2		57
TI	<	0.122
P	<	0.610
SR		0.02
BA	<	0.610
V	<	1.22
CR	<	0.049
MN	<	0.244
CO	<	0.024
NI	<	0.122
CU	<	0.061
MO	<	1.22
PB	<	0.244
ZN	<	0.122
CD	<	0.061
AG	<	0.049
AU	<	0.098
AS	<	0.610
SB	<	0.732
BI	<	2.44
U	<	6.10
TE	<	1.22
SN	<	0.122
W	<	0.122
LI	<	0.049
BE	<	0.005
B	<	0.122
ZR	<	0.122
LA	<	0.122
CE		0.3
TH	<	2.44

THERMOCHEM/GEO

24 23A

ELEMENT		CONCENTRATION (PPM)
NA		115
K		1
CA		1
MG		0.6
FE		0.21
AL		1.2
SIO2		51
TI	<	0.122
P	<	0.610
SR		0.03
BA	<	0.610
V	<	1.22
CR	<	0.049
MN	<	0.244
CO	<	0.024
NI	<	0.122
CU	<	0.061
MO	<	1.22
PB	<	0.244
ZN	<	0.122
CD	<	0.061
AG	<	0.049
AU	<	0.098
AS	<	0.610
SB	<	0.732
BI	<	2.44
U	<	6.10
TE	<	1.22
SN	<	0.122
W	<	0.122
LI	<	0.049
BE	<	0.005
B	<	0.122
ZR	<	0.122
LA	<	0.122
CE		0.3
TH	<	2.44

THERMOCHEM/GEO

25 24A

ELEMENT		CONCENTRATION (PPM)
NA		137
K		1
CA		1
MG	<	0.488
FE		0.14
AL		1.0
SIO2		63
TI	<	0.122
P	<	0.610
SR		0.03
BA	<	0.610
V	<	1.22
CR	<	0.049
MN	<	0.244
CO	<	0.024
NI	<	0.122
CU	<	0.061
MO	<	1.22
PB	<	0.244
ZN	<	0.122
CD	<	0.061
AG	<	0.049
AU	<	0.098
AS	<	0.610
SB	<	0.732
BI	<	2.44
U	<	6.10
TE	<	1.22
SN	<	0.122
W	<	0.122
LI	<	0.049
BE	<	0.005
B	<	0.122
ZR	<	0.122
LA	<	0.122
CE		0.3
TH	<	2.44

THERMOCHEM/GEO

26 25A

ELEMENT		CONCENTRATION (PPM)
NA		438
K		20
CA		7
MG		16
FE		0.10
AL	<	0.610
SIO2		60
TI	<	0.122
P	<	0.610
SR		0.14
BA	<	0.610
V	<	1.22
CR	<	0.049
MN	<	0.244
CO	<	0.024
NI	<	0.122
[illegible]	<	0.061
MO	<	1.22
PB	<	0.244
ZN	<	0.122
CD	<	0.061
AG	<	0.049
AU	<	0.098
AS	<	0.610
SB	<	0.732
BI	<	2.44
U	<	6.10
TE	<	1.22
SN	<	0.122
W	<	0.122
LI		0.19
BE	<	0.005
B		4.9
ZR	<	0.122
LA	<	0.122
CE	<	0.244
TH	<	2.44

THERMOCHEM/GEO

27 26A

ELEMENT		CONCENTRATION (PPM)
NA		127
K		1
CA		1
MG	<	0.488
FE		0.05
AL	<	0.610
SIO2		41
TI	<	0.122
P	<	0.610
SR		0.04
BA	<	0.610
V	<	1.22
CR	<	0.049
MN	<	0.244
CO	<	0.024
NI	<	0.122
CU	<	0.061
MO	<	1.22
PB	<	0.244
ZN	<	0.122
CD	<	0.061
AG	<	0.049
AU	<	0.098
AS	<	0.610
SB	<	0.732
BI	<	2.44
U	<	6.10
TE	<	1.22
SN	<	0.122
W	<	0.122
LI	<	0.049
BE	<	0.005
B		0.3
ZR	<	0.122
LA	<	0.122
CE		0.3
TH	<	2.44

THERMOCHEM/GEO

28 27A

ELEMENT		CONCENTRATION (PPM)
NA		101
K	<	1.22
CA		0.5
MG	<	0.488
FE	<	0.024
AL	<	0.610
SIO2		35
TI	<	0.122
P	<	0.610
SR		0.02
BA	<	0.610
V	<	1.22
CR	<	0.049
MN	<	0.244
CO	<	0.024
NI	<	0.122
CU	<	0.061
MO	<	1.22
PB	<	0.244
ZN	<	0.122
CD	<	0.061
AG	<	0.049
AU	<	0.098
AS	<	0.610
SB	<	0.732
BI	<	2.44
U	<	6.10
TE	<	1.22
SN	<	0.122
W	<	0.122
LI	<	0.049
BE	<	0.005
B	<	0.122
ZR	<	0.122
LA	<	0.122
CE		0.4
TH	<	2.44

THERMOCHEM/GEO

29 28A

ELEMENT		CONCENTRATION (PPM)
NA		112
K		2
CA		1
MG		0.6
FE		0.08
AL		0.9
SIO2		53
TI	<	0.122
P	<	0.610
SR		0.04
BA	<	0.610
V		1
CR	<	0.049
MN	<	0.244
CO	<	0.024
NI	<	0.122
CU	<	0.061
MO	<	1.22
PB	<	0.244
ZN	<	0.122
CD	<	0.061
AG		0.08
AU	<	0.098
AS	<	0.610
SB	<	0.732
BI	<	2.44
U	<	6.10
TE	<	1.22
SN	<	0.122
W	<	0.122
LI		0.05
BE	<	0.005
B	<	0.122
ZR	<	0.122
LA		0.2
CE		0.6
TH	<	2.44

THERMOCHEM/GEO

30 29A

ELEMENT		CONCENTRATION (PPM)
NA		720
K		3
CA		29
MG		7
FE		5.79
AL	<	0.610
SIO2		104
TI	<	0.122
P	<	0.610
SR		0.41
BA		0.9
V	<	1.22
CR	<	0.049
MN		0.8
CO	<	0.024
NI	<	0.122
CU	<	0.061
MO	<	1.22
PB	<	0.244
ZN		1.1
CD	<	0.061
AG	<	0.049
AU	<	0.098
AS	<	0.610
SB	<	0.732
BI	<	2.44
U	<	6.10
TE	<	1.22
SN	<	0.122
W	<	0.122
LI		0.07
BE	<	0.005
B	<	0.122
ZR	<	0.122
LA	<	0.122
CE	<	0.244
TH	<	2.44

THERMOCHEM/GEO

31 30A

ELEMENT	CONCENTRATION (PPM)
NA	207
K	< 1.22
CA	3
MG	1
FE	0.76
AL	1.5
SIO2	81
TI	< 0.122
P	< 0.610
SR	0.09
BA	< 0.610
V	< 1.22
CR	< 0.049
MN	< 0.244
CO	< 0.024
NI	< 0.122
CU	< 0.061
MO	< 1.22
PB	< 0.244
ZN	< 0.122
CD	< 0.061
AG	< 0.049
AU	< 0.098
AS	< 0.610
SB	< 0.732
BI	< 2.44
U	< 6.10
TE	< 1.22
SN	< 0.122
W	< 0.122
LI	< 0.049
BE	< 0.005
B	< 0.122
ZR	< 0.122
LA	< 0.122
CE	< 0.244
TH	< 2.44

THERMOCHEM/GEO

32 31A

ELEMENT		CONCENTRATION (PPM)
NA		224
K	<	1.22
CA		3
MG		1
FE		1.83
AL		4.1
SIO2		125
TI	<	0.122
P	<	0.610
SR		0.07
BA	<	0.610
V	<	1.22
CR	<	0.049
MN	<	0.244
CO	<	0.024
NI	<	0.122
CU	<	0.061
MO	<	1.22
PB	<	0.244
ZN		0.3
CD	<	0.061
AG	<	0.049
AU	<	0.098
AS	<	0.610
SB	<	0.732
BI	<	2.44
U	<	6.10
TE	<	1.22
SN	<	0.122
W	<	0.122
LI	<	0.049
BE	<	0.005
B	<	0.122
ZR	<	0.122
LA	<	0.122
CE	<	0.244
TH	<	2.44

THERMOCHEM/GEO

33 32A

ELEMENT		CONCENTRATION (PPM)
NA		167
K	<	1.22
CA		2
MG		1.0
FE		0.85
AL		2.4
SIO2		92
TI	<	0.122
P	<	0.610
SR		0.06
BA	<	0.610
V	<	1.22
CR	<	0.049
MN	<	0.244
CO	<	0.024
NI	<	0.122
CU	<	0.061
MO	<	1.22
PB	<	0.244
ZN	<	0.122
CD	<	0.061
AG	<	0.049
AU	<	0.098
AS	<	0.610
SB	<	0.732
BI	<	2.44
U	<	6.10
TE	<	1.22
SN	<	0.122
W	<	0.122
LI	<	0.049
BE	<	0.005
B		0.1
ZR	<	0.122
LA	<	0.122
CE	<	0.244
TH	<	2.44

THERMOCHEM/GEO

34 33A

ELEMENT		CONCENTRATION (PPM)
NA		145
K	<	1.22
CA		2
MG		1
FE		1.10
AL		2.9
SIO2		104
TI	<	0.122
P	<	0.610
SR		0.05
BA	<	0.610
V	<	1.22
CR	<	0.049
MN	<	0.244
CO	<	0.024
NI	<	0.122
CU	<	0.061
MO	<	1.22
PB	<	0.244
ZN	<	0.122
CD	<	0.061
AG	<	0.049
AU	<	0.098
AS	<	0.610
SB	<	0.732
BI	<	2.44
U	<	6.10
TE	<	1.22
SN	<	0.122
W	<	0.122
LI	<	0.049
BE	<	0.005
B	<	0.122
ZR	<	0.122
LA	<	0.122
CE		0.3
TH	<	2.44

FIGURE C1

VOLCANIC STRATIGRAPHY AND BOTTOM HOLE TEMPERATURES DURING DRILLING FOR GEO N-3, NEWBERRY VOLCANO, OREGON. Because BHTs are generalized in this figure, the reader should refer to Table B1 for more detailed information. Note the bimodal character with more felsic units from (3200-3753) feet. The lithographic column was constructed as a result of geologic logging and comparisons to geochemical analyses. Temperature data comes from drilling reports, and GEO personnel are responsible for the stratigraphic interpretations. The whole-rock analyses are included in Tables C 1/1 and C 1/2.

TEMPERATURE GRADIENT CORE HOLE SUMMARY

Name GEO CORE HOLE N-3

Company GEO NEWBERRY Lease ______ County DESCHUTES

Location 4100' N and 500' E of SW Corner Sec 24 T 20S R 12E

Spud Date 6-2-86 Completed 7-31-86 Depth 4002'

BOTTOM HOLE TEMPERATURES WHILE DRILLING

☒ Feet ☐ Meters ☒ °F ☐ °C

DEPTH	TEMP	DEPTH	TEMP	DEPTH	TEMP
565.5	< 60	2767.5	< 60		
663	< 60	2864	64		
942	< 60	3061	77/78		
1177	60	3160	103/103		
1272	64	3213	103/103		
1381.5	63	3320	94/94		
1477	< 60	3377.5	92/92		
1572	< 60	3422	110/110		
1670.5	< 60	3463.5	123		
1783	< 60	3509	103/103		
1845	< 60	3612	103/101		
1947	< 60	3562	106/105		
2044	< 60	3709	105/90		
2092	< 60	3662	101/101		
2182	< 60	3763	102/103		
2288.5	< 60	3858.5	103/104		
2359.5	< 60	3812	135/136		
2401	< 60	3908.5	130/130		
2563	64	3961	118/120		
2663	60				

COMMENTS:

ARTESIAN FLOW ~ 3800'

WATER ENTRIES:

HOT WATER ENTERS ~3800' FLOWS UP TO ~1900'

LITHOLOGY — MINERALOGY

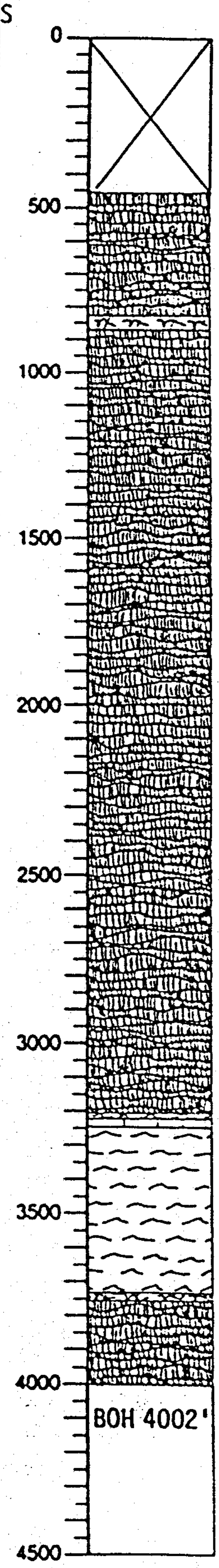

INTERVAL/FT.	DESCRIPTION
0-450	No sample.
450-820	Basalt flows intercalated with interflow breccias and scoria deposits.
820-862	Andesite flow.
862-3195	Basalt and basaltic andesite flow intercalated with interflow breccias and scoria deposits. Minor sporadic lithic tuffs and vitric tuffs ranging from rhyodacite to andesite in composition.
3195-3209	Rhyodacite flow.
3209-3242	Basalt flows.
3242-3729	Rhyodacite flows and rhyodacitic black glass flows.
3729-3753	Andesitic lithic tuffs.
3753-4002	Basalt flows intercalated with interflow breccias and scoria deposits.

Figure C1

TABLE C 1/1

WHOLE ROCK ANALYTICAL RESULTS OF CORE HOLE GEO N-3

Sample# GEO	Depth in ft.	Name	Si	Al	Fe	Mg	CA	NA	K	Ti	LOI	BA	Total
			Reported as percentage oxides										
31	487	B	54.9	18.8	7.8	4.3	9.6	3.8	0.8	1.1	<0.05	0.029	101.455
32	852	A	61.5	16.3	7.3	2.3	5.1	4.9	1.7	1.1	<0.05	0.074	100.809
33	1062	B	52.8	19.3	8.8	4.1	9.6	3.8	0.7	1.3	<0.05	0.029	100.787
34	1702	BA	55.1	16.7	9.3	4.8	8.6	4.0	0.9	1.4	<0.05	0.045	101.330
35	1796	*B (T)	49.9	27.8	7.2	1.1	2.2	1.7	0.6	1.2	9.15	0.166	92.220
36	1862	B	54.0	19.5	7.4	4.0	9.2	3.5	0.9	1.0	0.09	0.033	99.842
37	1949	BA	55.7	19.5	7.1	4.0	8.7	3.9	1.0	1.0	<0.05	0.037	101.127
38	2216	BA	56.3	17.6	9.1	4.6	7.8	4.2	1.0	1.3	<0.05	0.039	102.179
39	2275	B	52.3	20.8	7.5	4.1	10.5	3.5	0.7	1.0	<0.05	0.029	100.629
40	2343	B	53.9	19.9	7.4	3.9	9.6	3.8	0.9	1.1	<0.05	0.034	100.704
41	2387	B	52.8	17.0	10.0	5.3	8.6	3.4	0.7	1.5	<0.05	0.032	100.325
42	2441	B	52.3	16.7	10.7	5.5	9.0	3.9	0.7	1.5	<0.05	0.031	100.910
43	2511	RD (T)	71.7	13.6	2.5	0.5	1.4	3.5	4.4	0.3	2.29	0.122	98.111
44	2538	B	48.7	16.8	10.5	8.8	10.14	3.1	0.3	1.4	<0.05	0.011	100.116
45	2644	B	50.3	16.6	9.2	6.8	9.7	3.1	0.5	1.4	0.47	0.021	97.999
46	2799	B	50.4	16.8	10.5	6.7	9.8	3.4	0.4	1.4	<0.05	0.018	99.663
47	2881	B	49.2	16.6	10.5	7.7	9.4	3.1	0.5	1.3	1.16	0.021	98.678
48	3098	B	51.7	17.1	10.2	5.3	8.4	4.0	0.7	1.4	0.05	0.033	99.185
49	3132	A (T)	62.8	14.8	6.4	1.5	3.2	2.1	4.2	1.1	2.35	0.084	96.539
50	3239	B	54.4	19.6	6.8	3.4	8.8	3.8	0.9	0.93	0.96	0.040	98.910
51	3262	RD	71.7	13.7	3.0	0.2	1.1	5.0	3.7	0.4	0.56	0.124	98.914
52	3311	RD	72.2	14.0	3.0	0.2	0.9	5.1	3.7	0.4	0.28	0.122	99.729
53	3365	RD	71.3	14.7	3.6	0.3	1.4	5.6	3.3	0.5	0.47	0.111	101.005
54	3472	RD	72.0	14.5	3.8	0.3	1.2	5.9	3.4	0.5	0.64	0.112	101.824
55	3608	RD	70.9	14.5	3.9	0.4	1.2	5.7	3.3	0.5	0.51	0.109	100.638
56	3741	BA (T)	58.1	14.8	10.3	2.5	5.5	4.8	1.6	1.9	<0.05	0.061	100.217
57	3790	B	48.7	18.9	10.3	4.2	11.1	3.3	0.3	1.3	2.03	0.022	98.411
58	3961	B	49.7	17.0	10.3	6.4	9.7	3.2	0.5	1.4	1.16	0.019	98.552

* (T) denotes analysis of ash in tuff unit

Basalt	< 55%	SiO2
Basaltic andesite	55-60%	SiO2
Andesite	60-65%	SiO2
Dacite	65-70%	SiO2
Rhyodacite	70-75%	SiO2
Rhyolite	> 75%	SiO2

TABLE C 1/2

WHOLE ROCK ANALYTICAL RESULTS OF CORE HOLE GEO N-3

Reported as trace elements ppm

Sample # GEO	Depth in ft.	Name	Sr	Cr	Co	Ni	Cu	Zn	Li	Be	Zr	La	Ce	LOI	Total
31	487	B	489	129	34	42	85	71	6	1.3	87	18	ND**	<0.05	101.455
32	852	A	374	43	22	17	20	87	13	1.7	143	22	ND	<0.05	100.809
33	1062	B	499	72	36	34	59	80	7	1.4	94	18	ND	<0.05	100.787
34	1702	BA	458	141	28	46	67	86	9	1.6	134	24	ND	<0.05	101.330
35	1796	*B (T)	283	22	7	10	22	125	99	4.0	560	46	71	9.15	92.220
36	1862	B	495	133	40	69	119	69	7	1.3	92	18	ND	0.09	99.842
37	1949	BA	481	125	30	65	50	65	7	1.4	104	19	ND	<0.05	101.127
38	2216	BA	435	112	31	53	70	85	8	1.6	111	19	ND	<0.05	102.179
39	2275	B	528	118	30	49	61	62	7	1.3	83	24	16	<0.05	100.629
40	2343	B	488	115	33	41	56	71	10	1.4	99	24	14	<0.05	100.704
41	2387	B	443	117	37	48	85	83	8	1.6	103	24	13	<0.05	100.325
42	2441	B	414	160	41	56	95	91	9	1.7	111	25	15	<0.05	100.910
43	2511	RD (T)	100	8	20	5	9	44	27	2.0	176	32	42	2.29	98.111
44	2538	B	277	273	55	176	80	74	6	1.5	100	22	ND	<0.05	100.116
45	2644	B	358	171	39	108	49	72	9	1.5	103	25	17	0.47	97.999
46	2799	B	360	144	49	95	147	96	7	1.5	96	23	11	<0.05	99.663
47	2881	B	290	241	45	127	168	89	12	1.6	99	23	11	1.16	98.678
48	3098	B	475	109	38	19	27	93	8	1.6	104	25	19	0.30	99.185
49	3132	A (T)	364	8	20	7	17	109	18	2.3	252	34	46	2.35	96.539
50	3239	B	475	93	24	55	45	71	9	1.5	118	25	15	0.96	98.910
51	3262	RD	90	23	19	11	7	56	28	2.6	411	35	49	0.56	98.914
52	3311	RD	89	20	9	10	6	60	9	2.5	405	30	40	0.28	99.729
53	3365	RD	122	143	16	60	9	98	21	2.7	415	39	60	0.47	101.005
54	3472	RD	116	66	9	29	8	91	19	2.8	451	34	49	0.64	101.824
55	3608	RD	119	54	18	24	7	92	18	2.8	427	36	55	0.51	100.638
56	3741	BA (T)	272	26	26	15	22	122	10	2.4	241	31	33	<0.05	100.217
57	3790	B	436	193	41	136	89	89	20	1.5	90	23	ND	2.03	98.411
58	3961	B	338	173	42	129	72	79	8	1.4	90	20	ND	1.16	98.552

* (T) denotes analysis of ash in tuff unit

** ND = not detected.

Basalt	< 55%	SiO2
Basaltic andesite	55-60%	SiO2
Andesite	60-65%	SiO2
Dacite	65-70%	SiO2
Rhyodacite	70-75%	SiO2
Rhyolite	> 75%	SiO2

FIGURE C8

K/AR AGE DATES FOR CORE HOLE GEO N-3. Samples were submitted to the University of Arizona Laboratory of Isotope Geochemistry where rocks were ground, sieved to 100-150 mesh, and the feldspar-rich fraction concentrated using magnetic and heavy-liquid separation techniques. The basic data is included in Table C8.

CORE HOLE GEO N-3
K/AR AGE DATES
NEWBERRY VOLCANO, OREGON

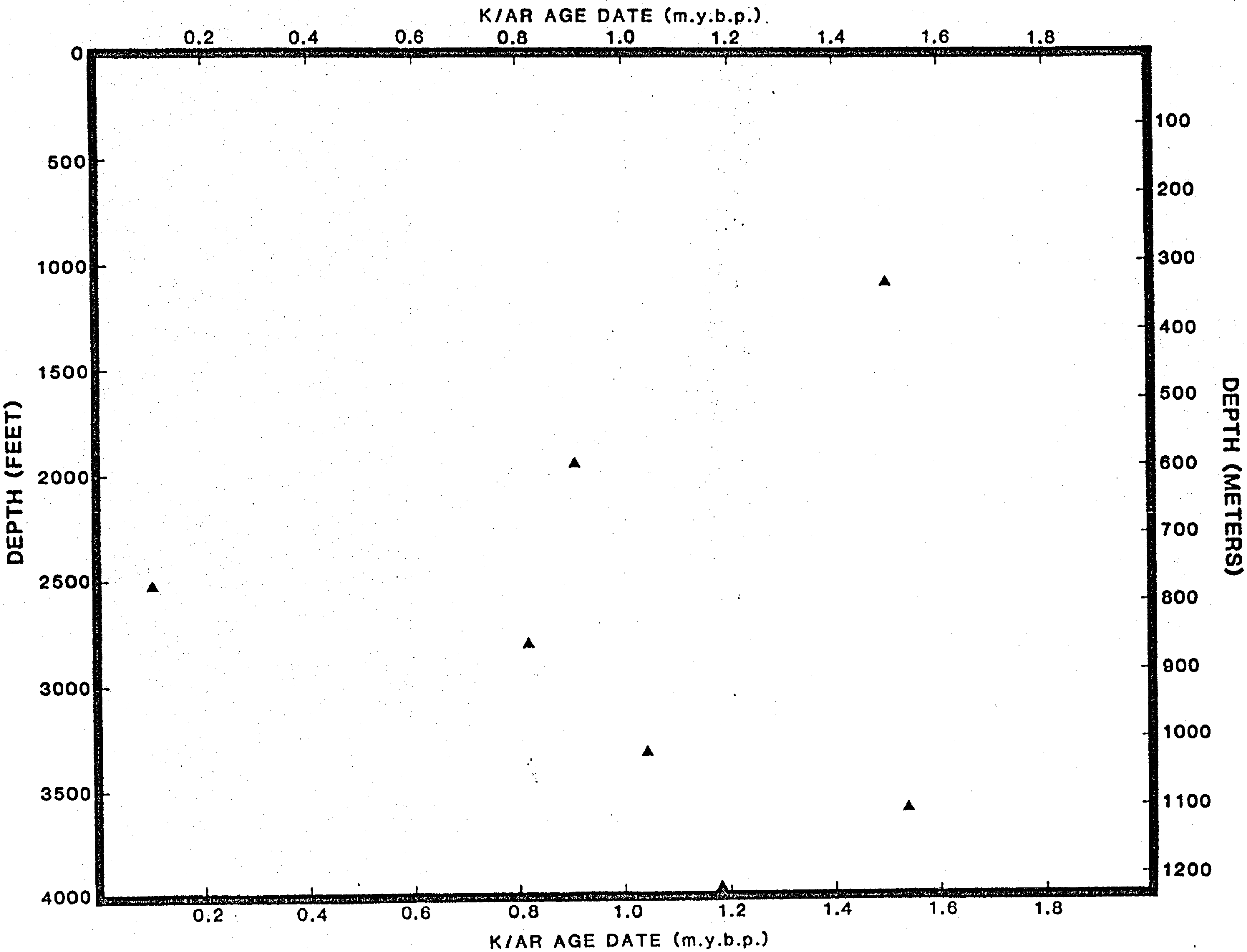

Figure C8

TABLE C8

K/AR AGE DATES: CORE HOLE GEO N-3

Newberry Volcano, Oregon

Sample # GEO	Sample # U.A.*	Depth/ft.	Description	Age (mybp)
1	86-207	1062	phyric basalt	1.50 + 0.63
2	86-208	1949	phyric basaltic andesite	0.911 + 0.188
3	86-209	2524	lithic tuff	0.109 + 0.081
4	86-210	2799	basalt	0.819 + 0.113
5	86-211	3312	rhyodacitic flow	1.04 + 0.03
6	86-212	3608	rhyodacitic flow	1.54 + 0.05
7	86-213	3961	basalt	1.18 + 0.30

* University of Arizona Isotope Laboratory

University of Arizona
Isotope Geochemistry Laboratory
Date of Report: 9 Feb 1987

Project: GEO-NEWBERRY Crater Inc
Cliff Walkey
Walter Randall

Sample Number
UAKA 86-207   Originator's - N-3 #1

Sample Information
Basalt, groundmass feldspar concentrate,
Newberry Volcano, east of High Cascade axis, Oregon

Analytical Data

Potassium Data	Potassium Mean	Radiogenic Ar pm/g Data	Radiogenic Ar pm/g Mean	% Atm. Ar Data	% Atm. Ar Mean	Reported Date + Err
0.471	0.472	1.376	1.232	99.0	98.8	1.50 + 0.63
0.472		1.136		98.7		
0.472		1.171		99.0		
0.474		1.209		99.0		
		1.270		98.6		

Sample Number
UAKA 86-208   Originator's - N-3 # 2

Sample Information
Basalt, groundmass feldspar concentrate,
Newberry Volcano, east of High Cascade axis, Oregon

Analytical Data

Potassium Data	Potassium Mean	Radiogenic Ar pm/g Data	Radiogenic Ar pm/g Mean	% Atm. Ar Data	% Atm. Ar Mean	Reported Date + Err
0.727	0.728	1.249	1.151	95.9	96.3	0.911 +0.188
0.728		1.173		96.2		
0.730		1.117		96.4		
		1.066		96.8		

University of Arizona
Isotope Geochemistry Laboratory
Date of Report: 9 Feb 1987

Project: GEO-NEWBERRY Crater Inc
Cliff Walkey
Walter Randall

Sample Number
UAKA 86-209 Originator's - N-3 #3

Sample Information
Lithic tuff, feldspar concentrate with some glass,
Newberry Volcano, east of High Cascade axis, Oregon

Analytical Data

Potassium		Radiogenic Ar pm/g		% Atm. Ar		Reported
Data	Mean	Data	Mean	Data	Mean	Date + Err
3.604	3.614	0.696	0.686	99.7	99.4	0.109 +0.081
3.626		0.777		99.6		
3.648		0.404		99.8		
3.577		0.868		98.7		

Sample Number
UAKA 86-210 Originator's - N-3 #4

Sample Information
Basalt, groundmass feldspar concentrate,
Newberry Volcano, east of High Cascade axis, Oregon

Analytical Data

Potassium		Radiogenic Ar pm/g		% Atm. Ar		Reported
Data	Mean	Data	Mean	Data	Mean	Date + Err
0.388	0.387	0.487	0.550	95.1	94.5	0.819 +0.113
0.383		0.605		94.0		
0.384		0.5		95.4		
0.398		0.607		93.7		
0.386						
0.381						

University of Arizona
Isotope Geochemistry Laboratory
Date of Report: 9 Feb 1987

Project:GEO-NEWBERRY Crater Inc
Cliff Walkey
Walter Randall

Sample Number
UAKA 86-211 Originator's - N-3 # 5

Sample Information
Rhyodacite, groundmass feldspar concentrate,
Newberry Volcano, east of High Cascade axis, Oregon

Analytical Data

Potassium Data	Potassium Mean	Radiogenic Ar pm/g Data	Radiogenic Ar pm/g Mean	% Atm. Ar Data	% Atm. Ar Mean	Reported Date + Err
2.892	2.906	5.400	5.241	64.0	65.7	1.04 + 0.03
2.906		5.272		65.7		
2.919		5.050		67.1		
		5.241		65.9		

Sample Number
UAKA 86-212 Originator's - N 3 # 6

Sample Information
Rhyodacite, groundmass feldspar concentrate,
Newberry Volcano, east of High Cascade axis, Oregon

Analytical Data

Potassium Data	Potassium Mean	Radiogenic Ar pm/g Data	Radiogenic Ar pm/g Mean	% Atm. Ar Data	% Atm. Ar Mean	Reported Date + Err
2.549	2.574	6.896	6.882	58.3	59.0	1.54 + 0.05
2.578		6.917		59.1		
2.594		6.855		59.4		
		6.860		59.3		

Sample Number
UAKA 86-213 Originator's - N-3 #7

Sample Information
Basalt, groundmass feldspar concentrate,
Newberry Volcano, east of High Cascade axis, Oregon

Analytical Data

Potassium Data	Potassium Mean	Radiogenic Ar pm/g Data	Radiogenic Ar pm/g Mean	% Atm. Ar Data	% Atm. Ar Mean	Reported Date + Err
0.351	0.354	0.762	0.722	97.6	97.8	1.18 + 0.30
0.354		0.773		97.6		
0.357		0.631		98.1		

Thin Section Descriptions
Newberry Crater Core Hole N-3

Depth: 487'

Rock Type: (from whole rock geochemistry) Basaltic Andesite

Description: Holocrystalline, seriate-glomeroporphyritic; Phenocrysts of subhedral to euhedral labradorite plagioclase laths up to 2.1mm, minor subhedral to euhedral olivine crystals up to 0.9mm and trace rounded to subhedral augite crystals up to 0.6mm in an intergranular matrix of labradorite microlaths, granular clinopyroxene <.01mm and granular iron ore <.01mm.

Depth: 848'

Rock Type: Andesite

Description: Holocrystalline, very fine grained equigranular, pilotaxitic. Flow banded euhedral laths and microlaths of labradorite plagioclase up to 0.4mm in an intergranular matrix of granular clinopyroxene <.01mm and granular iron ore.

Depth: 1062'

Rock Type: Basaltic Andesite

Description: Holocrystalline, seriate-glomeroporphyritic, locally subophitic; Euhedral laths of labradorite plagioclase, 0.1 to 2.6mm, and trace phenocrysts of subhedral to rounded olivine up to 0.8mm in a subophitic to granular matrix of clinopyroxene with very rare granular iron ore <.01mm.

Depth: 1266'

Rock Type: N/A

Description: Hypohyaline, crystal lapilli tuff, unwelded; Globular to arcuate lapilli of phenocryst-bearing glass and pumice up to 6.0mm and minor (10%) lapilli of basaltic cinder scoria, 0.1 to 3.0mm, in a frothy vitroclastic glass groundmass. Phenocrysts consist of euhedral to subhedral labradorite laths, <.01 to 0.4mm, and rare euhedral columnar augite, <0.1 to 0.2mm. Glass and pumice has been altered to a yellow brown to red brown palagonite.

Depth: 1353'

Rock Type: Basaltic Andesite

Description: Holocrystalline, seriate-glomeroporphyritic, vesicular; Euhedral laths of labradorite, .01 to 1.8mm, and subhedral to rounded grains of olivine up to 0.8mm in an intergranular matrix of rounded to anhedral grains of clinopyroxene, 0.005 to 0.2mm, and rare iron ores <.01mm. Vesicles are elongate, generally rounded cavities up to 2.5mm in length; diktytaxitic.

Depth: 1702'

Rock Type: Basaltic Andesite

Description: Holocrystalline, fine grained equigranular, weakly pilotaxitic, vesicular. Euhedral laths of labradorite plagioclase, <0.01 to 0.6mm, and minor subhedral to rounded grains of olivine and augite, up to 0.3mm, in an intergranular matrix of granular clinopyroxene, olivine and trace iron oxides <.01mm. Vesicles are subrounded bubble cavities up to 0.4mm; diktytaxitic.

Depth: 1791'

Rock Type: N/A

Description: Hypohyaline, crystal lapilli tuff, unwelded; Crystal-bearing glassy lapilli and rare pumiceous fragments up to 7.0mm rounded fragments of cinder scoria and basalt up to 6.0mm in a crystal-rich ashy matrix. Abundant euhedral laths of plagioclase (labradorite?), <0.1 to 0.6mm, very minor columnar to anhedral phenocrysts of augite up to 0.5mm and very rare olivine crystals up to 0.4mm. Glass material has been altered to yellow brown palagonite.

Depth: 1796'

Rock Type: Basalt

Description: Hypohyaline, vitric tuff, densely welded. Agglomerated lapilli and fiamme of yellow brown glass up to 1cm in length in a matrix of yellow brown to reddish brown crystal-rich ash and vitroclastic material. Fluidal banding well developed. Phenocrysts include plagioclase, clinopyroxene and iron ore. Also contains lithic fragments of cinder scoria, basalt and rhyodacite(?).

Depth: 1827'

Rock Type: N/A (Basaltic Andesite?)

Description: Hypohyaline, porphyritic, vesicular; Euhedral laths of labradorite plagioclase, <0.01 to 1.0mm, with trace subhedral to rounded grains of clinopyroxene and very rare olivine <0.1mm in a frothy, vesicular green glass groundmass. Round bubble-shaped vesicles up to 0.5mm are also present.

Depth: 1861'

Rock Type: Basaltic Andesite

Description: Hypocrystalline, seriate-glomeroporphyritic; Euhedral laths of labradorite plagioclase, <0.01 to 3.4mm, with minor subhedral, embayed olivine, <0.01 to 1.2mm, and trace subhedral to granular augite, <0.01mm to 0.6mm, in an intersertal dark green glassy groundmass. Groundmass contains abundant microlites and cryptolites of plagioclase, clinopyroxene and iron ore.

Depth: 1949'

Rock Type: Basaltic Andesite

Description: Holocrystalline, seriate-glomeroporphyritic; Euhedral laths of labradorite plagioclase, 0.02 to 4.0mm, with rare subhedral, embayed crystals of olivine up to 1.1mm and very rare subhedral columnar augite up to 0.35mm, in an intergranular matrix of plagioclase microlites, granular clinopyroxene and granular iron ore. Olivine is partially altered to iddingsite.

Depth: 2102'

Rock Type: N/A (Basaltic Andesite?)

Description: Holocrystalline, seriate glomeroporphyritic; Euhedral laths of labradorite plagioclase, 0.02 to 3.0mm, with rare subhedral to rounded grains up to 0.3mm of olivine and augite in an intergranular matrix of plagioclase microlites and granular clinopyroxene and iron ore <0.01mm. Olivines are partially altered to iddingsite.

Depth: 2216'

Rock Type: Basaltic Andesite

Description: Holocrystalline, seriate, pilotaxitic. Euhedral and embayed and sieve-textured bytownite plagioclase laths (approximately 5% of total rock) up to 2.3mm and rare embayed grains of olivine up to 0.3mm in an intergranular matrix of labradorite plagioclase laths, granular clinopyroxene and granular iron ore. Microlites display subparallel orientations.

Depth: 2275'

Rock Type: Basaltic Andesite

Description: Holocrystalline, seriate-glomeroporphyritic, vesicular; Euhedral laths of labradorite plagioclase, 0.2 to 4.0mm, with minor subhedral to rounded grains of augite, up to 0.4mm, and rare subhedral, embayed grains of olivine, up to 0.7mm, in an intergranular matrix of plagioclase microlites, granular clinopyroxene and granular iron oxides. Vesicles are rounded to elongate cavities, 0.2 to 0.8mm; diktytaxitic.

Depth: 2343'

Rock Type: Basaltic Andesite

Description: Holocrystalline, seriate-glomeroporphyritic, Euhedral laths of labradorite plagioclase, 0.1 to 3.2mm, with rare subhedral, embayed olivine grains up to 0.3mm and subhedral, embayed augite grains up to 0.4mm in an intergranular matrix of plagioclase microlites, granular clinopyroxene and granular iron ore.

Depth: 2387'

Rock Type: Basaltic Andesite

Description: Holocrystalline, very fine grained equigranular, ophimottled, pilotaxitic, vesicular; Euhedral labradorite plagioclase laths, 0.1 to 0.3mm with rare phenocrysts up to 0.6mm in an intergranular matrix that grades from granular clinopyroxene with subordinant granular iron ore to subophitic clinopyroxene to intermeshed ophimottle plates of clinopyroxene up to 0.4mm. Vesicles are irregular to rounded cavities up to 0.75mm; diktytaxitic. Plagioclase microlaths display subparallel orientations.

Depth: 2441'

Rock Type: Basaltic Andesite

Description: Holocrystalline, very fine grained equigranular, pilotaxitic; Euhedral laths of labradorite plagioclase, <.01mm to 0.2mm, in an intergranular matrix of granular clinopyroxene and granular iron oxides. Very minor, <5%, intersertal green glass.

Depth: 2511'

Rock Type: Rhyodacite

Description: Holohyaline, pumice lapilli tuff, poorly welded; Rounded to irregularly-shaped pumice fragments up to 3mm and trace cinder and basaltic clasts up to 0.8mm in a vitroclastic matrix of glass shards and ash. Rare embayed plagioclase phenocrysts up to 0.2mm.

Depth: 2524'

Rock Type: N/A (Rhyodacite?)

Description: Holohyaline, pumice lapilli tuff, poorly welded. Pumice lapilli up to 5mm, and lithic fragments of cinders and basalt up to 4mm, in a vitroclastic matrix of glass shards and ash. Similar to 2511' but has a higher percentage of lithics and larger pumice lapilli.

Depth: 2538'

Rock Type: Tholeiitic Basalt

Description: Holohyaline, seriate; Euhedral laths of labradorite plagioclase, 0.1 to 0.7mm, with abundant rounded grains of olivine, 0.1 to 0.4mm, infilled by subophitic (locally granular) clinopyroxene. Very rare granules of iron ore <0.1mm. Sample has a microdiabasic texture. Olivines are commonly rimmed by iddingsite.

Depth: 2644'

Rock Type: Tholeiitic Basalt

Description: Holocrystalline, seriate, vesicular; Euhedral laths of labradorite plagioclase, 0.1 to 1.8mm, with minor amounts of rounded to subhedral olivine grains, <0.1 to 0.2mm, infilled by subophitic clinopyroxene and granular iron ore. Very minor amount (<2%) of intersertal brown glass. Vesicles are rounded cavities which are commonly lined with brown glass; diktytaxitic. Very similar to 2538'.

Depth: 2799'

Rock Type: Tholeiitic Basalt

Description: Hypocrystalline, fine grained equigranular; Euhedral laths of labradorite plagioclase, <0.1 to 0.5mm, and rare subhedral to rounded grains of olivine, <0.1mm, infilled by subophitic to weakly ophimottled clinopyroxene. Minor amount, approximately 5%, of intersertal dark brown opaque devitrified glass.

Depth: 2881'

Rock Type: Tholeiitic Basalt

Description: Hypocrystalline, fine grained equigranular; ophimottled; Euhedral laths of Labradorite plagioclase, <0.1 to 0.6mm, and very rare subhedral, embayed olivine up to 0.4mm, infilled partially by ophitic crystals of clinopyroxene up to 1.4mm across and partially by intersertal brownish green glass. Clinopyroxene to glass ratio is approximately 2:1. Very rare granular iron ore.

Depth: 3020'

Rock Type: N/A (Tholeiitic Basalt)

Description: Hypocrystalline, very fine grained equigranular, vesicular; Euhedral microlaths of Labradorite plagioclase, up to 0.4mm but generally <0.1mm, with very minor granular clinopyroxene and iron ore, <0.01mm, in a highly vesicular intersertal groundmass of dark brown opaque devitrified glass. Vesicles are small, <0.2mm, and round.

Depth: 3087'

Rock Type: N/A (Tholeiitic Basalt?)

Description: Holocrystalline, very fine grained equigranular; Euhedral laths of labradorite plagioclase, <0.1 to 0.3mm, with rare phenocrysts up to 0.9mm, in an intergranular matrix of granular clinopyroxene <0.01mm and granular iron ore <0.01mm.

Depth: 3098'

Rock Type: Tholeiitic Basalt

Description: Holocrystalline, fine grained equigranular, pilotaxitic; Euhedral laths of labradorite plagioclase, <0.1mm to 0.2mm with rare phenocrysts up to 4.0mm, and minor amounts of rounded to subhedral olivine, <0.1mm to 0.2mm, in an intergranular matrix of granular clinopyroxene <0.01mm and granular iron ore <0.01mm. Olivine crystals are pervasively to completed replaced by iddingsite and iron oxides.

Depth: 3122'

Rock Type: Dacite

Description: Hypohyaline, lithic lapilli crystal tuff, welded; Globular to spindle-shaped lapilli and fiamme of crystal-bearing devitrified glass up to 15mm in length in a crystal-rich vitroclastic matrix of arcuate glass shards, ash and glass dust. Phenocrysts in the glass lapilli and matrix are identical consisting of andesine plagioclase laths, <0.05 to 0.8mm, and rare columnar crystals of augite, <0.01 to 0.15mm. Tuff also contains approximately 20% lithic fragments ranging up to 6.0mm in length. Lithics are basalt, cinders, rhyodacite(?) and pumice. Glass and matrix are brown to yellow brown.

Depth: 3143'

Rock Type: N/A (Dacite or Andesite)

Description: Hypohyaline, lithic vitric tuff, welded. Subangular to rounded lithic fragments, <0.1 to 10mm, in a crystal-bearing dusky red brown glassy matrix. Lithic fragments are extremely varied: several basalts, basaltic cinder scoria, pumice, rhyodacite and frothy red brown glassy material (pre-existing tuff?). Phenocrysts includes euhedral, partially embayed labradite plagioclase laths up to 1.1mm in length and subhedral to euhedral columnar augite up to 0.4mm in length.

Depth: 3204'

Rock Type: N/A (Basaltic Andesite)

Description: Hypocrystalline, very fine grained equigranular; Microlites and microlaths of labradorite plagioclase up to 0.3mm in length, rare subhedral, embayed crystals of clinopyroxene up to 0.2mm and rare polygonal iron ore up to 0.1mm in an intersertal matrix of pale green glass. Basaltic cinder scoria inclusions, <0.1 to 1.4mm are also incorporated in the glassy matrix.

Depth: 3239'

Rock Type: Basaltic Andesite

Description: Hypocrystalline, seriate-glomeroporphyritic, vesicular. Euhedral labradorite plagioclase laths, 0.1 to 5mm, in an intergranular matrix of plagioclase microlites, granular clinopyroxene <0.05mm and opaque iron ore <0.01mm. Approximately 20% of the groundmass is intersertal dark greenish gray dust-filled, devitrified glass. Vesicles, <0.1 to 1.5mm, comprise approximately 15% of total area. Cavities range from irregular arcuate to rounded geometries. Vesicles are partially to completely filled with greenish tc greenish brown clays. There is also very minor replacement of plagioclase by greenish brown clays.

Depth: 3263'

Rock Type: N/A (Rhyolite?)

Description: Holohyaline, glass flow; Agglomerate of rounded, arcuate and spindle-shaped pale green glassy fragments up to 5mm. Glass displays flow banding and contains abundant crystalline of plagioclase. Individual glass fragments have devitrified rims and open into irregular arcuate void spaces partly filled by black opaque material, yellow brown clays and spherical crystals of cristobalite up to .125mm.

Depth: 3311'

Rock Type: Rhyolite

Description: Hypocrystalline, cryptocrystalline, pilotaxitic; Microlites of plagioclase, <0.1mm, in a cryptocrystalline groundmass with abundant crystallites of plagioclase and iron ore with some very pale green glass. Rock composed of planar bands ranging from approximately 0.075 to 0.15mm. Platy fractures well developed along planar lamina with red brown opaque iron oxides and intergrowths of euhedral trydymite and cristobalite crystals lining open voids.

Depth: 3352'

Rock Type: N/A (Basalt?)

Description: Hypocrystalline, seriate, fine grained equigranular, pilotaxitic, vesicular; Microlaths of labradorite plagioclase, 0.1 to 0.2mm, with rare phenocrysts up to 0.75mm in an intergranular matrix of clinopyroxene and iron ore granules <.05mm grading into an intersertal groundmass of pale green glass. Glass constitutes approximately 20% of groundmass. Very rare of olivine up to 1.1mm in length completely replaced by a fine grained mixture of iddingsite, iron oxides and sphene. Vesicles, up to 0.6mm in length, are rounded elongate cavities partially filled by greenish clays; diktytaxitic.

Depth: 3365'

Rock Type: Rhyodacite

Description: Hypocrystalline, porphyritic; Embayed laths of andesine plagioclase up to 0.8mm, subhedral embayed columnar augite up to 0.3mm, and polygonal iron ore grains up to 0.1mm, in a cryptofelsic groundmass. Rock is flow banded, characterized by irregular lamina of holocrystalline cryptofelsic material alternating with cryptofelsic material grading into dark opaque green glass. Sporadic fractures parallel to the flow banding, <0.2mm, partially infilled with very fine grained cristobalite and calcite crystals.

Depth: 3472'

Rock Type: Rhyodacite

Description: Holocrystalline, porphyritic; Subhedral embayed andesine plagioclase, laths up to 2.1mm, subhedral embayed columnar clinopyroxene up to 0.7mm and polygonal to granular iron ore up to 0.1mm in a cryptofelsic groundmass. Rare fractures, <0.1mm, are partially infilled by cristobalite and yellow brown clays.

Depth: 3541'

Rock Type: Rhyodacite

Description: Holocrystalline, porphyritic, pilotaxitic; Subhedral embayed andesine plagioclase, laths up to 1.95mm, rare subhedral embayed columnar augite up to 0.3mm, and very rare iron ore up to 0.1mm, in a cryptofelsic groundmass. Flow banded with minor fractures subparallel to flow banding up to 0.95mm in width. Fractures contain drusy crystals of tridymite with interstitial calcite and iron oxides and also layers of yellow brown clays.

Depth: 3608'

Rock Type: Rhyodacite

Description: Holocrystalline, porphyritic; Trace amounts of phenocrysts consisting of subhedral embayed andesine laths up to 1.0mm, subhedral embayed augite crystals up to 0.2mm and granular iron ore <0.05mm in a cryptofelsic groundmass.

Depth: 3741'

Rock Type: Basaltic Andesite

Description: Hypocrystalline, seriate, vesicular; Euhedral laths of labradorite plagioclase, <0.1mm to 2.45mm, and minor rounded to subhedral columnar augite, <0.1mm to 0.5mm, in an intersertal matrix of dark gray green glass with abundant crystallites of clinopyroxene and iron ore. Approximately 20% of slide composed of lithic inclusions ranging from 1.2mm to 8.0mm in length. Lithics include rhyodacite, basaltic cinder scoria and flow basalts of widely varying textures. Rims of some inclusions, especially rhyodacite, show evidence of partial melting. Vesicles range from <.1mm to 2.2mm in length characterized by rounded to elongate geometries. Vesicles are partially to completely filled with massive to euhedral saucer-shaped siderite crystals and red to yellow brown clays. Minor patchy replacement of glassy groundmass by siderite is also present adjacent to siderite-bearing vesicles.

Depth: 3790'

Rock Type: Tholeiitic Basalt

Description: Hypocrystalline, seriate-fine grained equigranular, pilotaxitic, vesicular; Euhedral laths of labradorite plagioclase, 0.05 to 0.35mm, with rare rounded grains of augite less than 0.2mm in an intersertal matrix of black opaque devitrified glass with minor inclusions of granular clinopyroxene and iron ore <.01mm. Pseudomorphs of olivine completely replaced by red brown clays and carbonate are also present. Large round vesicles constitute approximately 5% of total area and range in size from 0.5 to 8mm. Vesicles are partially to completely infilled by botryoidal masses of clays (opaque black, dusky reddish brown, greenish brown, dark green), euhedral saucer-shaped siderite, and drusy aggregates of colorless calcite crystals.

Depth: 3961'

Rock Type: Tholeiitic Basalt

Description: Hypocrystalline, seriate-microdiabasic, vesicular; Euhedral laths of labradorite plagioclase, <0.1mm to 0.9mm, surrounded by subophitic platlets of augite up to 0.3mm and partially by intersertal devitrified, altered glass with minor granules of iron ore <0.05mm. Glass is pervasively altered to red brown to brown clays. Vesicles are rare and consist of rounded cavities up to 0.6mm which are partially to completely infilled by greenish brown clays, radiating spherical crystals of siderite and very fine-grained mosaic aggregates of carbonate.

JNS:bk
GE87-150.jns

N-3

Amygdaloidal and Fracture-Filling Secondary Mineral Assemblages in Samples from a Geothermal Field

by
Lori A. Bettison, M.S.

n.

RECEIVED
DATE 10/1/86 TIME mail
BY
GEO NEWBERRY

SUMMARY

Ten samples from various drill hole depths were examined with X-ray diffraction and secondary electron imaging on the scanning electron microscope. The following fracture and vesicle filling secondary minerals were identified: calcite, aragonite, siderite, marcasite, pyrite, tridymite, and magnesite. Table 1 lists the secondary phases identified at the depth represented by each sample.

	calcite	aragonite	siderite	marcasite	pyrite	tridymite	magnesite
2882'		X					
3412'				X	X	X	
3470'			X			X	
3540'			X	X	X	X	
3580'			X	X	X	X	
3705'			X	X	X	X	
3770'	X					X	
3948'	X	X	X			?	
3970'			X				X
3980'			X				X

Table 1

labeled "area" indicate the realtive abundance of a particular element within the area analyzed. However, these numbers cannot be used to estimate a quantitative analysis of a specimen. Not also that the X-ray anaysis cannot detect the presence of elements lighter (i.e., with atomic numbers less) than magnesium. Thus, the carbon in the carbonate analyses is not identified in the EDS print out. In addition, Cu and Fe characteristic X-ray lines can be excited from the objective lens pole pieces of the SEM.

RESULTS

Ten specimens from various drill hole depths were examined. Table 1 presents a summary of the fracture and vesicle mineralogy of each sample.

2882 feet: Clear, elongate, vesicle filling crystals were identified as aragonite with XRD.

3412 feet: X-ray diffraction indicates the presence of two sulfides on the surface of fractures: marcasite and pyrite. Interpretation of the XRD pattern suggests that marcasite is predominant. Qualitative analysis presented in Table 2A and s.e.i. confirms the presence of an Fe-sulfide (see s.e.i. photo 1). The presence of tridymite is also suggested by the XRD and EDS data.

3470 feet: Greenish-brown "balls: on the surface of fractures were identified as siderite using XRD. Qualitative analysis presented in Table 2B indicates that the phase is not pure (substitution of Ca and Mn for Fe^{2+}). The botryoidal or "ball" form of siderite, characteristic of samples in this study, is shown in photo 2. Tridymite identified from the XRD pattern is also shown in the s.e.i. photo.

3540 feet, 3580 feet, and 3705 feet: Materials scraped off the fracture surfaces of these three samples show similar X-ray diffraction patterns. The presence of tridymite (milky white crystals), marcasite and pyrite (green material), and minor siderite is indicated. Quantitative analyses presented in Tables 2C and 2D confirm the presence of these minerals. The presence of minor amounts of a phyllosilicate (smectite or illite) is suggested by EDS results; however, this is not confirmed by XRD.

3770 feet: The white blocky crystals were identified as calcite and the green "balls" as siderite from the XRD pattern.

3948 feet: Three forms of minerals were examined individually with XRD: 1) clear crystals, 2) milky white crystals, and 3) cream colored balls. The minerals were identified as: 1) aragonite, 2) calcite + aragonite, and 3) siderite. Siderite forms balls of webby textured crystals (photo 3), unlike the platy form from 3470 feet shown in photo 2 or columnar stacks which form the acicular needles shown in the sample from 3970 feet.

3970 feet: The blue amygdule-lining material and balls were identified as magnesite with XRD. SEM qualitative analysis presented in Table 2E confirms the presence of Mg and Ca. The acicular green crystals radiating outward from amygdule walls were identified as siderite with XRD and confirmed with qualitative analysis presented in Table 2F. Photo 4 is an s.e.i. picture of the relationship between these two phases.

3980 feet: The amygdule filling minerals in this sample are the same as those at 3970 feet: magnesite and siderite. S.e.i. photo 5 shows siderite in balls of platy crystals and in the webby texture described at 3948 feet.

QUALITATIVE ANALYSES

TABLE 2A: Fe-sulfide, tridymite

```
QUALITATIVE ELEMENT IDENTIFICATION

SAMPLE ID:3412

POSSIBLE IDENTIFICATION
  FE KA KB
  SI KA OR  RB LA
  S  KA OR  MO LA OR  TL MA?
  AU LA
  CU KA
```

PEAK LISTING

	ENERGY	AREA	EL. AND LINE
1	1.743	855	SI KA
2	2.294	271	S KA OR TL MA?
3	6.387	2099	FE KA
4	7.039	367	FE KB
5	8.024	137	CU KA
6	9.693	174	AU LA

TABLE 2B: siderite

```
QUALITATIVE ELEMENT IDENTIFICATION

SAMPLE ID:3470

POSSIBLE IDENTIFICATION
  FE KA KB
  CA KA
  MN KA OR  EU LA
  NB LA OR  AU LA MA
```

PEAK LISTING

	ENERGY	AREA	EL. AND LINE
1	2.144	198	AU MA
2	3.689	617	CA KA
3	5.891	341	MN KA
4	6.390	2055	FE KA
5	7.030	253	FE KB
6	9.684	198	AU LA

TABLE 2C: Fe-sulfide

QUALITATIVE ELEMENT IDENTIFICATION

SAMPLE ID:3540

POSSIBLE IDENTIFICATION
S KA OR MO LA OR TL MA? MZ1
FE KA KB
AU LA
CL KB OR PD LA
CU KA
ZN KA OR RE LA

PEAK LISTING

	ENERGY	AREA	EL. AND LINE
1	1.729	728	TL MZ1
2	2.304	20586	S KA OR TL MA?
3	2.841	720	PD LA
4	6.385	15130	FE KA
5	7.039	2040	FE KB
6	8.027	394	CU KA
7	8.590	282	RE LA
8	9.674	1238	AU LA

TABLE 2D: siderite, tridymite

QUALITATIVE ELEMENT IDENTIFICATION

SAMPLE ID:3540

POSSIBLE IDENTIFICATION
FE KA KB
CA KA KB
MN KA OR EU LA
NB LA OR AU LA MA
SI KA OR RB LA
CL KB OR PD LA
CU KA
MG KA OR AS LA?

PEAK LISTING

	ENERGY	AREA	EL. AND LINE
1	1.264	226	MG KA OR AS LA?
2	1.734	738	SI KA
3	2.150	1749	AU MA
4	2.843	358	PD LA
5	3.690	2103	CA KA
6	4.021	285	CA KB
7	5.887	1845	MN KA
8	6.389	15060	FE KA
9	7.039	1855	FE KB
10	8.027	274	CU KA
11	9.701	677	AU LA

TABLE 2E: magnesite

QUALITATIVE ELEMENT IDENTIFICATION

SAMPLE ID:3970

POSSIBLE IDENTIFICATION
- CA KA KB
- FE KA
- NB LA OR AU LA MA
- SI KA OR RB LA
- MG KA OR AS LA?

PEAK LISTING

	ENERGY	AREA	EL. AND LINE
1	1.251	89	MG KA OR AS LA?
2	1.736	160	SI KA
3	2.164	435	AU MA
4	3.690	3978	CA KA
5	4.014	562	CA KB
6	6.389	680	FE KA
7	9.671	224	AU LA

TABLE 2F: siderite

QUALITATIVE ELEMENT IDENTIFICATION

SAMPLE ID:3970

POSSIBLE IDENTIFICATION
- FE KA KB
- CA KA
- SI KA OR RB LA
- CU KA

PEAK LISTING

	ENERGY	AREA	EL. AND LINE
1	1.740	210	SI KA
2	3.686	621	CA KA
3	6.389	3767	FE KA
4	7.032	496	FE KB
5	8.038	135	CU KA

FIGURE B2

DRESSER ATLAS TEMPERATURE LOG OF 7-28-86 FOR GEO N-3, NEWBERRY VOLCANO, OREGON. This profile was constructed by GEO personnel from data taken from a continuous temperature log (see Table B2) which began 4 hours after last circulation of the core hole. Note the conductive slope for the last 100 plus feet.

TABLE B2

GEO CORE HOLE N-3

Temperature (F°) Log from Dresser Atlas of 7/28/86

Depth	0	10	20	30	40	50	60	70	80	90
0						52	52	52	52	52
100	52	52	52	52	52	51	51	51	51	51
200 to 690 = 51°										
700	51	51	50	50	50	50	50	50	50	50
800 to 1590 = 50°										
1600	50	50	51	52	53	53	53	53	54	53
1700	53	53	53	53	53	53	53	53	53	54
1800	54	54	54	54	54	55	55	55	55	55
1900	55	56	56	57	57	58	58	62	76	98
2000	101	103	104	105	106	106	106	107	107	107
2100	107	107	107	107	108	108	108	108	108	109
2200	109	109	109	109	109	109	110	110	110	110
2300	110	110	110	111	111	111	111	111	111	111
2400	112	112	112	112	112	112	113	113	113	113
2500	113	113	113	113	113	114	114	114	114	114
2600	114	114	114	115	115	115	115	115	115	115
2700	115	115	115	115	116	116	116	116	116	116
2800	116	116	116	117	117	117	117	117	117	117
2900	117	117	117	117	117	117	117	117	118	118
3000	118	118	118	118	118	118	118	118	119	119
3100	119	119	119	119	119	119	119	119	119	119
3200	119	119	119	119	119	119	120	120	120	120
3300	120	120	120	120	120	120	120	120	120	120
3400	120	121	121	121	121	121	121	121	121	121
3500 to 3690 = 121°										
3700	121	121	121	121	121	121	121	122	122	122
3800	122	122	122	121	121	121	121	121	121	122
3900	122	122	122	122	123	123	124	125	126	126
4000	125									
4002 BHT = 126°										

Note: this table was compiled from an analog record and was rounded to the nearest degree.

Logging operations begin 4 hours after last circulation of core hole.

Spud date: 6/2/86
Date TD reached: 7/29/86

TABLE B2

GEO CORE HOLE N-3

Temperature (F°) Log from Dresser Atlas of 7/28/86

Depth	0	10	20	30	40	50	60	70	80	90
0						52	52	52	52	52
100	52	52	52	52	52	51	51	51	51	51
200 to 690 = 51°										
700	51	51	50	50	50	50	50	50	50	50
800 to 1590 = 50°										
1600	50	50	51	52	53	53	53	53	54	53
1700	53	53	53	53	53	53	53	53	53	54
1800	54	54	54	54	54	55	55	55	55	55
1900	55	56	56	57	57	58	58	62	76	98
2000	101	103	104	105	106	106	106	107	107	107
2100	107	107	107	107	108	108	108	108	108	109
2200	109	109	109	109	109	109	110	110	110	110
2300	110	110	110	111	111	111	111	111	111	111
2400	112	112	112	112	112	112	113	113	113	113
2500	113	113	113	113	113	114	114	114	114	114
2600	114	114	114	115	115	115	115	115	115	115
2700	115	115	115	115	116	116	116	116	116	116
2800	116	116	116	117	117	117	117	117	117	117
2900	117	117	117	117	117	117	117	117	118	118
3000	118	118	118	118	118	118	118	118	119	119
3100	119	119	119	119	119	119	119	119	119	119
3200	119	119	119	119	119	119	120	120	120	120
3300	120	120	120	120	120	120	120	120	120	120
3400	120	121	121	121	121	121	121	121	121	121
3500 to 3690 = 121°										
3700	121	121	121	121	121	121	121	122	122	122
3800	122	122	122	121	121	121	121	121	121	122
3900	122	122	122	122	123	123	124	125	126	126
4000	125									
4002 BHT = 126°										

Note: this table was compiled from an analog record and was rounded to the nearest degree.

Logging operations begin 4 hours after last circulation of core hole.

Spud date: 6/2/86
Date TD reached: 7/29/86

FIGURE B5

BLACKWELL TEMPERATURE LOG OF 9/26/86 FOR CORE HOLE GEO N-3. This profile was constructed by GEO personnel from selected data in Table B5. The precision and accuracy of the temperature measurements are 0.01°F and 1°F. Temperatures were measured at 6.6 foot intervals. Note the conductive slope for the last 100 feet.

BLACKWELL TEMPERATURE LOG OF 9/26/86

NEWBERRY VOLCANO, OREGON

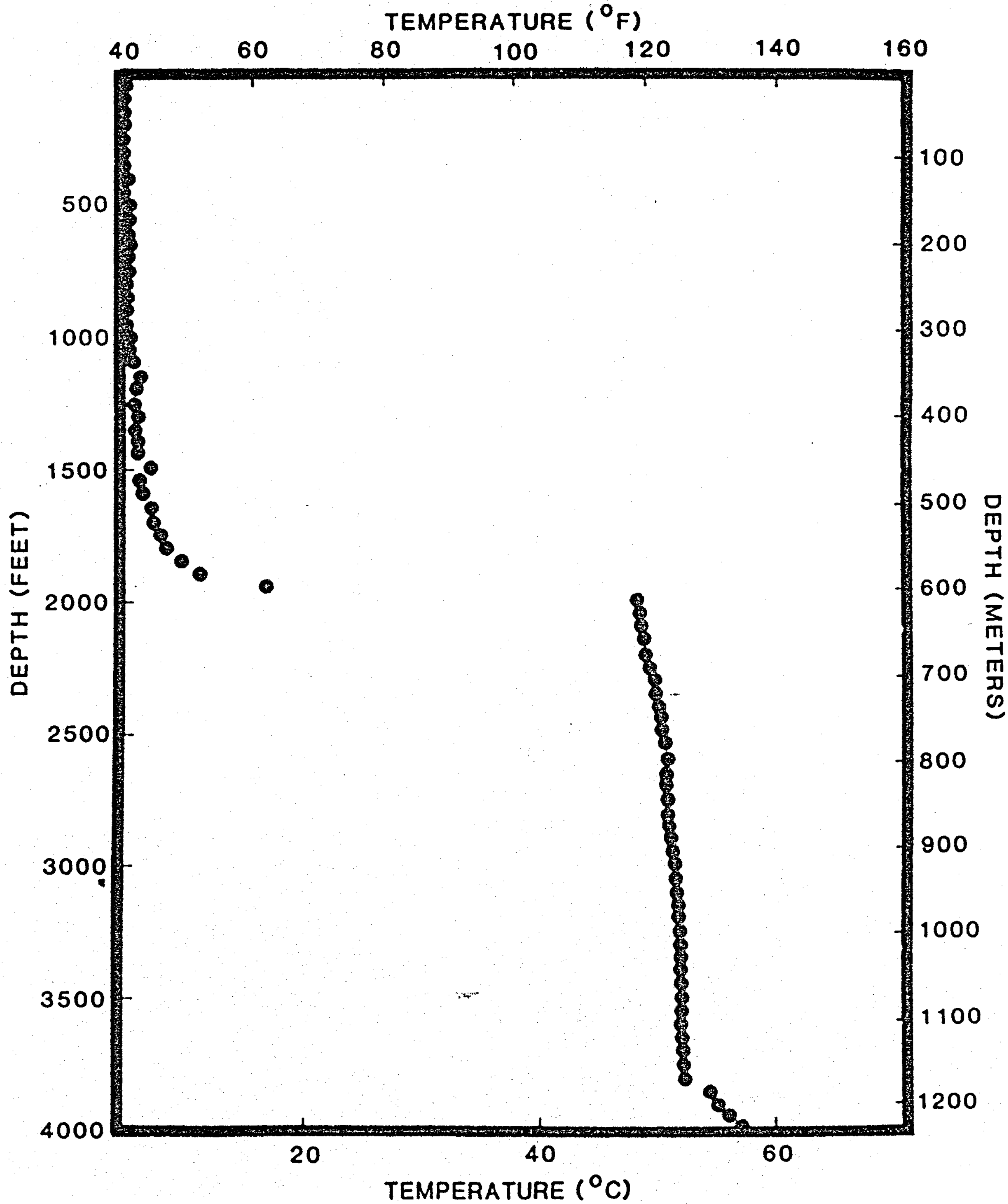

TABLE B5

GEO N-3

Temperature/Depth Data

Blackwell: 9/26/86

Depth Feet	Temperature Deg. F	Gradient Deg.F/100 Ft	Depth Feet	Temperature Deg. F	Gradient Deg.F/100 Ft
13.1	40.54	0.0	282.2	40.12	-1.0
19.7	40.77	3.5	288.7	40.24	1.7
26.2	40.93	2.4	295.3	40.47	3.5
32.8	41.06	2.1	301.8	40.64	2.7
39.4	41.18	1.8	308.4	40.94	4.6
45.9	41.29	1.6	315.0	41.22	4.2
52.5	41.39	1.7	321.5	41.27	0.8
59.1	41.67	4.2	328.1	41.18	-1.4
65.6	41.85	2.7	334.6	41.11	-1.2
72.2	41.80	-0.8	341.2	41.08	-0.4
78.7	41.71	-1.3	347.8	41.08	0.0
85.3	41.37	-5.2	354.3	41.07	-0.1
91.9	41.13	-3.6	360.9	41.02	-0.7
98.4	41.09	-0.6	367.5	40.99	-0.4
105.0	41.21	1.7	374.0	41.03	0.5
111.5	41.53	5.0	380.6	41.07	0.7
118.1	42.03	7.6	387.1	41.11	0.5
124.7	41.95	-1.3	393.7	41.21	1.5
131.2	41.48	-7.1	400.3	41.63	6.5
137.8	41.10	-5.8	406.8	42.20	8.6
144.4	40.88	-3.4	413.4	42.14	-0.9
150.9	40.96	1.3	419.9	41.96	-2.7
157.5	41.34	5.7	426.5	41.70	-4.0
164.0	41.51	2.6	433.1	41.46	-3.7
170.6	41.36	-2.2	439.6	41.21	-3.8
177.2	40.95	-6.3	446.2	40.98	-3.6
183.7	40.80	-2.3	452.8	40.87	-1.6
190.3	40.76	-0.7	459.3	40.82	-0.8
196.9	40.74	-0.2	465.9	40.83	0.2
203.4	40.79	0.7	472.4	40.87	0.6
210.0	40.96	2.6	479.0	40.92	0.7
216.5	41.38	6.5	485.6	40.97	0.8
223.1	42.20	12.4	492.1	41.05	1.2
229.7	42.11	-1.3	498.7	41.16	1.7
236.2	41.55	-8.7	505.2	41.30	2.2
242.8	41.14	-6.2	511.8	41.47	2.6
249.3	40.93	-3.1	518.4	41.66	2.9
255.9	40.83	-1.6	524.9	41.67	0.1
262.5	40.83	0.0	531.5	41.56	-1.8
269.0	40.73	-1.5	538.1	41.51	-0.7
275.6	40.19	-8.2	544.6	41.52	0.1

TABLE B5

GEO N-3

Temperature/Depth Data

Blackwell: 9/26/86

Depth Feet	Temperature Deg. F	Gradient Deg.F/100 Ft	Depth Feet	Temperature Deg. F	Gradient Deg.F/100 Ft
551.2	41.53	0.2	820.2	42.29	-0.8
557.7	41.52	-0.2	826.8	41.93	-5.5
564.3	41.51	-0.1	833.3	41.64	-4.4
570.9	41.50	-0.2	839.9	41.41	-3.5
577.4	41.50	0.1	846.5	41.28	-2.0
584.0	41.49	-0.2	853.0	41.23	-0.7
590.6	41.47	-0.3	859.6	41.24	0.2
597.1	41.45	-0.2	866.1	41.38	2.1
603.7	41.43	-0.3	872.7	41.57	2.8
610.2	41.41	-0.3	879.3	41.58	0.1
616.8	41.40	-0.2	885.8	41.56	-0.3
623.4	41.38	-0.3	892.4	41.52	-0.5
629.9	41.42	0.6	899.0	41.46	-1.0
636.5	41.55	2.0	905.5	41.39	-1.1
643.0	41.68	2.0	912.1	41.39	0.1
649.6	41.68	0.0	918.6	41.40	0.2
656.2	41.58	-1.5	925.2	41.41	0.2
662.7	41.53	-0.8	931.8	41.43	0.2
669.3	41.48	-0.7	938.3	41.43	0.0
675.9	41.51	0.4	944.9	41.40	-0.4
682.4	41.67	2.4	951.4	41.37	-0.6
689.0	41.79	1.8	958.0	41.36	-0.1
695.5	41.73	-0.9	964.6	41.41	0.8
702.1	41.63	-1.5	971.1	41.47	0.8
708.7	41.55	-1.3	977.7	41.52	0.8
715.2	41.52	-0.4	984.3	41.57	0.7
721.8	41.69	2.7	990.8	41.58	0.2
728.3	41.70	0.1	997.4	41.70	1.8
734.9	41.67	-0.4	1003.9	41.73	0.5
741.5	41.74	1.1	1010.5	41.65	-1.3
748.0	41.93	2.8	1017.1	41.53	-1.8
754.6	42.27	5.2	1023.6	41.47	-0.9
761.2	42.48	3.2	1030.2	41.47	0.0
767.7	42.20	-4.3	1036.7	41.56	1.3
774.3	41.52	-10.4	1043.3	41.75	3.0
780.8	41.31	-3.2	1049.9	41.82	1.1
787.4	41.26	-0.7	1056.4	41.77	-0.7
794.0	41.29	0.4	1063.0	41.77	-0.1
800.5	41.44	2.3	1069.6	41.81	0.6
807.1	41.90	7.1	1076.1	41.87	0.9
813.6	42.34	6.6	1082.7	41.91	0.7

TABLE B5

GEO N-3

Temperature/Depth Data

Blackwell: 9/26/86

Depth Feet	Temperature Deg. F	Gradient Deg.F/100 Ft	Depth Feet	Temperature Deg. F	Gradient Deg.F/100 Ft
1089.2	41.97	0.8	1358.3	42.40	1.6
1095.8	42.06	1.4	1364.8	42.51	1.6
1102.4	42.10	0.6	1371.4	42.59	1.3
1108.9	42.09	-0.2	1378.0	42.65	0.8
1115.5	42.32	3.5	1384.5	42.71	0.9
1122.0	42.88	8.6	1391.1	42.80	1.4
1128.6	43.34	6.9	1397.6	42.92	1.8
1135.2	43.31	-0.3	1404.2	43.06	2.2
1141.7	43.20	-1.8	1410.8	43.17	1.6
1148.3	43.03	-2.5	1417.3	43.20	0.5
1154.9	42.54	-7.6	1423.9	43.17	-0.5
1161.4	42.14	-6.1	1430.4	43.10	-1.1
1168.0	41.99	-2.3	1437.0	43.00	-1.5
1174.5	42.02	0.5	1443.6	42.90	-1.5
1181.1	42.31	4.4	1450.1	42.79	-1.6
1187.7	42.60	4.5	1456.7	42.73	-0.9
1194.2	42.67	1.0	1463.3	42.73	0.0
1200.8	42.54	-2.0	1469.8	42.81	1.3
1207.3	42.39	-2.3	1476.4	42.98	2.6
1213.9	42.27	-1.7	1482.9	43.21	3.4
1220.5	42.27	-0.1	1489.5	43.51	4.7
1227.0	42.25	-0.3	1496.1	43.90	5.9
1233.4	42.24	-0.1	1502.6	44.34	6.6
1240.2	42.20	-0.6	1509.2	44.70	5.5
1246.7	42.19	-0.2	1515.7	44.62	-1.1
1253.3	42.19	0.1	1522.3	44.09	-8.1
1259.8	42.04	-2.3	1528.9	43.61	-7.4
1266.4	41.82	-3.4	1535.4	43.35	-3.9
1273.0	42.20	5.9	1542.0	43.27	-1.2
1279.5	42.34	2.0	1548.6	43.27	0.1
1286.1	42.48	2.1	1555.1	43.30	0.4
1292.7	42.55	1.1	1561.7	43.32	0.3
1299.2	42.48	-1.0	1568.2	43.36	0.6
1305.8	42.35	-1.9	1574.8	43.43	1.1
1312.3	42.23	-1.9	1581.4	43.53	1.6
1318.9	42.15	-1.2	1587.9	43.59	0.9
1325.5	42.11	-0.6	1594.5	43.66	1.1
1332.0	42.12	0.2	1601.0	43.74	1.2
1338.6	42.17	0.7	1607.6	43.89	2.2
1345.1	42.23	0.9	1614.2	44.07	2.8
1351.7	42.30	1.1	1620.7	44.23	2.5

TABLE B5

GEO N-3

Temperature/Depth Data

Blackwell: 9/26/86

Depth Feet	Temperature Deg. F	Gradient Deg.F/100 Ft	Depth Feet	Temperature Deg. F	Gradient Deg.F/100 Ft
1627.3	44.38	2.3	1896.3	52.36	7.9
1633.9	44.54	2.4	1902.9	52.79	6.5
1640.4	44.71	2.5	1909.4	53.35	8.6
1647.0	44.90	3.0	1916.0	54.17	12.5
1653.5	45.22	4.8	1922.6	54.87	10.6
1660.1	45.70	7.3	1929.1	56.18	19.9
1666.7	46.14	6.7	1935.7	56.90	11.0
1673.2	46.41	4.0	1942.3	58.66	26.9
1679.8	46.24	-2.6	1948.8	62.91	64.7
1686.4	45.91	-4.9	1955.4	70.02	108.5
1692.9	45.64	-4.2	1961.9	81.01	167.6
1699.5	45.51	-2.0	1968.5	93.25	186.6
1706.0	45.46	-0.8	1975.1	107.00	209.6
1712.6	45.46	0.0	1981.6	116.80	149.4
1719.2	45.51	0.8	1988.2	119.28	37.8
1725.7	45.58	1.1	1994.8	119.44	2.4
1732.3	45.72	2.2	2001.3	119.47	0.5
1738.8	46.01	4.4	2007.9	119.52	0.7
1745.4	46.26	3.8	2014.4	119.55	0.4
1752.0	46.53	4.0	2021.0	119.58	0.6
1758.5	46.82	4.5	2027.6	119.59	0.1
1765.1	47.11	4.5	2034.1	119.60	0.1
1771.7	47.39	4.3	2040.7	119.61	0.1
1778.2	47.57	2.7	2047.2	119.63	0.3
1784.8	47.68	1.7	2053.8	119.69	1.0
1791.3	47.63	-0.7	2060.4	119.77	1.3
1797.9	47.67	0.5	2066.9	119.85	1.2
1804.5	47.82	2.3	2073.5	119.91	0.9
1811.0	48.03	3.2	2080.1	119.98	1.1
1817.6	48.28	3.8	2086.6	120.06	1.1
1824.1	48.54	4.0	2093.2	120.14	1.2
1830.7	48.82	4.2	2099.7	120.20	0.9
1837.3	49.06	3.7	2106.3	120.22	0.3
1843.8	49.29	3.5	2112.9	120.23	0.1
1850.4	49.47	2.6	2119.4	120.24	0.2
1857.0	49.57	1.6	2126.0	120.25	0.2
1863.5	50.04	7.1	2132.5	120.27	0.3
1870.1	50.52	7.4	2139.1	120.31	0.7
1876.6	50.90	5.8	2145.7	120.38	1.0
1883.2	51.46	8.5	2152.2	120.44	1.0
1889.8	51.85	5.9	2158.8	120.52	1.2

TABLE B5

GEO N-3

Temperature/Depth Data

Blackwell: 9/26/86

Depth Feet	Temperature Deg. F	Gradient Deg.F/100 Ft	Depth Feet	Temperature Deg. F	Gradient Deg.F/100 Ft
2165.4	120.60	1.2	2434.4	122.84	0.8
2171.9	120.66	0.9	2440.9	122.90	0.9
2178.5	120.73	1.1	2447.5	122.94	0.7
2185.0	120.81	1.1	2454.1	123.00	0.8
2191.6	120.88	1.2	2460.6	123.04	0.7
2198.2	120.95	1.1	2467.2	123.09	0.7
2204.7	121.01	0.9	2473.8	123.13	0.7
2211.3	121.05	0.5	2480.3	123.18	0.6
2217.8	121.09	0.7	2486.9	123.16	-0.2
2224.4	121.13	0.5	2493.4	123.16	-0.1
2231.0	121.14	0.1	2500.0	123.19	0.5
2237.5	121.14	0.1	2506.6	123.29	1.6
2244.1	121.16	0.2	2513.1	123.35	0.9
2250.7	121.25	1.4	2519.7	123.39	0.6
2257.2	121.30	0.8	2526.2	123.42	0.4
2263.8	121.36	1.0	2532.8	123.44	0.3
2270.3	121.42	0.8	2539.4	123.47	0.4
2276.9	121.47	0.8	2545.9	123.53	1.0
2283.5	121.53	0.9	2552.5	123.57	0.6
2290.0	121.58	0.7	2559.1	123.61	0.6
2296.6	121.63	0.8	2565.6	123.62	0.1
2303.1	121.68	0.7	2572.2	123.62	0.0
2309.7	121.74	1.0	2578.7	123.63	0.2
2316.3	121.79	0.7	2585.3	123.66	0.4
2322.8	121.83	0.7	2591.9	123.69	0.5
2329.4	121.92	1.3	2598.4	123.71	0.3
2336.0	121.99	1.1	2605.0	123.75	0.7
2342.5	122.06	1.1	2611.5	123.77	0.3
2349.1	122.11	0.8	2618.1	123.80	0.4
2355.6	122.19	1.2	2624.7	123.81	0.3
2362.2	122.26	1.0	2631.2	123.83	0.3
2368.8	122.31	0.8	2637.8	123.84	0.0
2375.3	122.38	1.0	2644.4	123.84	0.1
2381.9	122.41	0.5	2650.9	123.86	0.2
2388.5	122.51	1.5	2657.5	123.86	0.1
2395.0	122.57	1.0	2664.0	123.87	0.0
2401.6	122.62	0.8	2670.6	123.87	0.0
2408.1	122.67	0.8	2677.2	123.88	0.1
2414.7	122.71	0.5	2683.7	123.90	0.3
2421.3	122.76	0.8	2690.3	123.91	0.2
2427.8	122.79	0.4	2696.9	123.97	0.8

TABLE B5

GEO N-3

Temperature/Depth Data

Blackwell: 9/26/86

Depth Feet	Temperature Deg. F	Gradient Deg.F/100 Ft	Depth Feet	Temperature Deg. F	Gradient Deg.F/100 Ft
2703.4	123.99	0.4	2972.4	124.93	0.5
2710.0	124.01	0.3	2979.0	124.95	0.4
2716.5	124.01	0.0	2985.6	124.98	0.4
2723.1	124.01	0.0	2992.1	125.00	0.4
2729.7	124.04	0.4	2998.7	125.03	0.5
2736.2	124.05	0.2	3005.2	125.06	0.3
2742.8	124.06	0.0	3011.8	125.08	0.3
2749.3	124.06	0.1	3018.4	125.09	0.2
2755.9	124.06	0.0	3024.9	125.11	0.3
2762.5	124.06	-0.1	3031.5	125.14	0.4
2769.0	124.08	0.4	3038.1	125.16	0.4
2775.6	124.11	0.5	3044.6	125.19	0.3
2782.2	124.14	0.4	3051.2	125.21	0.4
2788.7	124.17	0.5	3057.7	125.24	0.5
2795.3	124.20	0.4	3064.3	125.26	0.2
2801.8	124.23	0.5	3070.9	125.28	0.3
2808.4	124.26	0.5	3077.4	125.31	0.6
2815.0	124.29	0.4	3084.0	125.33	0.2
2821.5	124.30	0.2	3090.6	125.35	0.4
2828.1	124.26	-0.7	3097.1	125.37	0.3
2834.6	124.36	1.6	3103.7	125.40	0.4
2841.2	124.40	0.6	3110.2	125.42	0.3
2847.8	124.42	0.3	3116.8	125.44	0.3
2854.3	124.45	0.5	3123.4	125.45	0.2
2860.9	124.48	0.4	3129.9	125.47	0.3
2867.5	124.51	0.5	3136.5	125.49	0.2
2874.0	124.53	0.2	3143.0	125.50	0.2
2880.6	124.57	0.6	3149.6	125.52	0.3
2887.1	124.60	0.4	3156.2	125.54	0.3
2893.7	124.63	0.5	3162.7	125.54	0.1
2900.3	124.66	0.4	3169.3	125.56	0.2
2906.8	124.67	0.2	3175.9	125.56	0.0
2913.4	124.70	0.4	3182.4	125.58	0.2
2919.9	124.72	0.3	3189.0	125.59	0.2
2926.5	124.75	0.4	3195.5	125.60	0.2
2933.1	124.77	0.3	3202.1	125.62	0.2
2939.6	124.79	0.3	3208.7	125.63	0.2
2946.2	124.82	0.3	3215.2	125.64	0.1
2952.8	124.84	0.4	3221.8	125.65	0.2
2959.3	124.87	0.4	3228.3	125.67	0.3
2965.9	124.89	0.3	3234.9	125.69	0.3

TABLE B5

GEO N-3

Temperature/Depth Data

Blackwell: 9/26/86

Depth Feet	Temperature Deg. F	Gradient Deg.F/100 Ft	Depth Feet	Temperature Deg. F	Gradient Deg.F/100 Ft
3241.5	125.69	0.1	3510.5	126.13	0.0
3248.0	125.67	-0.3	3517.1	126.13	0.0
3254.6	125.73	0.8	3523.6	126.14	0.2
3261.2	125.75	0.3	3530.2	126.14	0.0
3267.7	125.76	0.2	3536.7	126.15	0.1
3274.3	125.78	0.3	3543.3	126.15	0.0
3280.8	125.78	0.1	3549.9	126.16	0.1
3287.4	125.80	0.2	3556.4	126.16	0.0
3294.0	125.82	0.3	3563.0	126.15	-0.2
3300.5	125.83	0.2	3569.6	126.19	0.6
3307.1	125.84	0.1	3576.1	126.20	0.1
3313.6	125.82	-0.2	3582.7	126.20	0.0
3320.2	125.88	0.8	3589.2	126.18	-0.2
3326.8	125.89	0.2	3595.8	126.20	0.4
3333.3	125.90	0.1	3602.4	126.21	0.1
3339.9	125.90	0.0	3608.9	126.22	0.1
3346.5	125.88	-0.3	3615.5	126.20	-0.3
3353.0	125.93	0.8	3622.0	126.23	0.4
3359.6	125.94	0.1	3628.6	126.24	0.1
3366.1	125.95	0.2	3635.2	126.25	0.1
3372.7	125.96	0.1	3641.7	126.25	0.0
3379.3	125.97	0.1	3648.3	126.24	-0.1
3385.8	125.98	0.2	3654.9	126.25	0.2
3392.4	125.98	0.0	3661.4	126.27	0.3
3399.0	125.99	0.2	3668.0	126.28	0.1
3405.5	126.00	0.1	3674.5	126.28	0.1
3412.1	126.01	0.1	3681.1	126.27	-0.1
3418.6	126.02	0.2	3687.7	126.29	0.3
3425.2	126.03	0.1	3694.2	126.30	0.2
3431.8	126.03	0.1	3700.8	126.31	0.1
3438.3	126.04	0.1	3707.3	126.31	0.0
3444.9	126.05	0.2	3713.9	126.30	-0.1
3451.4	126.05	0.1	3720.5	126.32	0.4
3458.0	126.07	0.2	3727.0	126.32	0.1
3464.6	126.06	-0.1	3733.6	126.33	0.0
3471.1	126.09	0.4	3740.2	126.32	-0.1
3477.7	126.09	0.1	3746.7	126.33	0.2
3484.3	126.10	0.1	3753.3	126.35	0.2
3490.8	126.11	0.1	3759.8	126.34	0.0
3494.4	126.11	0.1	3766.4	126.36	0.2
3503.9	126.13	0.2	3773.0	126.37	0.1

TABLE B5

GEO N-3

Temperature/Depth Data

Blackwell: 9/26/86

Depth Feet	Temperature Deg. F	Gradient Deg.F/100 Ft	Depth Feet	Temperature Deg. F	Gradient Deg.F/100 Ft
3779.5	126.43	1.0	3897.6	131.34	1.1
3786.1	126.43	0.0	3904.2	131.36	0.3
3792.7	126.44	0.2	3910.8	131.52	2.5
3799.2	126.44	0.0	3917.3	132.47	14.5
3805.8	126.43	-0.2	3923.9	132.49	0.4
3812.3	126.45	0.4	3930.4	132.69	3.0
3818.9	126.55	1.5	3937.0	132.92	3.5
3825.5	126.75	3.1	3943.6	133.10	2.7
3832.0	126.71	-0.7	3950.1	133.34	3.7
3838.6	128.58	28.5	3956.7	133.47	2.1
3845.1	130.16	24.2	3963.3	133.63	2.3
3851.7	130.46	4.6	3969.8	133.71	1.3
3858.3	130.71	3.7	3976.4	133.90	2.8
3864.8	130.71	0.0	3982.9	134.09	2.9
3871.4	130.77	1.0	3989.5	134.25	2.4
3878.0	130.96	2.9	3996.1	134.64	6.1
3884.5	131.07	1.7	4002.6	134.76	1.7
3891.1	131.27	3.0			

Spud date: 6/2/86
Date TD reached: 7/29/86

Half-splits of core from GEO N-3 of 0-4000 feet were provided to the University of Utah Research Institute (UURI) personnel on August 20, 1986 in Bend, Oregon.